

Correlation functions in the QCD vacuum

Edward V. Shuryak

Department of Physics, State University of New York, Stony Brook, New York 11794

Correlation functions are one of the key tools used to study the structure of the QCD vacuum. They are constructed out of the fundamental fields and can be calculated using quantum-field-theory methods, such as lattice gauge theory. One can obtain many of these functions using the rich phenomenology of hadron physics. They are also the object of study in various quark models of hadronic structure. This review begins with available phenomenological information about the correlation functions, with their most important properties emphasized. These are then compared with predictions of various theoretical approaches, including lattice numerical simulations, the operator product expansion, and the interacting instanton approximation.

CONTENTS

I. Introduction	1
A. Preface	1
B. Why the correlation functions?	2
C. Different types of correlation functions	3
D. General relations and inequalities	5
II. Phenomenology of Mesonic Correlation Functions	6
A. Vector currents and correlators	6
B. Vector $I=1$ (or ρ) channel	7
C. ω and ϕ channels	8
D. Strange vector (or K^*) channel	10
E. Axial $I=1$ (or A_1) channel	11
F. Pseudoscalar correlation functions for the SU(3) octet (the π, K, η channels)	13
G. The SU(3) singlet correlation functions: axial, pseudoscalar, and gluonic ones	14
H. General properties of the scalar correlators	16
III. Theory of Mesonic Correlation Functions	17
A. Potential models and heavy quarkonia	17
B. Operator product expansion and QCD sum rules	19
C. Interacting instanton approximation	22
IV. Other Correlation Functions	24
A. Light-and-heavy mesons	24
B. Does the constituent quark model make sense?	26
C. Diquarks and baryons containing a heavy quark	28
D. Ordinary baryons. Why is the nucleon so light?	28
V. Correlation Functions at Nonzero Temperatures and/or Densities	31
A. Melting the QCD vacuum	31
B. The low-temperature and low-density limits	33
C. Quark propagation in the quark-gluon plasma at high temperatures	34
D. Lattice data	35
1. Screening masses	35
2. Binding of $\bar{q}q$ pairs propagating in spatial direction	36
3. Baryonic number susceptibility	37
E. Sum rules based on the operator product expansion at finite temperatures and densities	37
1. Modifications of the operator product expansion	38
2. Operator expectation values	38
3. Some results	39
VI. Summary and Discussion	40
A. Summary of phenomenological observations	40
B. What new experiments are needed?	41
C. Further lattice studies	42
D. Theoretical problems	42
Notes added in proof	43
Acknowledgments	44
References	44

I. INTRODUCTION

A. Preface

It is widely recognized that one of the central problems of strong-interaction physics is in understanding the structure of the ground state of quantum chromodynamics, the QCD vacuum. This “vacuum” is composed of gauge and quark fields interacting in a complicated non-perturbative way. A general introduction to this subject and references to original papers can be found in many reviews, including Shuryak (1984, 1988a) and Shifman (1992).

This review deals with a part of the problem, that related to correlation functions. Our purpose is to collect the available phenomenological information and compare it with predictions of various theoretical approaches. We do not discuss the theoretical ideas in depth, and in many places we ignore the related technicalities. Instead, we proceed from a qualitative discussion directly to the specific results. We concentrate on the main phenomena to be explained by the theory and comment to what extent this goal has been achieved.

An important motivation for surveying the field is that theorists working on strong-interaction physics are divided into several poorly interacting communities, according to the method they follow. The main theoretical approaches are (1) lattice gauge theory (LGT); (2) QCD sum rules, based on the operator product expansion (OPE); (3) interacting instanton approximation (IIA); and (4) quark potential models for hadronic spectroscopy and reactions.

We hope that this review can bridge the theoretical gaps and bring these isolated communities together. Our main target is to make better connections between lattice calculations and the other theoretical analyses. The lattice community, having the most powerful methods based on first principles, has great opportunities for making better contact with the phenomenology of strong-interaction physics.

As a common denominator for our discussion, we have chosen the point-to-point correlation function in the coordinate representation, with which it becomes possible to compare phenomenological information and

theoretical predictions. As we shall see, it is quite straightforward to “translate back” the main results of the OPE and instanton frameworks to the coordinate representation of the correlators.

Unfortunately, most lattice studies of correlation functions use either sources in the form of three-dimensional “walls” or even more complicated nonlocal sources. However, the point-to-point correlators are the basic objects; they carry more information and can be measured by simple modification of the existing techniques. Apart from the qualitatively new short-range phenomena to be learned, one may obtain more accurate and reliable comparisons between lattice and empirical correlators. This contrasts with the traditional technique of only studying the asymptotic large-distance behavior of the correlators related to the masses of the lightest hadrons.

It is hoped that some part of this review may be of interest to experimentalists working in different branches of strong-interaction physics. We comment often on the mutual consistency of various sets of data, on most desirable new experiments, on the main source of experimental uncertainties, etc. A brief summary of the experimental side of the problem can be found in Sec. VI.B.

The paper is organized as follows. In Sec. II we discuss the available phenomenological information about mesonic correlation functions, outlining a set of major facts to be explained by the theory. Section III is devoted to theoretical predictions, which we consider only briefly on a matter-of-fact level, concentrating on the results and their relation to experiment. In Sec. IV we discuss some other correlation functions, including light- and heavy mesons and baryons, as well as ordinary baryons, pointing out several other important observations related to quark properties and interactions. There also we consider experimental information and theoretical ideas together. Section V is devoted to correlation functions at nonzero temperature and/or density. The hadrons are expected to “melt” at some critical temperature into free quarks and gluons, and one can study this phenomenon using the correlation functions. Our conclusions and suggestions are summarized in Sec. VI.

The reader who would like to see from the start which operators and correlation functions are considered in this review is invited to look at Table I.

B. Why the correlation functions?

Here we define what we mean by the correlation functions, discuss their asymptotic behavior at small and large distances, and then try to explain why they play such an important role in studies of the QCD vacuum.

Below we deal with two types of operators: mesonic ones of the type

$$O_{\text{mes}}(x) = \bar{\psi}_i \psi_j \delta_{ij} , \quad (1.1)$$

and baryonic ones,

$$O_{\text{bar}}(x) = \psi_i \psi_j \psi_k \epsilon^{ijk} . \quad (1.2)$$

Here the color indices i, j, k are explicitly shown; we shall omit them below. Other indices like spin and flavor are not here specified, but shall be later. As all color indices are properly contracted and all quark fields are taken at the same point x , these operators are manifestly gauge invariant.

The correlation function is defined as the vacuum expectation value (VEV) of the product¹ of two operators taken at two points x and y :

$$K(x-y) = \langle 0 | O(x) O(y) | 0 \rangle . \quad (1.3)$$

The first comment is that the vacuum is homogeneous; so one of the points can be the origin of the coordinate system, say, $y=0$. A second comment is that we assume throughout this paper that the separation between the points $(x-y)$ is spacelike. The reason is we prefer to deal with virtual propagation of quarks or hadrons from one point to another, to have simple decaying functions instead of functions having a complicated oscillatory behavior.

There is an old question that one inevitably asks at this point: why is there a correlation between fields outside the light cone? It was essentially answered by Feynman: particles can propagate along any path going from x to y . Depending on the reference frame, an observer can consider the path to be a sequence of spontaneous pair-creation and annihilation events. This correlation does not contradict causality, because one cannot use it for signal transfer. See textbooks on quantum field theory for more.

One can look at the pairs of points of the correlator in two ways. Either they are two points in space, taken at the same instant of time and separated by the spatial distance x , or they are two events separated by some interval in imaginary or Euclidean time: $ix_0 - iy_0 = \tau$. Below we use both interpretations, depending on which is more convenient at the moment. We hope the reader will not be confused by our using the symbols x and τ interchangeably.

Let us now discuss the behavior of the correlation functions at small and large distances. At small x (remember, $y=0$) the asymptotic freedom of QCD tells us that quarks and gluons propagate freely, up to small and calculable radiative corrections. Therefore $K(x)$ in the mesonic (baryonic) case is essentially the square (or cube) of the free-quark propagator, $S(x) = \langle \bar{q}(x) q(0) \rangle$, depending on whether a mesonic or baryonic correlator is under consideration. From dimensional arguments, the quark propagator $S(x)$ is seen to scale as $S(x) \sim x^{-3}$,

¹Actually, it is the time-ordered product that is usually denoted by T : it is always implied below. We do not go into details here, but only mention that such T -ordering just corresponds to using the standard path integrals and Feynman propagators for particles propagating from x to y .

ignoring small quark masses.² So for the mesonic or baryonic correlators, there follows a small x limit $K(x) \sim x^{-6}$ (or $\sim x^{-9}$) from the simple dimensional arguments³ alone.

If quarks are allowed to propagate to larger distances, they start interacting more strongly with vacuum fields. If corrections are not too large, one can take these effects into account using the operator product expansion (OPE) formalism (see Sec. III.B). At intermediate distances, description of the correlation functions becomes, in general, very complicated, and one may only evaluate them by using either lattice numerical simulations or some vacuum models (e.g., the instanton model described in Sec. III.C).

At large distances one can again understand the behavior of the correlation functions, using now completely different kinds of arguments. Instead of thinking in terms of fundamental fields, one may just use the formal relation for the time evolution of an operator $O(t) = e^{iHT}O(0)e^{-iHt}$, where H is a Hamiltonian, and then insert a complete set of physical intermediate states between the two operators:

$$K(t) = \sum_n |\langle 0|O(0)|n\rangle|^2 e^{-iE_n t}. \quad (1.4)$$

Now one can analytically continue the correlation function into the Euclidean time $\tau = it$ and get a sum over decreasing exponents.⁴

Physically, application of such relations in QCD means that one consider propagation of physical excitations or hadrons between our two points, leading to the prediction that $K(x) \sim \exp(-mx)$ for large x , where m is the mass of the lightest particle with the corresponding quantum numbers. This is essentially the idea of Yukawa, to relate the range of the nuclear forces with the pion mass.

It is now easy to understand why the correlation functions are so important in nonperturbative QCD and hadronic physics. The reason is that the same function can be considered on two different levels: (1) in terms of the fundamental QCD fields, quark and gluons, or (2) in terms of the physical intermediate states, using the vast hadronic phenomenology of masses, coupling constants, form factors, etc.

Moreover, there is a third approach to the correlation functions. There are useful models originating from the

original quark model of the '60s based on "constituent" quarks and their effective interactions. It is instructive to explain what we want to learn from the correlation functions in this language: it is the interquark effective interaction.

Application of these models to hadronic spectroscopy reminds one of nuclear physics in its early days, when only limited information about the nuclear forces was known. Besides knowledge of the bound states, such as the deuteron, one had only qualitative information that the potential was attractive and of short range.

Indeed, potential-type quark models are successfully applied to the evaluation of hadronic parameters. This is discussed in detail by Godfrey and Isgur (1985) for mesons and by Capstick and Isgur (1986) for baryons. One obtains the average characteristics of the few lowest hadronic states in each channel, and the theory is sensitive mainly to interquark interaction averaged over the size of these states. The hadronic phenomenology demonstrates the existence of flavor- and spin-independent confining forces, complemented by some short-range spin-spin interaction.

However, we lack detailed knowledge of how the interquark interaction depends on distance and momenta. Returning to the analogy with nuclear physics, we comment that only the extensive studies of nucleon-nucleon scattering eventually showed all the details of nuclear forces with their complicated spin-isospin structure.

Although qq or $\bar{q}q$ scattering is experimentally impossible to study, due to confinement, a set of various mesonic correlation functions $K(x)$ plays essentially the same role as that played in nuclear physics by the scattering phase shifts. These correlation functions are discussed below. Roughly speaking, we shall describe virtual $\bar{q}q$ or qq scattering, using wave packets of variable size instead of physical hadrons.

C. Different types of correlation functions

The correlation functions in Euclidean space-time $K(x)$ [or $K(\tau)$] defined above are the objects of our discussion in what follows. As their argument x is the distance between the two points in Euclidean space-time, we call them point-to-point correlation functions, or correlators.

We use this specific name because in various applications people have used other representations of correlators related to the above ones by some integral transformation. We compare here their definitions and briefly comment on their advantages and disadvantages.⁵

If one makes a Fourier transform of $K(x)$, the resulting function $K_{\text{mom}}(q^2)$ depends on the momentum transfer q flowing from one operator to another. For

²The coefficient is also easy to find by solving the Dirac equation for free massless particles: $S(x) = (i\gamma_\mu \partial_\mu)(1/4\pi^2 x^2)$.

³Of course, QCD does have a dimensional parameter Λ_{QCD} , which eventually fixes the scale of all dimensional quantities. However, in perturbation theory it only comes in via the radiative corrections. Therefore, at small x , those produce corrections to our estimates above containing $\alpha_s(x) \sim 1/\ln(x\Lambda)$.

⁴A reader who does not like Euclidean time can repeat this exercise for spatially separated points and sum over virtual momenta of the intermediate states. The result is the same, due to the four-dimensional symmetry of the Euclidean space-time.

⁵As we actually do not use any of them in what follows, the reader may well skip this section.

clarity we use the following notations, introducing momentum squared with a negative sign $Q^2 = -q^2$. We are interested in spacelike momentum transfers, as in scattering experiments, for which $q^2 < 0$ and $Q^2 > 0$.

Due to causality, the Fourier transform of the point-to-point correlation function satisfies the usual dispersion relation,

$$K_{\text{mom}}(q^2) = (1/\pi) \int ds \frac{\text{Im}K_{\text{mom}}(s)}{(s - q^2)}. \quad (1.5)$$

The numerator on the right-hand side, $\text{Im}K_{\text{mom}}(s)$, is the physical spectral density. It describes the squared matrix elements of the operator in question between the vacuum and all hadronic states with the invariant mass $s^{1/2}$, and is nonzero only for positive s . Because we are considering only negative q^2 , we never come across a vanishing denominator and therefore may ignore $i\epsilon$, which is usually put in the denominator. This simplification is possible because our discussion is restricted to virtual processes, although in the right-hand side we shall use information coming from the real processes of particle creation and annihilation.⁶

Equation (1.5) is the basis of the so-called QCD sum rules. Their general idea is as follows. Suppose one knows $K_{\text{mom}}(q^2)$ in some region. This implies that some integral of the spectral density is known, which can be used to fix a set of physical parameters. Unfortunately, such finite-energy sum rules are not very productive, because the dispersion integrals are usually divergent, leading to useful sum rules only after some subtractions. This introduces extra parameters and significantly undetermines their predictive power.

Let us be more specific, taking the mesonic correlation functions as an example. As mentioned earlier, the mesonic correlators are given by a simple loop diagram for small x , corresponding in the coordinate representation to the free-quark propagator squared. It is not difficult to see that the imaginary part of this diagram, corresponding to the production of a $\bar{q}q$ pair, is $\text{Im}K_{\text{mom}}(s) \sim s$. This is also obvious on dimensional grounds. Then from the dispersion integral we see that at large s the Fourier-transformed correlator depends on s as $K_{\text{mom}}(s) \sim s \ln(-s)$. However, the dispersion integral is also divergent, which signals that something is missing in the last argument. One simple way to get around this difficulty is to consider the second derivative over Q^2 : then one deals with the function $K''_{\text{mom}}(s)$, which is defined by a convergent dispersion relation. However, while going back to the original function $K_{\text{mom}}(s)$, one has to fix two integration constants corresponding to the missing terms in $K_{\text{mom}}(s)$ of the type

$c_1 s + c_2$, which have no imaginary part. We can safely ignore them below in our discussion of $K(x)$, provided x is never zero, because these correspond in the coordinate space to contact terms, δ functions, and their derivatives. However, in finite-energy sum rules, these two undefined constants need to be determined also from the data.

Several other ideas have been suggested to improve these sum rules. First, after taking a sufficient number of derivatives, one may take $Q=0$ and arrive at the so-called moments of the spectral density,

$$M_n = (1/\pi) \int ds \text{Im}K_{\text{mom}}(s)/s^{n+1}. \quad (1.6)$$

Following ideas presented in the original paper of Shifman, Vainshtein, and Zakharov (1979a), this method is commonly used in the discussion of "charmonium sum rules," which are related to correlators of $\bar{c}c$ currents.

Another idea, suggested in the same paper (Shifman *et al.*, 1979a), is to introduce the Borel transform of the function $K_{\text{mom}}(Q)$, defined as follows,

$$K_{\text{bor}}(m) = \lim_{\substack{n \rightarrow \infty \\ s \rightarrow \infty \\ m^2 = Q^2/n^2}} \frac{Q^{2n}}{(n-1)!} (-d/dQ^2)^n K_{\text{mom}}(Q^2). \quad (1.7)$$

Applying this to the dispersion relation (1.5), we obtain the sum rules in the Borel-transformed representation:

$$K_{\text{bor}}(m) = (1/\pi) \int ds \text{Im}K_{\text{mom}}(s) \exp(-s/m^2). \quad (1.8)$$

Now the integral is cut off at large s by the exponential function. This formula also has another useful feature: usually we know the contribution of the lowest states (the first resonance) better than the contribution of the multi-body high-energy part; so the exponential cutoff hides our ignorance and is therefore welcomed. Such forms of the sum rules have been used in many papers based on the OPE (see, e.g., references in Shuryak, 1984, 1988a and Shifman, 1992).

However, most of the results obtained by this technique can also be presented in a much simpler way. Instead of the Borel transformation, one can Fourier transform back to coordinate space; then the dispersion relation has the transparent form (Shuryak, 1984, 1988a)

$$K(x) = (1/\pi) \int ds \text{Im}K_{\text{mom}}(s) D(s^{1/2}, x). \quad (1.9)$$

Here function $\text{Im}K_{\text{mom}}(s)$ describes the amplitude of production of all intermediate states of mass $s^{1/2}$, while the function

$$D(m, x) = (m/4\pi^2 x) K_1(mx) \quad (1.10)$$

is nothing more than the propagator of these states to a point x . In practice there is not much difference between this equation and Borel sum rules. At large x the propagator goes as $\exp(-mx)$; therefore one has an exponential cutoff, but with the factor $\exp(-s^{1/2}x)$ instead of $\exp(-s/m^2)$. However, the space-time dispersion rela-

⁶In principle, virtual processes contain all the information; but, of course, in practice, it is much more difficult to go in the opposite direction and reproduce the physical spectral density from the point-to-point correlators.

tion has a much clearer physical interpretation, and we shall keep to it in what follows.

For completeness, let us also mention one more type of correlation function, the one traditionally used in lattice gauge theory. This is the so-called plane-to-plane correlation function obtained from $K(x)$ by an integration over a three-dimensional plane:

$$K_{\text{plane to plane}}(\tau) = \langle \int d^3x O(x, \tau) O(0, 0) \rangle. \quad (1.11)$$

In other words, a spatial integration selects intermediate states of momentum zero; so dispersion relations are done in energy only. The above function can be related to a physical spectral density by

$$K_{\text{plane to plane}}(\tau) = (1/\pi) \int dm \operatorname{Im} K_{\text{mom}}(m) \exp(-\tau m). \quad (1.12)$$

The mass of the lowest hadron can be obtained directly from the logarithmic derivative of this function at large τ . However, its essential disadvantage is that it mixes contributions of small and large distances. This makes it difficult to match with the OPE-derived functions at small distances, and also obscures the physics going on at intermediate distances.

However, in the important case of heavy-light mesons (see Sec. IV.A), a lattice evaluation of point-to-point correlation functions has been made. In this case there is no difference between point-to-point and plane-to-plane ones, because the super-heavy quark does not propagate in space; so the integral in (1.11) has only a δ function contribution.

To summarize this section, we have noted five different correlation functions in use: (1) the original point-to-point function $K(x)$ in coordinate space; (2) the Fourier transform $K_{\text{mom}}(q^2)$; (3) the moments of the spectra density M_n ; (4) the Borel-transform function $K_{\text{mom}}(m)$; and (5) the plane-to-plane correlation function $K_{\text{plane to plane}}(\tau)$.

Although each correlation function has its advantages, we suggest that for the understanding of the underlying physics it is better to use the original point-to-point function $K(x)$, and we shall do so in what follows.

D. General relations and inequalities

One can classify correlation functions according to quark paths, recognizing two different types of diagrams: (1) the one-loop diagrams, in which quarks produced by one operator go to another one, and (2) the two-loop diagrams, where quark lines are closed on the same operator.

For example, in the isospin $I=1$ channels like π^+ , one has operators like $\bar{u}\Gamma d$, where Γ is any Dirac matrix. In this case, obviously, only the one-loop diagrams contribute. On the other hand, considering the nondiagonal correlators in flavor, say, $\langle \bar{u}(x)\Gamma u(x)\bar{d}(0)d(0) \rangle$, one is restricted to the second type. For most $I=0$ cases, one

has both types of contributions. Lattice calculations deal mainly with one-loop diagrams, and therefore with the $I=1$ channels, for technical reasons. Some general statements can be made about the one-loop diagrams, which we would like to outline here, following Weingarten (1983).⁷

To derive the relations, we first note the following formula for the propagator in the backward direction,⁸

$$S(x, y) = -\gamma_5 S^+(y, x) \gamma_5. \quad (1.13)$$

One next decomposes it into Dirac matrices $S = \sum a_i \Gamma_i$, where $\Gamma_i = 1, \gamma_5, \gamma_\mu, i\gamma_5\gamma_\mu, i\gamma_\mu\gamma_\nu$ ($\mu \neq \nu$). Finally, one considers all diagonal one-loop correlators of the type $\Pi = \operatorname{Tr}[S(x, y)\Gamma_i S(y, x)\Gamma_i]$ and evaluates the traces.

The most interesting result appears for the pseudoscalar (pion) correlator: in this case one has a sum of all coefficients squared,

$$\Pi_{\text{PS}}/\Pi_{\text{PS}}^{\text{free}} = (|a_1|^2 + |a_5|^2 + |a_\mu|^2 + |a_{\mu 5}|^2 + |a_{\mu\nu}|^2)/|a_0|^2, \quad (1.14)$$

while, for example, the scalar one is

$$\begin{aligned} \Pi_S/\Pi_S^{\text{free}} &= (-|a_1|^2 - |a_5|^2 + |a_\mu|^2 + |a_{\mu 5}|^2 - |a_{\mu\nu}|^2)/|a_0|^2. \end{aligned} \quad (1.15)$$

Here we have normalized the correlator to its asymptotically free version, containing free propagators of massless quarks. Assuming that the propagation takes place in the time direction, the propagator is $S_{\text{free}} = \gamma_0/(2\pi^2 x_0^3)$, and the only nonzero coefficient is $a_0 = 1/(2\pi^2 x_0^3)$. Comparing the above two equations, we obtain the Weingarten inequality. This states that the pseudoscalar correlator exceeds the scalar one at all distances, $|\Pi_{\text{PS}}| \geq |\Pi_S|$.

The nontrivial thing is that the physical pion is very light, while scalars are heavy; therefore for $x > 0.5$ fm the scalar correlator is practically zero, while the pseudoscalar ratio is very large. This requires a very delicate cancellation between the different a_i in the propagator.

Additional information is provided by similar relations for vector (ρ) and axial (A_1) channels,

$$\Pi_V/\Pi_V^{\text{free}} = (2|a_1|^2 - 2|a_5|^2 + |a_\mu|^2 - |a_{\mu 5}|^2)/|a_0|^2, \quad (1.16)$$

$$\Pi_A/\Pi_A^{\text{free}} = (-2|a_1|^2 + 2|a_5|^2 + |a_\mu|^2 - |a_{\mu 5}|^2)/|a_0|^2, \quad (1.17)$$

⁷In preparation of this section J. Verbaarschot has helped a lot toward the understanding of the meaning of these relations. He also found a few new ones.

⁸Readers who wonder why γ_5 is needed should take as an example a free massive propagator and notice that the terms proportional to $(x-y)_\mu\gamma_\mu$ and to m behave differently under the transformation $x \leftrightarrow y$.

TABLE I. Set of the operators and correlation functions discussed in this paper.

Channel	Current	Section	Info
ρ	$(\bar{u}\gamma_\mu u - d\gamma_\mu d)/2^{1/2}$	II.B	$e^+e^- \rightarrow N\pi, N$ even
ω	$(\bar{u}\gamma_\mu u + d\gamma_\mu d)/2^{1/2}$	II.C	$e^+e^- \rightarrow N\pi, N$ odd
ϕ	$\bar{s}\gamma_\mu s$	II.C	$e^+e^- \rightarrow \bar{K}K + N\pi$
K^*	$\bar{u}\gamma_\mu\gamma_5 s$	II.D	decay $\tau \rightarrow \nu_\tau + K^*$
A_1	$\bar{u}\gamma_\mu\gamma_5 d$	II.E	decay $\tau \rightarrow \nu_\tau + N\pi, N$ odd
π	$\bar{u}\gamma_5 u - \bar{d}\gamma_5 d)(i/2^{1/2})$	II.F	pion decay
K	$\bar{u}i\gamma_5 s$	II.F	K decay
η	$(\bar{u}\gamma_5 u - \bar{d}\gamma_5 d - 2\bar{s}\gamma_5 s)/(i/6^{1/2})$	II.F	
η'	$(\bar{u}\gamma_5\gamma_\mu u + \bar{d}\gamma_5\gamma_\mu d + \bar{s}\gamma_5\gamma_\mu s)/(1/3^{1/2})$	II.G	$J/\psi \rightarrow \gamma + \eta$ etc.
η'	$G\bar{G}$	II.G	$J/\psi \rightarrow \gamma + \eta$ etc.
scalars	$\bar{q}q$	II.H	masses, generalities
Υ	$\bar{b}\gamma_\mu ub$	III.A	$e^+e^- \rightarrow \bar{B}B +$ pions
B -type mesons	$\bar{Q}\Gamma q$	IV.A	masses of heavy flavored mesons
heavy baryons	$q^T C \Gamma_q Q$	IV.C	masses
N	$(u^T C d)u - (u^T C \gamma_5 d)\gamma_5 u$	IV.D	OPE predictions
Δ	$(u^T C \gamma_\mu u)u$	IV.D	OPE predictions

and the following inequalities may be proven⁹:

$$\Pi_{PS}/\Pi_{PS}^{\text{free}} > \frac{1}{2}(\Pi_V/\Pi_V^{\text{free}} + \Pi_A/\Pi_A^{\text{free}}) \quad (1.18)$$

$$\Pi_{PS}/\Pi_{PS}^{\text{free}} > \frac{1}{4}(\Pi_V/\Pi_V^{\text{free}} - \Pi_A/\Pi_A^{\text{free}}) . \quad (1.19)$$

Witten (1983) has found another interesting inequality between vector and axial correlators, but it applies only to the momentum representation, and we do not discuss it here.

As these inequalities are identities, they are satisfied for any configuration of the gauge field, and they therefore are not very restrictive from a theoretical point of view. However, they can be used to check consistency of experimental data, as discussed below.

On the other hand, the diagonal correlators themselves are positive monotonously decreasing functions, as is clear from the spectral decomposition discussed in the previous section. This condition is trivial to satisfy from the empirical determination of correlators; but from the theoretical point of view, it produces nontrivial limitations for the ensemble of vacuum fields. Some configurations do produce negative correlators, especially in the scalar channel. If their weight in the ensemble of vacuum fields is too large, the positivity and monotonicity may be violated. These conditions may provide interesting new conditions on the models of the vacuum.

II. PHENOMENOLOGY OF MESONIC CORRELATION FUNCTIONS

A. Vector currents and correlators

We start the discussion of the correlation functions with vector currents for an obvious reason: these

currents really exist in nature, evidenced by their coupling to weak and electromagnetic fields, in contrast to many other operators to be discussed. In several cases the complete spectral density of the corresponding correlation functions is experimentally known, subject, of course, to some experimental uncertainty, from e^+e^- annihilation into hadrons.

The vector currents and their correlation functions to be discussed below will be denoted by the name of the lightest meson in the corresponding channel; in particular, we define the ρ , the ω , and the ϕ currents as the following quark currents,

$$j_\mu^\rho = (1/2^{1/2})[\bar{u}\gamma_\mu u - \bar{d}\gamma_\mu d] \text{ or } \bar{u}\gamma_\mu d , \quad (2.1)$$

$$j_\mu^\omega = (1/2^{1/2})[\bar{u}\gamma_\mu u + \bar{d}\gamma_\mu d] , \quad (2.2)$$

$$j_\mu^\phi = \bar{s}\gamma_\mu s . \quad (2.3)$$

Further definitions may be found in Table I. The electromagnetic current is the following combination of the quark currents:

$$\begin{aligned} j_\mu^{\text{em}} &= \frac{2}{3}\bar{u}\gamma_\mu u - \frac{1}{3}\bar{d}\gamma_\mu d + \dots \\ &= (1/2^{1/2})j_\mu^\rho - (1/2^{1/2}3)j_\mu^\omega + \dots . \end{aligned} \quad (2.4)$$

The vector correlation functions are defined as

$$\Pi_{i,\mu\nu}(x) = \frac{1}{2}\langle 0 | T j_{i,\mu}(x) j_{i,\nu}(0) | 0 \rangle , \quad (2.5)$$

and the Fourier transform (in Minkowski space-time) is traditionally written as

$$i \int d^4x e^{iqx} \Pi_{i,\mu\nu}(x) = \Pi_i(q^2)(q_\mu q_\nu - q^2 g_{\mu\nu}) . \quad (2.6)$$

The right-hand side is explicitly transverse, i.e., it vanishes when multiplied by momentum q . This is necessary for conservation of the vector current.

The dispersion relations for the scalar functions $\Pi_i(q^2)$ are

⁹These were shown to me by J. Verbaarschot (private communication).

$$\Pi_i(Q^2 = -q^2) = (1/\pi) \int ds \frac{\text{Im}\Pi_i(s)}{(s+Q^2)}, \quad (2.7)$$

where the physical spectral density $\text{Im}\Pi_i(s)$ is directly related to the cross section of e^+e^- annihilation into hadrons. As this quantity is dimensionless, it is proportional to the normalized cross section

$$R_i(s) = \sigma_{e^+e^- \rightarrow i}(s) / \sigma_{e^+e^- \rightarrow \mu^+\mu^-}(s), \quad (2.8)$$

where the cross section of muon pair production (neglecting the muon mass) is just $\sigma_{e^+e^- \rightarrow \mu^+\mu^-} = (4\pi\alpha^2/3s)$ and α is the fine-structure constant. If both quarks in the current considered have the same flavor, as, for example, the $s\bar{s}$ in the ϕ current, one obtains

$$\text{Im}\Pi_i(s) = R_i(s) / (12\pi e_q^2), \quad (2.9)$$

where e_q is quark electric charge. Generalization to ρ, ω channels is straightforward: instead of the charge there stands a corresponding coefficient in the equation for the electromagnetic current, e.g.,

$$\text{Im}\Pi_\rho(s) = \frac{1}{6\pi} R_\rho(s). \quad (2.10)$$

The reader may wonder how the different vector correlators are distinguished experimentally. It is clear enough for the charge and beauty heavy flavors: if the final state has a pair of such quarks, it is much more likely that they were directly produced in the electromagnetic current than that they were produced by final-state interactions. We shall also use this argument later for the strange quark, although it is less justified in that case. To separate the light quark ρ, ω channels, we make use of their isospin and G parity. The two channels have a different isospin $I=1,0$ which is conserved by any strong final-state interaction. As it is well known, C parity plus isotopic invariance leads to the so-called G -parity conservation, and pions have negative G parity. Therefore strong interactions do not mix states with even and odd numbers of pions. The currents j_ρ, j_ω have fixed G parity as well, and therefore pionic states created by them can have only even or odd numbers of pions, respectively.

Let us start with a simple example to show how these relations lead to definite predictions. The ratios $R_i(s)$ have a very simple limit at high energies s , because in this limit quarks and antiquarks are produced as free particles. For currents containing only one quark flavor q , the only difference with the muon is a different electric charge and a color factor:

$$\lim_{s \rightarrow \infty} R_q(s) = e_q^2 N_c, \quad (2.11)$$

which for the ϕ case gives $\lim_{s \rightarrow \infty} R_\phi(s) = \frac{1}{3}$. For the ρ and ω cases, we expand the electromagnetic current equation (2.4) in terms of (2.1) and (2.2) and obtain from that representation

$$\lim_{s \rightarrow \infty} R_\rho(s) = \frac{3}{2}, \quad \lim_{s \rightarrow \infty} R_\omega(s) = \frac{1}{6}. \quad (2.12)$$

As we shall see shortly, these relations are well satisfied experimentally. In fact, this was historically one of the first and simplest justifications for QCD.

Coming back to coordinate representation of the dispersion relation, one obtains

$$\begin{aligned} \Pi_{i,\mu\nu}(x) &= (\partial^2 g_{\mu\nu} - \partial_\mu \partial_\nu) \frac{1}{12\pi^2} \\ &\times \int_0^\infty ds R_i(s) D(s^{1/2}, x), \end{aligned} \quad (2.13)$$

where, we recall, $D(m, x)$ from Eq. (1.10) is just the propagator of a scalar mass- m particle to point x . Contracting indices and using the equation $-\partial^2 D(m, x) = m^2 D(m, x) + \text{contact term}$, which we disregard, the dispersion relation finally becomes

$$\Pi_{i,\mu\mu}(x) = (1/4\pi^2) \int_0^\infty ds s R_i(s) D(s^{1/2}, x). \quad (2.14)$$

This is our experimental definition of the vector correlation functions.

A final comment related to our notation: as correlators are very strongly decreasing functions of x , it is more convenient to plot them normalized to the free propagators, namely, as $\Pi_{\mu\mu}(x) / \Pi_{\mu\mu}^{\text{free}}(x)$ where $\Pi_{\mu\mu}^{\text{free}}(x)$ corresponds to the simple loop diagram describing free-quark propagation. In such ratios all uninteresting normalization factors, such as the quark electromagnetic charges, drop out. At small distances these ratios are all close to 1 due to asymptotic freedom.

B. Vector $I=1$ (or ρ) channel

Figure 1 shows a sample of experimental data on $R_\rho(s)$ at low energies. One can see that this function consists of two quite different parts: (1) the prominent ρ -meson resonance, seen in the 2π channel, and (2) a mixture of multipion states, which starts with (at least) two ‘‘primed’’ resonances, ρ' (1450) and ρ' (1700), seen mainly in the four-pion channel. However, taken together with the six-pion channel, they add up to a rather smooth nonresonance ‘‘continuum,’’ and already at energies of about 1.5 GeV this spectral density follows the prediction $R_\rho = \frac{3}{2}$ made above.

We have parametrized the data in Fig. 1 by the following function, shown as the solid line:

$$\begin{aligned} R_\rho(E) &= \frac{9}{1 + 4(E - m_\rho)^2 / \Gamma_\rho^2} \\ &+ \frac{3}{2} (1 + \alpha_s(E) / \pi) \frac{1}{1 + \exp[(E_0 - E) / \delta]}, \end{aligned} \quad (2.15)$$

where $E_0 = 1.3$ GeV, $\delta = 0.2$ GeV, and $\alpha_s(E) = 0.7 / \ln E / 0.2$ GeV). This parametrization includes all essential ingredients of the data: the resonance peak and (smoothed) transition to the asymptotic behavior, corresponding to the famous cross section of free-quark production. For the high-energy contribution, we used a smoothed function instead of the θ function, as it is traditionally done in QCD sum rules. The physical meaning

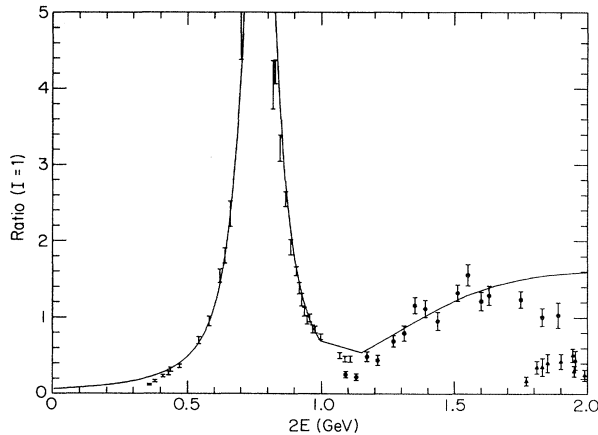


FIG. 1. Ratio of $\sigma(e^+e^- \rightarrow n\pi) / \sigma(e^+e^- \rightarrow \mu^+\mu^-)$ with n even, as a function of the total invariant mass of the hadronic system. The data points correspond to the following states: the error bars without points to 2π (Barkov *et al.*, 1985); stars to 4π (Cosme *et al.*, 1979; Cordier *et al.*, 1982a; Barkov *et al.*, 1988; Kurdadze *et al.*, 1988); and triangles to 6π states (Cosme *et al.*, 1979; Dolinsky *et al.*, 1989). The solid line is our fit to the sum of all contributions with n even for the total cross section in the $I=1$ channel. We have not shown all data points available near the top of the ρ peak, nor the region $2E > 2$ GeV, where the agreement between data points and our fitted curve is very good.

of the parameter E_0 is the same: it is the energy above which the asymptotic freedom is restored and simple quark model estimates for cross section become valid.

We now calculate the correlation function using this parametrization and the dispersion relation (2.14), taking the integral over all energies. The resulting curve is shown in Fig. 2, where the contributions of two components of the spectral density mentioned above are also

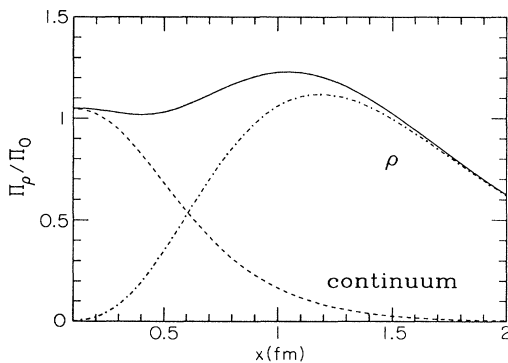


FIG. 2. Ratio of the $I=1$ vector correlation function to that corresponding to free-quark propagation vs the distance x . The dot-dashed curve is the ρ -meson contribution calculated as the contribution to the integral of the region below a total energy of 1 GeV. The dashed curve labeled “continuum” is the complementary contribution of all hadronic states above 1 GeV, and the solid curve is their sum.

shown separately. The first striking observation is that, starting with the rather complication function $\text{Im}\Pi_{\mu\mu}(s)$, we arrived at a very smooth function of the separation x . Clearly, the way back from the coordinate representation to physical spectral density would be much more difficult.

The second striking observation (Shuryak, 1989a) is that the contributions of the lowest meson and continuum complement each other in such a way that the ratio $\Pi(x) / \Pi_{\text{free}}(x)$ remains close to 1 up to distances as large as 1.5 fm. We call this fine tuning of all parameters superduality. As we shall show, it persists in all vector channels. For small distances it is nothing more than asymptotic freedom. At $x \sim 0.3$ fm, it is a consequence of the so-called duality between hadronic and quark description. However, from 0.3 to 1.5 fm, where the correlator drops by more than four orders of magnitude, it is an unexpected and remarkable phenomenon!

Completing this section, let us examine the errors in the determination of the correlators. Of course, the experimental uncertainties are there, and their magnitudes are seen in Fig. 1. In the ρ region (due essentially to VEPP-2M data from Novosibirsk), the resulting error at large $x > 0.6$ fm in the correlator is about 5%. The high-energy domain is covered by SPEAR data from SLAC, which fix the normalization of small- x region also to within a few percent. However, in the most interesting medium distances, we have contributions from the ρ' energy region, and here the situation is actually even more uncertain than our Fig. 1 indicates: the Frascati and Orsay data do not agree, and the problem is not statistical. It is quite probable that in this region our parametrization of the cross section is off by as much as 30%, which may lead to error bars for the ratio $\Pi(x) / \Pi_{\text{free}}(x)$ plotted in Fig. 2 of about 15% at $x \sim 0.6$ fm. In view of the apparent systematic deviation of the two sets of data, it would not be useful to display statistical error bars on the plots of the correlators.

C. ω and ϕ channels

The next channel we discuss is the isoscalar channel having the quantum numbers of the ω meson. The corresponding data for the cross section of e^+e^- annihilation into an odd number of pions, now summed over all channels, are shown in Fig. 3. The top of the ω peak is not shown because here the Breit-Wigner curve (with the width value taken from *Review of Particle Properties*, Hernández *et al.*, 1990) is very accurate: the peak value of R_ω is about 12. One can also see a trace of the ϕ peak due to the ω - ϕ mixing, which will be disregarded in our parametrization. Note the change of scale and the essentially larger error bars compared to the $I=1$ channel. Within uncertainties the continuum magnitude approaches its asymptotic value $R_\omega = \frac{1}{6}$ at about the same energies as in the $I=1$ channel.

For narrow resonances, we include the resonance contribution in the simple form

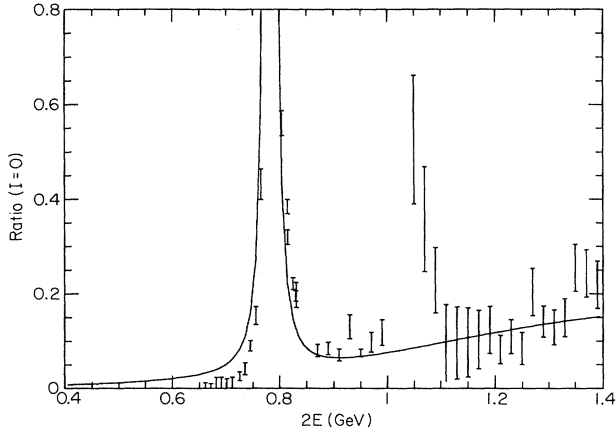


FIG. 3. As in Fig. 1, the isospin $I=0$ final states, defined as those having an odd number of pions. Data points are summed over all channels, compiled in Dolinsky *et al.* (1989), while the curve is our fit discussed in the text.

$$\Pi_{\mu\mu}(\tau)|_{\text{res}} = 3f_{\text{res}}^2 m_{\text{res}}^2 D(m_{\text{res}}, \tau), \quad (2.16)$$

where the coupling constants of the currents to mesons are defined as follows¹⁰:

$$\langle 0 | j_{\mu}^{\text{em}} | \text{resonance} \rangle = f_{\text{res}} m_{\text{res}} \epsilon_{\mu}. \quad (2.17)$$

Here the ϵ_{μ} is the polarization vector of the vector meson. These couplings and the partial widths to the e^+e^- channel are related as follows:

$$f_{\text{res}}^2 = \frac{3m_{\text{res}} \Gamma(\text{res} \rightarrow e^+e^-)}{4\pi\alpha^2}. \quad (2.18)$$

For reference, the accepted values of the coupling constants of the ρ , ϕ , and ω mesons are $f_{\omega} = 46$ MeV, $f_{\phi} \approx 79$ MeV, $f_{\rho} \approx 152$ MeV.

Next Fig. 4 shows the correlation function $\Pi_{\omega}(x)/\Pi_{\text{free}}(x)$, again with contributions from the ω resonance and the continuum state shown separately and in sum. The curve corresponds to the following parametrization of the cross section:

$$R_{\omega}(E) = \frac{12}{1 + 4(E - m_{\omega})^2 / \Gamma_{\omega}^2} + \frac{1}{6} (1 + \alpha_s(E)/\pi) \frac{1}{1 + \exp[(E_0 - E)/\delta]}, \quad (2.19)$$

where now $E_0 = 1.1$ GeV and $\delta = 0.2$ GeV. The experimental error on the ϕ contribution is about 3%, but about 20% for the continuum.

In spite of completely different final hadronic states

¹⁰There will, of course, be some ambiguity in these definitions, if the resonance is broad.

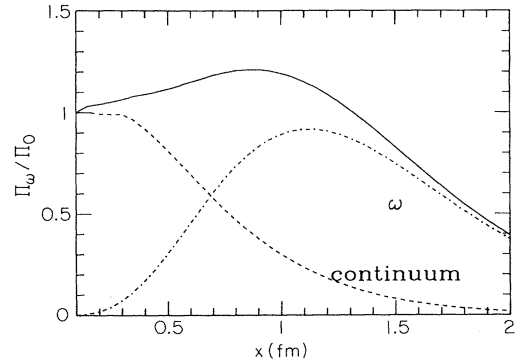


FIG. 4. Same as in Fig. 2, but for the $I=0$ vector correlator, the ω channel.

and a much smaller cross section, the correlator in the ω channel is similar to the ρ correlator. Figure 2 for the ρ channel and Fig. 4 for ω agree to within uncertainties, and the only difference between them appears at distances as large as about 2 fm!

To understand what this phenomenon means, let us look at the difference between the ρ and ω correlators. As the former current has the $\bar{u}u - \bar{d}d$ flavor structure, and the latter $\bar{u}u + \bar{d}d$, this difference is the vector flavor-changing correlator

$$K_{ud}^V(x) = \langle \bar{u} \gamma_{\mu} u(x) \bar{d} \gamma_{\mu} d(0) \rangle = 2(\Pi_{\omega, \mu\mu} - \Pi_{\rho, \mu\mu}). \quad (2.20)$$

Thus the data presented above tell us that this amplitude is for some reason extremely small. Unfortunately, we do not really know how small it is at intermediate distances, up to 1 fm or so, because it is within the experimental uncertainties. Only at distances as large as 2 fm does the difference between the ω and ρ correlators become clearly observable. It means that the flavor-changing correlation function (2.20) becomes comparable to the flavor-diagonal ones¹¹ only when the latter drops by many orders of magnitude.

There are two more striking experimental observations that suggest that the famous Zweig rule, forbidding the flavor-changing transitions, is indeed surprisingly strict in the vector channels: (1) the ρ - ω mass difference is only 12 MeV; (2) the ω - ϕ mixing angle is only $1^\circ - 3^\circ$.

No general reasons for such strong suppression of flavor-changing transitions in vector channels are known, although some interesting hints have been suggested. In particular, a perturbative analysis leads to the idea that in the vector case one needs at least three gluons in the intermediate state, not two as in the pseudoscalar case. However, this argument should not be applicable to distances of the order of 1 fm and beyond. In this respect,

¹¹We show below that for pseudoscalar correlators such deviation happens at much smaller distances, where the correlation function is about four orders of magnitude larger.

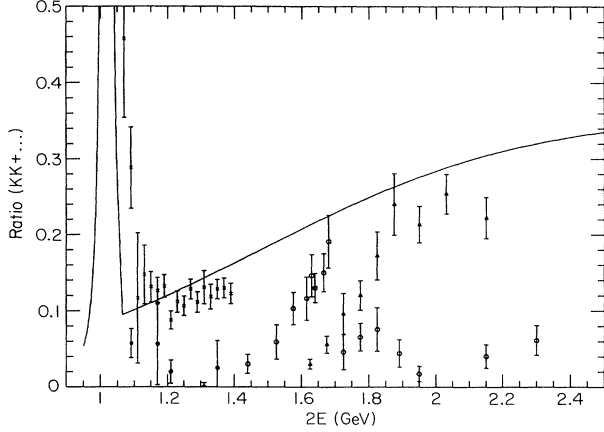


FIG. 5. Same as in Fig. 1, but for the channels containing a pair of K mesons. The points marked by crosses, closed dots, open dots, and triangles correspond to the following final states: K^+K^- (Ivanov *et al.*, 1981); $K_S^0K_L^0, K_S^0K^- \pi^+ + K_S^0K^+ \pi^-$ (Mané *et al.*, 1982); and $K^+K^- \pi^+ \pi^-$ (Cordier *et al.*, 1982b), respectively. The solid curve is our fit to their sum. We do not show the fit near the top of the ϕ peak (which in this case is very high, R being about 50), because it is perfect there.

an important observation can be made from nonperturbative considerations to be discussed later (Sec. III.C). It is that vector and axial channels do not have a direct instanton contribution in first order in 't Hooft interaction, in contrast to pseudoscalar and scalar ones. However, this argument also cannot account for the smallness of this transition up to very large distances, where multi-instanton effects become important.

Now we show one more figure related to e^+e^- annihilation experiments, Fig. 5, which presents the cross section of the production of channels with $\bar{K}K$ plus pions. We assume in this case that the $\bar{s}\gamma_\mu s$ current dominates in strangeness production, which may not be well justified. As above, we do not display the fit near the top of the ϕ peak, because it is nearly perfect; the maximal value is $R_\phi \sim 50$. Instead we show how our fit reproduces the sum of all other contributions, shown by the solid line. The parametrization used here was

$$\frac{B(\tau \rightarrow \nu_\tau + K^*)}{B(\tau \rightarrow \nu_\tau + \rho)} = \tan^2(\theta_c) \left[\frac{f_{K^*}}{f_\rho} \right]^2 \frac{(1 - m_{K^*}^2/m_\tau^2)^2 (1 + 2m_{K^*}^2/m_\tau^2)}{(1 - m_\rho^2/m_\tau^2)^2 (1 + 2m_\rho^2/m_\tau^2)}, \quad (2.22)$$

where θ_c is the Cabibbo angle. Inserting on the left-hand side the experimental ratio 0.0143 ± 0.0031 (from *Review of Particle Properties*, Hernández *et al.*, 1990), one obtains the following ratio of the coupling constants:

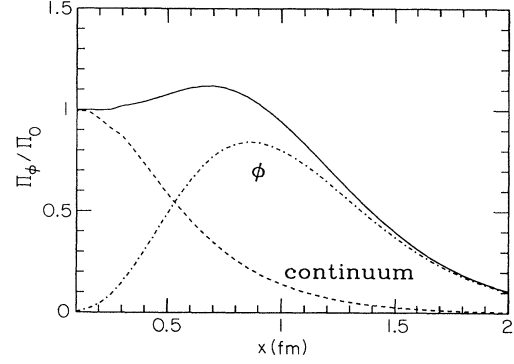


FIG. 6. Same as in Fig. 2, but for the ϕ correlator.

$$R_\phi(E) = \frac{52.4}{1 + 4(E - m_\phi)^2/\Gamma_\phi^2} + \frac{1}{\frac{1}{3}(1 + \alpha_s(E)/\pi) \frac{1}{1 + \exp[(E_0 - E)/\delta]}}, \quad (2.21)$$

where $E_0 = 1.5$ GeV and $\delta = 0.4$ GeV.

Finally, we present in Fig. 6 the correlator $\Pi_\phi(x)/\Pi_{\text{free}}(x)$, which is also surprisingly similar¹² to the ρ, ω correlators shown above.

D. Strange vector (or K^*) channel

For completeness, let us also consider the strange vector channel. Here the current is $j_{K^*} = \bar{u}\gamma_\mu s$ and the lowest meson is the $K^*(892)$. Phenomenological analysis in this case is not based on electromagnetic processes, but rather on the vector part of weak currents. The data come in this case from the weak decay process $\tau \rightarrow \nu_\tau + \text{hadrons}$. Since the hadrons are produced from a virtual W instead of virtual photon, we obtain an admixture of the strange current from the Cabibbo mixing of the weak current.

Comparing the Cabibbo suppressed production of K^* to the Cabibbo allowed production of ρ in this decay, one can obtain the following relation,

$$\frac{f_{K^*}}{f_\rho} = 1.1 \pm 0.1. \quad (2.23)$$

We do not have sufficient information about the cross

¹²Here our presentation is somewhat illogical, because we still measure the correlator in units of $\Pi_{\mu\mu}^{\text{free}}$, corresponding to the free propagation of massless quarks. The decrease of $R_\phi(x)$ with distance is partly kinematical, due to nonzero strange quark mass. We have not included this correction, in order to make comparison with nonstrange correlators in the same figure.

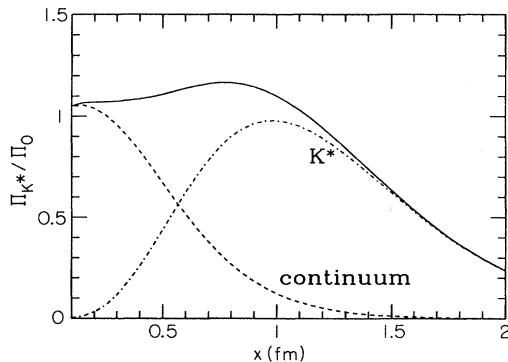


FIG. 7. Same as in Fig. 2, but for the K^* correlator.

section of weak production of nonresonance states with such quantum numbers, K and pions. In addition, the τ lepton mass sets a rather restrictive limit on the available energy. However, one can still make some arguments based on spectroscopic data. Indeed, in the strange vector channel there are two primed resonances, at 1415 and 1715 MeV, very much similar to two ρ' resonances near 1600 MeV. We shall thus assume that the nonresonance part of both K^* and ρ cross sections are similar. Therefore the same nonresonant contribution as that for the ρ channel will be taken in the parametrization, scaled, of course, to a different limit at infinite energies.

The corresponding curves for $\Pi_{K^*}/\Pi_{\text{free}}(x)$ are given in Fig. 7. The resulting curve fits perfectly between the ρ and ϕ curves discussed above, suggesting that all these completely different sets of data are, in fact, deeply connected to each other.

E. Axial $I=1$ (or A_1) channel

Now we turn from vector to axial-vector channels, concentrating on the $I=1$ channel. This has the quantum numbers of the A_1 meson and is related to the following current:

$$j_\mu^{A_1} = \bar{u} \gamma_\mu \gamma_5 d. \quad (2.24)$$

Data corresponding to this channel are also obtainable from the τ lepton decay into the corresponding neutrino and hadrons, because the weak current has both vector and axial components. Since we deal with the charge current associated with the W exchange, we do not have an $I=0$ component; so production of odd numbers of pions is now entirely due to the axial part of the current.¹³

¹³Decays into neutrino and an even number of pions are, as in the e^+e^- annihilation, related to the vector ρ -type current. The corresponding data are consistent with the e^+e^- annihilation data, although they are much less accurate.

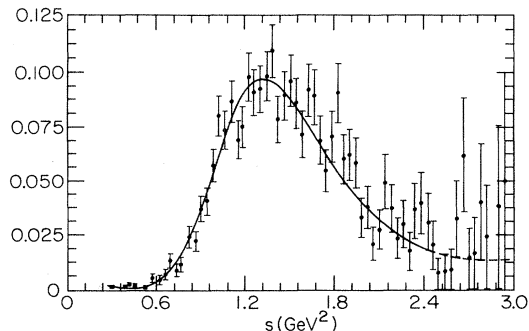


FIG. 8. Contribution of the 3π channels to the spectral density of the axial current, measured in the τ lepton decay by the ARGUS Collaboration (Albrecht *et al.*, 1986; the five-pion one is small and rather uncertain). The curve is just a parametrization used in the theoretical paper by Peccei and Sola (1987), from which we took this figure, and it is not used here.

The experimentally measured distribution into three pions as a function of their invariant mass is shown in Fig. 8. The asymmetric peak around 1.2 GeV is the contribution of the A_1 meson.¹⁴ Its dominance is also confirmed by the observation that two channels with three pions, $\pi^-\pi^-\pi^+$ and $\pi^0\pi^0\pi^-$, have branching ratios (of all $\tau \rightarrow \nu_\tau + \text{hadrons}$ decays) equal to $(6.8 \pm 0.6)\%$ and $(7.5 \pm 0.9)\%$, respectively. They are equal within uncertainties, and this is precisely what should be the case if they are dominated by A_1 decays. For those reasons, we treat the peak seen in the τ decays as an “effective” A_1 meson.

Let us introduce coupling constants f_{A_1} similar to those of vector resonances:

$$\langle 0 | \bar{d} \gamma_\mu \gamma_5 u | A_1 \rangle = f_{A_1} m_{A_1} \epsilon_\mu. \quad (2.25)$$

From the experimental branching ratios and the theoretical equation

$$\frac{B(\tau \rightarrow \nu_\tau + A_1)}{B(\tau \rightarrow \nu_\tau + \rho)} = \left(\frac{f_{A_1}}{f_\rho} \right)^2 \frac{(1 - m_{A_1}^2/m_\tau^2)^2 (1 + 2m_{A_1}^2/m_\tau^2)}{(1 - m_\rho^2/m_\tau^2)^2 (1 + 2m_\rho^2/m_\tau^2)}, \quad (2.26)$$

one deduces a value for the coupling constant,

$$f_{A_1}/f_\rho = 1.0 \pm 0.07. \quad (2.27)$$

Having fixed the resonance contribution, we next

¹⁴The A_1 shape observed in the τ decay and hadronic reactions is somewhat different. This point is discussed in Isgur (1989), which also contains further references. The data shown in Fig. 8 seem to suggest an admixture of some nonresonance background at the largest energies, but the errors are still too large to allow any definite conclusions.

proceed to the continuum states at larger invariant masses. Unfortunately, the τ lepton is not heavy enough to produce final states in the asymptotic region; direct observation of the axial spectral density is limited by its mass, 1784 MeV. Moreover, as one can see from Fig. 8, the statistics of the existing experiments are only good up to $s^{1/2} \approx 1.4-1.5$ GeV. Therefore we do not see the most interesting region in which spectral density approaches its asymptotic limit.

However, we have some general arguments that allow one to fix the continuum contribution with reasonably small uncertainties. First, in the chiral limit, the following inequality has been proven¹⁵ (Witten, 1983):

$$\Pi_{\mu\mu}^{\rho}(q^2) - \Pi_{\mu\mu}^{A_1}(q^2) \geq 0 \quad (\text{for all } q^2 < 0). \quad (2.28)$$

This condition should become an equality at large $|q^2|$ because the $O(1/q^2)$ terms, corresponding to the $O(1/x^2)$ terms in the coordinate representation of the correlators, should be the same for vector and axial correlators in the chiral limit. This statement is known as the second Weinberg sum rule¹⁶ (Weinberg, 1967):

$$\int ds (\text{Im}\Pi_{\mu\mu}^{A_1} - \text{Im}\Pi_{\mu\mu}^{\rho}) = 0. \quad (2.29)$$

As the resonance contribution is proportional to $m_{A_1}^2 f_{A_1}^2 - m_{\rho}^2 f_{\rho}^2 > 0$, the contribution of the nonresonance continuum should be negative. Assuming our previous parametrization of the continuum, we may therefore conclude that asymptotic freedom in the axial channel should be recovered at larger energies, $E_0^{A_1} > E_0^{\rho}$, which is indeed the case. The sum rule (2.29) is satisfied at $E_0^{A_1} \approx 1.5$ GeV, if we use the same shape as that used for the ρ case, with $\delta = 0.2$ GeV. This is quite a firm prediction, provided the shape of the continuum spectrum is the same. However, to show the sensitivity of the correlator to this uncertainty, we shall display two curves for the axial correlator, with $E_0^{A_1} = 1.5$ and 1.7 GeV. For a more detailed discussion of the axial spectral density, including, in particular, its relation to $m_{\pi^+} - m_{\pi^0}$, see Peci and Sola (1987).

Before plotting the correlation function, let us also clarify a theoretical point related to a general form of the axial correlators. If chiral symmetry were exact, with all quark masses zero, the nonsinglet axial currents would be conserved. Because of that, one might think that the Fourier transform of their correlators would have only a

transverse part, namely,

$$\Pi_{\mu\nu}^A(a) \sim (q_{\mu}q_{\nu} - g_{\mu\nu}q^2). \quad (2.30)$$

This is not the case. The existence of a Goldstone mode, the massless pion, coupled to the axial current, produces, in addition, a longitudinal contribution:

$$\Pi_{\mu\nu}^A(q) = \Pi_L(q^2)(q_{\mu}q_{\nu} - g_{\mu\nu}q^2) + f_{\pi}^2 q_{\mu}q_{\nu}/q^2. \quad (2.31)$$

In the coordinate representation, the second term just gives a singularity at $x=0$, which does not spoil current conservation.

Now we proceed further, discussing the real world in which quark masses are nonzero. We still have a longitudinal part due to a pion contribution, which now depends on x as $\partial_{\mu}\partial_{\nu}D(m_{\pi},x)$. Taking the divergence ∂_{μ} (or contracting indices $\mu\nu$), we obtain $\partial^2 D(m_{\pi},x) = -m_{\pi}^2 D(m_{\pi},x) + \text{contact term}$. Now we have a longitudinal contribution, nontrivially depending on distance, but it is proportional to m_{π}^2 . This result is not unexpected: although in the real world the axial current is not conserved, its divergence is $O(m_q) = O(m_{\pi}^2)$.

The conclusion from these theoretical considerations is that one can partially get rid of the pion signal in the A_1 correlation function by simply contracting the indices on the correlator. This will also make better contact to the correlators for the vector channels. The contraction leads to the following approximate relation for the axial correlator:

$$\begin{aligned} \Pi_{\mu\mu}^A(\tau) &= 3f_A^2 m_A^2 D(m_A, \tau) + f_{\pi}^2 m_{\pi}^2 D(m_{\pi}, \tau) \\ &+ \frac{3}{4\pi} \int dE E^3 D(E, \tau) \frac{1 + \alpha_s(E)/\pi}{1 + \exp[(E_0 - E)/\delta]}. \end{aligned} \quad (2.32)$$

The first two terms are the contributions of the A_1 and the π , and the third term is the nonresonant continuum. The latter is expressed in our usual way, with a perturbative contribution starting at some E_0 , taken to be 1.5 or 1.7 GeV. As before, we took $\delta = 0.2$ GeV.

Now everything is fixed, and the resulting correlator is shown in Fig. 9. Comparing it with the ρ correlator in Fig. 2, one observes that it has a completely different shape. The A_1 contribution can be slightly larger than the ρ one at small x (again, because $f_A^2 m_A^2 > f_{\rho}^2 m_{\rho}^2$), but at larger distances it drops due to larger A_1 mass. Eventually, at large x , the axial correlator grows again, due to the long-range pion contribution.

Finally let us emphasize that the difference between the vector and axial correlators is entirely due to the chiral asymmetry of the QCD vacuum. By studying how this difference develops as a function of distance, one can hope to learn something about the mechanisms creating this asymmetry.

¹⁵The author is indebted to S. Nussinov for bringing this theorem to his attention.

¹⁶This statement can be derived from the fact that, in the chiral limit, the only dimension-4 scalar operator is a gluonic field strength squared, which contributes the same amount to vector and axial correlators (see Sec. III.B). However, for nonzero quark masses, there appear contributions of the type $m_q \bar{q}q$, different for vector and axial correlators.

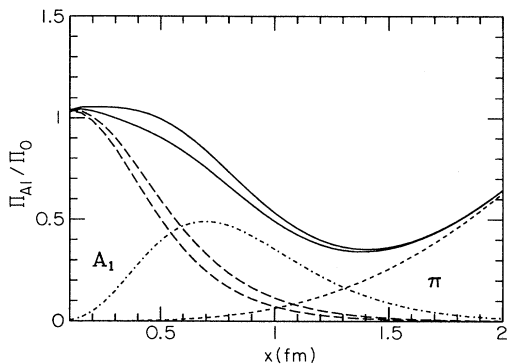


FIG. 9. Same as in Fig. 2, but for the axial current. The dot-dashed line is the contribution of the A_1 meson, while the short-dashed one is that of the pion. Two long-dashed lines show the contribution of the nonresonance continuum, if its threshold is $E_0=1.5$ or 1.7 GeV. Two solid lines show the sums of all contributions in these two cases; the true correlator is somewhere between them.

F. Pseudoscalar correlation functions for the SU(3) octet (the π, K, η channels)

Here we consider correlations of the octet pseudoscalar quark-antiquark operators

$$j_\pi = (i/2^{1/2})(\bar{u}\gamma^5 u - \bar{d}\gamma^5 d), \quad (2.33)$$

$$j_K = i\bar{u}\gamma^5 s, \quad (2.34)$$

$$j_\eta = (i/6^{1/2})(\bar{u}\gamma^5 u + \bar{d}\gamma^5 d - 2\bar{s}\gamma^5 s). \quad (2.35)$$

These correlators are very important for the understanding of QCD vacuum structure. One might naively think that because the pseudoscalars are the lowest excitations of the QCD vacuum, they tell us primarily about its long-range structure. However, as we shall see shortly, they also provide much puzzling information about its short-range structure as well.

Generally speaking, the pseudoscalar and scalar mesons are rather exceptional members of the family of hadrons. There are some surprisingly large numbers attached to them; in particular, the coupling constants to the corresponding currents are very large. Therefore the contributions of these particles to the correlators are also important at small x .

Before we come to correlation functions, some general comments about pseudoscalars are in order. Throughout the history of hadronic physics, from naive nonrelativistic quark models to modern lattice calculations, some puzzles related to these particles have presented difficulties, and they are in many cases still unexplained. New, surprising facts are revealed if one considers the correlation functions.

The well-known observation that the pion is extraordinarily light was, in fact, explained in classical works of the '60s, even before QCD was discovered: it is a Goldstone mode associated with chiral symmetry. In QCD

terms, its mass is small due to the near vanishing of the light quark masses. This subject is reviewed in detail by Gasser and Leutwyler (1987), which also has original references.

However, taking a closer look at this problem, one arrives at the opposite puzzling conclusion: the pion is surprisingly heavy, given the light quark masses. Indeed, the pion mass can be written as

$$m_\pi^2 = (m_u + m_d)K, \quad (2.36)$$

where the constant K is nonzero in the chiral limit. This constant is related to the quark condensate and the pion-decay constant $f_\pi = 2^{1/2}F_\pi = 131$ MeV by the famous relation (Gell-Mann, Oakes, and Renner, 1968)

$$K = 2|\langle \bar{u}u \rangle|/f_\pi^2. \quad (2.37)$$

We do not present its derivation here and only note that the standard values of the quark masses¹⁷ are (Gasser and Leutwyler, 1987)

$$m_d \approx 7 \text{ MeV}, \quad m_u \approx 4 \text{ MeV}. \quad (2.38)$$

One then finds a very large value of this constant associated with the quark condensate: $K \approx 1700$ MeV.¹⁸ Masses are external to QCD, but the value of K is an internal problem, which should be explained by QCD. We formulate this question in a slightly more general way as the first puzzle: (1) *Why are the masses of the pseudoscalar octet mesons so sensitive to small quark masses?*

The second well-known puzzle related to the pseudoscalar channels is the famous Weinberg (1975) " $U_A(1)$ problem," which is related to the SU(3) singlet channel and the η' meson. Ignoring the u, d quark masses and considering only the effect of m_s , one can easily see that chiral perturbation theory predicts η' to be lighter than the η meson: the former has $\frac{1}{3}$ of the "strange" component, while the latter has $\frac{2}{3}$ of it.¹⁹ Experimentally, $m_{\eta'} \approx 958$ MeV, which is much larger than these naive estimates. Let us now formulate this problem somewhat more generally: (2) *Why is the singlet channel so much*

¹⁷Quark masses are not physical, but are instead a kind of theoretical parameter; so their values depend on their exact definition. In particular, they have perturbative anomalous dimensions; so the numbers depend on "resolution" (normalization point μ_0) used. For example, speaking about bare quark masses in the lattice Lagrangian, one has resolution on the scale of lattice spacing $\mu_0 = a^{-1}$. The numbers mentioned correspond to the scale $\mu_0 = 1$ GeV.

¹⁸Accuracy of these "standard" numbers depends on whether extrapolation of chiral perturbation theory is good for the strange quark; see details in Gasser and Leutwyler (1987).

¹⁹We simplify discussion of this point for pedagogical reasons. The reader may consult the original paper (Weinberg, 1975) for his estimates of the upper limit of the η' , with and without $O(m_s)$ effects.

different from the octet ones? What is the mechanism responsible for this splitting?

The third problem we address is also an old one, related to the fact that in pseudoscalar channel we do not see even a trace of the Zweig rule. Namely, flavor changing is not suppressed in this channel, but rather enhanced: (3) *Why isn't the strange sector in the pseudoscalar multiplet separated from the nonstrange one, as in other multiplets? What is the mechanism of these mixings?*

We now proceed to discussion of the pseudoscalar correlation functions. The main point is that the coupling constants of the mesons to the pseudoscalar currents also can be expressed in terms of known parameters. For example, starting with the definition of the pion-decay constant

$$\langle 0 | \bar{u} \gamma_\mu \gamma_5 d | \pi, p_\mu \rangle = i f_\pi p_\mu, \quad (2.39)$$

one takes the divergence of the axial current and obtains

$$(m_u + m_d) \langle 0 | \bar{u} i \gamma_5 d | \pi, p_\mu \rangle = f_\pi m_\pi^2, \quad (2.40)$$

from which one obtains the needed pseudoscalar coupling constants

$$\lambda_\pi = \langle 0 | \bar{u} i \gamma_5 d | \pi, p_\mu \rangle = f_\pi K \approx (480 \text{ MeV})^2. \quad (2.41)$$

This λ_π is a large quantity, due to the large value of the factor K . This in turn can be traced to a large value of the quark condensate.

The axial current matrix element to the K meson is known from its weak decays, and the decay constant is

$$f_K \approx 1.24 f_\pi. \quad (2.42)$$

We shall extrapolate from the π and K cases to the η -decay constant with

$$f_\eta \approx \frac{4}{3} f_K - \frac{1}{3} f_\pi \approx 1.32 f_\pi. \quad (2.43)$$

We obtained this formula assuming that the deviations from the SU(3) symmetry were due to strangeness. The η is $\frac{2}{3}$ strange, while the K is only $\frac{1}{2}$ strange.

So far we only have information about π , K , η contributions to the axial correlators. However, in order to obtain their contributions to the pseudoscalar ones, we have to make additional assumptions. Here we assume that they scale in a way similar to the decay constants²⁰:

$$\lambda_K / \lambda_\pi \sim f_K / f_\pi, \lambda_\eta / \lambda_\pi \sim f_\eta / f_\pi. \quad (2.44)$$

In Fig. 10 we show the resulting π , K , and η pseudoscalar correlators in the form $K(x)/K_{\text{free}}(x)$. Apart from resonance contributions, we assumed a nonresonance continuum and selected a value $E_0 \approx 1.6$ GeV to smoothly bring the ratio to unity at small distances. In fact, the

²⁰In any case, a 10–20 % level of accuracy is good enough for most of our conclusions here, and at this level all couplings can just be considered as equal.

ambiguity in the E_0 value is important only in a very small window at about $x = 0.2$ fm.

Note the marked difference compared to the vector correlators considered above: instead of changes within 10–20 % in the region $x \sim 1$ fm, the ratio K/K_{free} has changed by two orders of magnitude.

The general reason for this behavior is the well-known feature of pseudoscalar mesons, that they are exceptionally light. In terms of $\bar{q}q$ interaction, this behavior implies that there is a strong attraction between quark and the antiquark in this channel, forcing them to move in a correlated manner. As a result, the correlation function is larger than the perturbative one.

Note also that up to distances of the order of 0.5 fm, there is no marked difference between the three curves, which implies that all effects proportional to the strange quark mass are irrelevant in this region. In fact, the heavier mesons have slightly larger couplings, making the curves for different channels even more similar.

Surprisingly, due to contributions from these lowest mesons alone, asymptotic freedom is violated at very small distances, about $\frac{1}{5}$ fm. This fact, noticed in Novikov *et al.* (1981), deserves to be considered as another general puzzle: (4) *Why do deviations from the perturbative behavior start at such small distances in the pseudoscalar channels?*

G. The SU(3) singlet correlation functions: axial, pseudoscalar, and gluonic ones

The SU(3) singlet channel, called η' for brevity, is traditionally discussed in relation to the axial current

$$j_{\eta'}^\mu = (\bar{u} \gamma^5 \gamma_\mu u + \bar{d} \gamma^5 \gamma_\mu d + \bar{s} \gamma^5 \gamma_\mu s) / 3^{1/2}. \quad (2.45)$$

Its matrix element is connected to $f_{\eta'}$ in the usual way:

$$\langle 0 | j_{\eta'}^\mu | \eta' \rangle = i f_{\eta'} k_\mu. \quad (2.46)$$

This axial current is subject to the famous Adler-Bell-Jackiw anomaly (Adler, 1969; Bell and Jackiw, 1969), which means that its divergence is not just proportional to the quark masses, but it also contains a gluonic operator²¹:

$$\partial_\mu j_{\eta'}^\mu = 3^{1/2} \left[2i m_s \bar{s} \gamma_5 s + \frac{3g^2}{16\pi^2} G\tilde{G} \right]. \quad (2.47)$$

In the above equation $G\tilde{G} \equiv \frac{1}{2} \epsilon_{\alpha\beta\mu\nu} G_{\alpha\beta} G_{\mu\nu}$ is the contraction of the gluonic field strength with its dual, analogous to $E \cdot B$ in electromagnetism.

Therefore, sandwiching this relation between vacuum and η' states, one does not find a direct relation between the couplings to pseudoscalar and axial currents $\lambda_{\eta'}$ and $f_{\eta'}$.

²¹Contributions proportional to the light quark masses are ignored here.

Several estimates of $f_{\eta'}$ have been put forward by Novikov *et al.* (1980), all suggesting it to be smaller than f_{π} :

$$f_{\eta'} = (0.5 - 0.7) f_{\pi}. \quad (2.48)$$

The simplest estimate is related to the J/ψ radiative decay, which is also important because it provides some direct information about the matrix elements of the gluonic operator entering the anomaly (Novikov *et al.*, 1980). Indeed, if the charmed quarks are sufficiently heavy, one can describe the $\bar{c}c$ annihilation in terms of local operators. We do not need to go into detail here, but only comment that, for the decays $J/\psi \rightarrow \gamma +$ pseudoscalar meson, one has to deal with the lowest-dimension²² pseudoscalar gluonic operator $G\tilde{G}$. The exact coefficient of this operator in the effective Lagrangian is irrelevant, because we shall only consider ratios of the decay probabilities:

$$\frac{\Gamma(\psi \rightarrow \gamma \eta')}{\Gamma(\psi \rightarrow \gamma \eta)} = \left| \frac{\langle 0 | G\tilde{G} | \eta' \rangle}{\langle 0 | G\tilde{G} | \eta \rangle} \right|^2 \left[\frac{p_{\eta'}}{p_{\eta}} \right]^3. \quad (2.49)$$

The last factor is the phase-space ratio for P -wave decays. Experimentally the left-hand-side ratio is 4.9 ± 0.5 ,²³ from which one finds the ratio of the matrix elements to be

$$\frac{\langle 0 | G\tilde{G} | \eta' \rangle}{\langle 0 | G\tilde{G} | \eta \rangle} = 2.46 \pm 0.1. \quad (2.50)$$

Since that work was published, another large contribution in radiative decay of ψ has been found, that of the decay into photon and $\eta(1430)$ (originally called ι). Repeating the same argument, one obtains an even slightly larger²⁴ matrix element for this particle:

$$\frac{\langle 0 | G\tilde{G} | \eta(1430) \rangle}{\langle 0 | G\tilde{G} | \eta' \rangle} = 1.12 \pm 0.2 \quad (2.51)$$

In order to evaluate the absolute magnitude of all these matrix elements, Novikov *et al.* (1980) proposed to sandwich the anomaly relation (2.47) between the vacuum and the η state. If the latter is an ideal member of the SU(3) octet,²⁵ it should vanish because the current is an SU(3) singlet. Thus one should have an exact cancellation between the $O(m_s)$ and anomalous parts, implying

$$\begin{aligned} \frac{3g^2}{16\pi^2} \langle 0 | G\tilde{G} | \eta \rangle &= -2im_s \langle 0 | \bar{s}\gamma_5 s | \eta \rangle \\ &= \left(\frac{3}{2}\right)^{1/2} f_{\eta} m_{\eta}^2. \end{aligned} \quad (2.52)$$

This fixes the absolute scale of these matrix elements. Now, ignoring the $O(m_s)$ term, we obtain the value for the coupling constant, $f_{\eta'} \approx 0.74 f_{\pi}$.

Armed with this information, let us return to the correlation functions. Unfortunately, the coupling constant of the pseudoscalar SU(3) singlet current remains unknown. Nevertheless, just for the sake of comparison with other pseudoscalar correlators, we have also plotted in Fig. 10 the η' contribution, making an ‘‘educated guess’’ based on the ratio of $f_{\eta'}/f_{\pi}$ just derived, $\lambda_{\eta'} \approx 0.74 \lambda_{\pi}$.

Whatever are the uncertainties in this coupling, a qualitative difference between the SU(3) octet and the singlet correlators is obvious. Even if the singlet $\Pi(x)/\Pi_{\text{free}}(x)$ is flat up to $x \sim 0.5$ fm, the splitting between them seems to begin at $x_{\text{splitting}} \sim 0.2$ fm. In the whole interval of intermediate distances $x = 0.3 - 1.5$ fm, the singlet correlation function is about one order of magnitude smaller than the η correlator.

Now we switch to another interesting subject: the correlation functions of the pseudoscalar gluonic operators. Generally, we know very little about them; we do not even have reliable experimental information about glueball masses. Heated discussions on whether particular hadronic resonances are glueballs take place at specialized conferences on hadronic spectroscopy, and we cannot go into this question here.

Let us make only a general comment that all glueball candidates are rather heavy, with masses in the region 1.5–2 GeV. This is qualitatively consistent with LGT

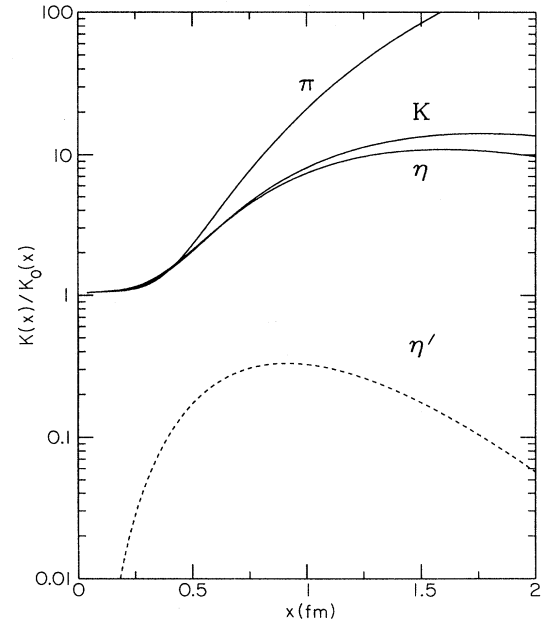


FIG. 10. Normalized pseudoscalar correlation functions vs distance x (in fm). The three solid lines show the π, K, η channels, while the dashed line corresponds to the contribution of the η' meson into the SU(3) singlet correlator.

²²Others are suppressed by powers of m_c .

²³These numbers are from Hernández *et al.* (1990).

²⁴Actually, this is an even lower limit of the matrix element, since the decay ratio branching into $\gamma \eta(1440)$ that we use actually contains the branching ratio of $\eta(1440) \rightarrow \bar{K}K \pi$.

²⁵In fact, the $\eta - \eta'$ mixing angle is approximately $\theta_{\text{mixing}} \approx 10^\circ - 20^\circ$ and corrections are very small, $O(\theta_{\text{mixing}}^2)$.

(lattice gauge theory) calculations [see reviews in Lattice 88 (1989), Lattice 89 (1990), Lattice 90 (1991), and Teraflop (1992)]. Quenched calculations also suggest that the lightest glueball is the scalar, with a mass of about 1.3–1.5 GeV, while pseudoscalars are about twice as heavy. Of course, results may be modified in calculations going beyond the quenched approximation.

The general question of why all glueballs have completely different mass scale, distinct from those typical of hadrons made of quarks, remains essentially unanswered.²⁶

The really relevant question is the contribution of various hadronic states to gluonic correlation functions, independent of whether or not we call them glueballs. From our discussion above we obtained several matrix elements of the pseudoscalar gluonic operator. Our estimates discussed above lead to

$$\begin{aligned} \langle 0|G\tilde{G}|\eta\rangle &\approx 0.9 \text{ GeV}^3, & \langle 0|G\tilde{G}|\eta'\rangle &\approx 2.2 \text{ GeV}^3, \\ \langle 0|G\tilde{G}|\eta(1440)\rangle &\approx 2.9 \text{ GeV}^3, \end{aligned} \quad (2.53)$$

where we have also taken α to be “frozen” at $\alpha_s \approx 0.3$. It is tempting to examine the contribution of these three states to the pseudoscalar gluonic correlation function. As before, in order to get an idea of whether the matrix elements obtained are large or small, it is instructive to normalize this contribution to the asymptotically free gluonic contribution, which is equal to

$$K_0(x) = \langle 0|G\tilde{G}(x)G\tilde{G}(0)|0\rangle = \frac{9(N_c^2 - 1)}{\pi^4 x^8}. \quad (2.54)$$

This equation is derived by propagating two gluons from point 0 to x . The x dependence is obvious, since the gluon operator $G\tilde{G}$ has mass dimension 4. Apart from the color factor, the formula is the same as in quantum electrodynamics.

The estimated contributions of the η 's to the gluon correlator are shown in Fig. 11. We see that the η' and $\eta(1440)$ matrix elements found above are indeed comparable to the perturbative ones already at distances as small as $\frac{1}{4}$ fm. Moreover, they become about an order of magnitude larger at only slightly larger distances.

It is amusing to note that the η' and $\eta(1440)$ together contribute to the gluonic pseudoscalar correlator in a way very similar to the π, K, η contributions to quark pseudoscalar current. The general tendency of a rapid rise suggests a strong attraction in this channel, starting at about the same distances.

One may further speculate that the “true gluonic

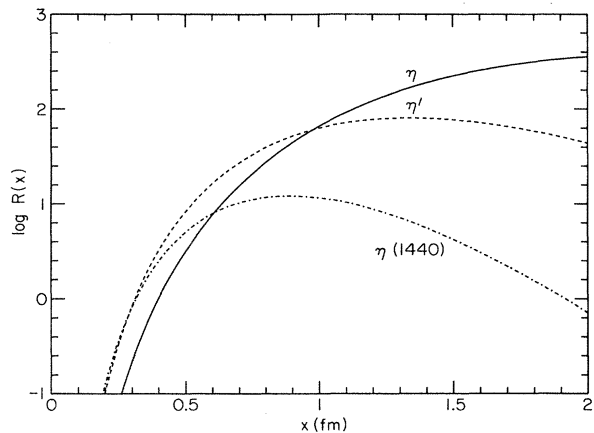


FIG. 11. Normalized pseudoscalar gluonic correlation function to that corresponding to the propagation of two free gluons. Three curves correspond to the contributions of $\eta, \eta', \eta(1440)$ mesons, respectively.

states” contribute roughly an amount that causes the $K(x)/K_{\text{free}}(x)$ ratio to level off at 1 for $x < \frac{1}{4}$ fm. If so, the threshold E_0 is expected to be rather high, of the order 2 GeV or so. In principle, one can tell whether it is true or not from studies of the radiative decay $\Upsilon \rightarrow \gamma + \text{hadrons(s)}$, in which hadronic systems with corresponding invariant mass are produced. Moreover, the local annihilation hypothesis is even better fulfilled here than for charmed quarks.

H. General properties of the scalar correlators

We conclude our survey of the phenomenology of the QCD correlation functions with some remarks about the scalar correlation functions.

From the phenomenological side the situation is far from clear. Historically, the first candidate for scalar mesons was the famous enhancement seen in the isoscalar $\pi\pi$ scattering near 500 MeV, known in literature as the “sigma meson.” This name was also used in the “sigma el” (Gell-Mann and Levi, 1960), in which the scalar particle is essentially the “radial” ($I=0$) oscillation of the quark condensate. It is not recognized as resonance, but still can be strongly coupled to the scalar $I=0$ current.

The next scalar mesons are isovector and isoscalar pairs of particles, $f_0(975)$ and $a_0(980)$. Their close masses and particular decay modes have led to the suspicion that they are not regular $\bar{q}q$ mesons, but rather four-body $\bar{q}q\bar{q}q$ mesons containing “intrinsic strangeness.”²⁷ This latter observation makes it very improbable that they play any role in the spectral density of non-strange quark currents $\bar{u}u, \bar{d}d$.

²⁶In fact, in the interacting instanton approximation the difference in mass scales is quite natural. In the IIA the quark and the gluon fields have completely different roles and different distribution in space-time. The former are distributed more or less homogeneously, while glue is concentrated in small spots of the strong field, the instantons.

²⁷The interested reader can consult the proceedings of any conference on hadronic spectroscopy, where this topic is repeatedly discussed.

The $I=0$ scalar channel has two more resonances listed in the *Review of Particle Properties*, the $f_0(1400)$ and $f_0(1590)$. The former decays predominantly into two pions and can therefore be plausibly assigned as a non-strange $\bar{q}q$ meson.²⁸

The $f_0(1590)$ was produced diffractively in one experiment only, and it has a very interesting dominant mode, $\eta'\eta$, in spite of the fact that it is very much suppressed by small phase space. Taking into account its production mechanism and specific decay pattern, with a “gluonic touch,” we see that it is a good candidate for scalar gluonium. Its mass value also fits well with what quenched lattice data tell us (see, e.g., Teraflop, 1992). Unfortunately, there are problems with this interpretation of $f_0(1590)$: in particular, there are strong experimental limitations on $J/\psi \rightarrow \gamma + \eta'\eta$. If correct, they imply that this particle cannot have a sufficiently strong coupling to the gluonic operator $\langle 0|G^2|f_0(1590)\rangle$.

No isovector scalar resonances (other than a_0 mentioned) are in the *Review of Particle Properties*; so one has to conclude that such mesons probably do not exist, or they are too heavy and wide.

Let us now discuss the qualitative behavior of scalar correlation functions. In the $I=1$ channel, $K(x)/K_{\text{free}}(x)$ should strongly fall off with x , because the lowest intermediate state has a mass of at least 1 GeV or more. In the $I=0$ channel the situation is different, because the correlation function

$$K_{\text{scalar}, I=0}(x) = \langle \bar{q}q(x)\bar{q}q(0) \rangle \quad (2.55)$$

possesses the factorizable contribution, $\langle \bar{q}q \rangle^2$, which does not fall off at large distances. Large mesonic masses in this case mean that transition to this region should be rather sharp.

Our point now is that it is possible to guess at what distances this transition takes place just by comparison of perturbative contributions. In terms of the ratio we usually use, $K(x)/K_{\text{free}}$, it means a rapid increase starting from the point where

$$K_{\text{scalar}, I=0}(x)/K_{\text{free}}(x) = \pi^4 \langle \bar{\psi}\psi \rangle^2 x^6 / 3 \sim 1. \quad (2.56)$$

This estimate tells us that this curve probably turns up starting from rather small distances, about $\frac{1}{3}$ fm (which is again related to and from a rather large magnitude of the quark condensate).

Summarizing, we have two important observations: one expects the curve for $K(x)/K_{\text{free}}$ (a) to curve up in the $I=0$ [or the SU(3) singlet] scalar case, but (b) to curve down in the $I=1$ [or the SU(3) octet] case. In other terms, one expects the existence of some attraction in the singlet and a repulsion in the octet channel. Let us now compare these conclusions with the behavior of the pseudoscalar channels. Note that their behavior is exact-

ly the opposite: a similar ratio (c) goes up for the octet (π, K, η), but (d) goes down for the singlet (η') case.

Let us reformulate these four statements in terms of somewhat different correlation functions. Considering for simplicity u, d quarks only, we define instead of the four previous correlation functions, scalar and pseudoscalar with $I=0$ and 1, the following linear combinations:

$$K_{++} = \bar{u}_L u_R \bar{u}_R u_L + \bar{d}_L d_R \bar{d}_R d_L, \quad (2.57)$$

$$K_{+-} = \bar{u}_L u_R \bar{u}_L u_R + \bar{d}_R d_L \bar{d}_R d_L, \quad (2.58)$$

$$K_{-+} = \bar{u}_L u_R \bar{d}_R d_L + \bar{d}_L d_R \bar{u}_R u_L, \quad (2.59)$$

$$K_{--} = \bar{u}_L u_R \bar{d}_L d_R + \bar{u}_R u_L \bar{d}_R d_L. \quad (2.60)$$

Here L, R stand for left and right chirality. The notations are as follows: the first \pm index here corresponds to flavor, the second to chirality, (+) means this quark property remains unchanged, (−) means it is changed. At small distances the dominant contribution comes from free-quark propagation, which corresponds to dominant K_{++} .

Based on the discussion above of both scalars and pseudoscalar correlators, with $I=0, 1$, one may reach two important conclusions: (1) The qualitative behavior of those correlation functions is consistent with the assumptions that the dominant term producing splitting in parity and isospin is K_{--} ; and (2) deviations from asymptotic freedom are much more radical than those in vector and axial channels, and they show up at much smaller distances, $x \approx \frac{1}{4} - \frac{1}{3}$ fm.

Consequences of these observations will be discussed in the next section, and we note here only that the K_{--} amplitude corresponds exactly to the quantum numbers of the instanton-induced 't Hooft interaction.

III. THEORY OF MESONIC CORRELATION FUNCTIONS

A. Potential models and heavy quarkonia

This section is somewhat separate from the others, because it applies to the physics of heavy quarks only. We have included it mainly for pedagogical reasons: here one can use simple nonrelativistic language based on the interaction potential between quarks, which, we hope, will make the discussion clear.

Our main goal is to show how studies of the correlation functions may help to reveal information that is nearly impossible to get from an analysis of stationary states. This discussion is based on a paper (Shuryak and Zhirov, 1987) that attempted to find experimental evidence for a strong Coulomb law.

Very heavy quarks and antiquarks form nonrelativistic bound states similar to positronium, with the interaction described by a Coulomb-type potential (Appelquist and Politzer, 1975). The force is as fundamental as a

²⁸However, the sigma meson of the sigma model (Gell-Mann and Levi, 1960) should be much wider at this mass.

Coulomb law of electrodynamics or the Newton law of gravity; so it is certainly worth trying to measure it more precisely. In fact, QCD does not predict exactly a Coulomb law, because of the running coupling constant, which effectively depends on the distance between quarks. The equation derived in Appelquist and Politzer (1975) for the potential is

$$V_{\text{QCD}} = -\frac{4}{3} \frac{\alpha_s(R)}{R} \\ = -\frac{8\pi}{(11N_c - 2N_f)\ln[1/(R\Lambda_{\text{Coulomb}})]} \frac{1}{R}, \quad (3.1)$$

where N_c and N_f are the number of colors and flavors. Note that this potential contains a parameter Λ_{Coulomb} . Its measurement is crucial for setting the absolute scale in QCD, which is also needed for lattice calculations (discussed below).²⁹ Heavy quarkonium is in principle an ideal place to measure the QCD scale, because the potential is perturbative in nature but still produces large observable effects.

Unfortunately, neither c nor even b quarks are heavy enough for this simple idea to be applicable. However, these mesons are very well described by an effective potential $V_{\text{eff}}(r)$, a combination of confining and Coulomb forces. To be specific, let us consider two potentials used: the Martin potential (Martin, 1981)

$$V = 6.87R^{0.1} + \text{const}, \quad (3.2)$$

and the Cornell potential (Eichten *et al.*, 1980)

$$V = -0.52/R + 0.18R, \quad (3.3)$$

where in the last two formulas all units are GeV or inverse GeV. Both potentials give about equally good descriptions of all states in the J/ψ and Υ families. However, the Martin potential has no Coulomb term at all! From this experts in quarkonium spectroscopy have concluded that there is not yet any direct evidence for a strong Coulomb law.

Now comes the main idea: if the stationary states, J/ψ and Υ mesons, are not small enough to be a Coulomb system, why not consider a virtual system, a wave packet of any desirable size? In particular, one can discuss a correlation function in which quarks propagate any distance (or Euclidean time) we want.

As for the light quarks already considered, these correlation functions can be recalculated from experimental data on e^+e^- annihilation into heavy quarks. What is important is that these data contain not only resonances (the upsilons), but also a continuum of excited states above the heavy quark-antiquark threshold. Therefore one can obtain information not only about lowest bound states, but also about the unbound (or scattering) states.

Realizing all this, let us consider a correlator of two vector currents made of b quarks placed at the same spatial point and separated by the Euclidean time τ . It is connected to the experimentally measurable cross section mentioned above by the following formula³⁰:

$$K(\tau) = \frac{3}{16\pi^3\alpha^2 e_b^2} \int ds s^2 \sigma_{e^+e^- \rightarrow \bar{b}b}(s) D(s^{1/2}, \tau). \quad (3.4)$$

We evaluate this using the following equation for the cross section,

$$\sigma_{e^+e^- \rightarrow \bar{b}b}(s) = \sum_{\Upsilon_s} (12\pi^2 \Gamma_{\Upsilon}/M_{\Upsilon}) \delta(s - M_{\Upsilon}^2) \\ + (4\pi\alpha^2/3s) R_b \theta(s - s_0). \quad (3.5)$$

The partial widths and masses of the four upsilon states are taken from *Particle Data Table*; s_0 is the threshold of the open beauty production, $(2m_B)^2$; and the constant R_b is taken from the averaged data to be $R_b = 0.31 \pm 0.06$, consistent with the free-quark value $R_b = \frac{1}{3}$ just above the threshold. Putting all this into the equation above, we obtain the ‘‘experimental’’ correlation function plotted in Fig. 12. This shows the logarithmic derivative

$$F(\tau) = -\frac{d}{d\tau} \ln \frac{K(\tau)}{K_{\text{free}}(\tau)}, \quad (3.6)$$

where $K_{\text{free}}(\tau)$ corresponds to free propagation of the $\bar{b}b$ pair.³¹ The function $K(\tau)$ decays very strongly, due to factors like $\exp(-2m_b\tau)$; so it is more informative to plot the logarithm. By definition, if the interaction potential is absent, $F(\tau)$ is just zero. Its physical meaning is, roughly speaking, the mean energy of the wave packet existing during the Euclidean time period τ .

The function $F(\tau)$ obtained in this way is shown in Fig. 12 by the dashed region (representing experimental error bars). Although the experimental accuracy is not very good, one can see that this function is decreasing toward the small τ , which, of course, means that some attraction is present at small distances. Thus one does observe a manifestation of the strong Coulomb law.

At this point we are finished with our phenomenological input and come to theoretical predictions. In the nonrelativistic case, with a potential-type interaction $V(R)$, this can be done just by solving the ordinary Schrödinger equation for the Green’s function with this potential. Another practical way to do it (Shuryak and Zhurov, 1987) is based on the equation

$$\frac{K(\tau)}{K_{\text{free}}(\tau)} = \left\langle \exp \left[- \int d\tau V[|\mathbf{r}_Q(\tau) - \mathbf{r}_{\bar{Q}}(\tau)|] \right] \right\rangle_{\text{free paths}}. \quad (3.7)$$

²⁹Some recent work done in the direction of fixing the scale from charmonium physics can be found in Mackenzie (1991).

³⁰In fact, in the nonrelativistic domain under consideration, $\tau m \gg 1$, the propagator can be taken in the nonrelativistic limit, $D(M, \tau) \sim M^{1/2} \tau^{-3/2} \exp(-M\tau)$.

³¹The b quark mass was taken to be 4.9 GeV.

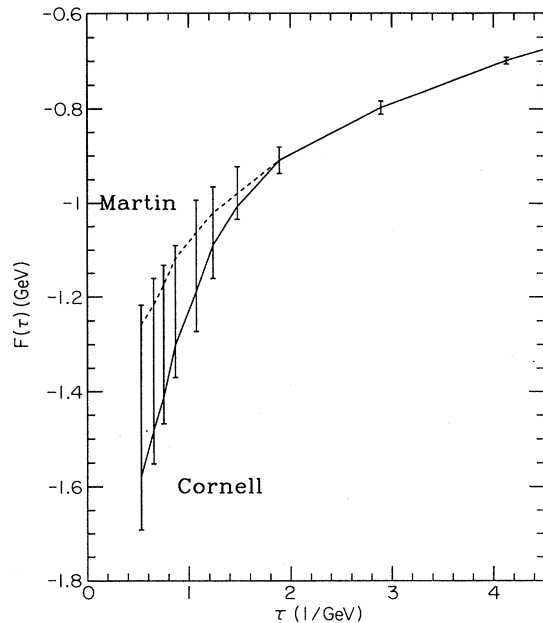


FIG. 12. $F(\tau) = -d \log(K/K_{\text{free}})/d\tau$, where $K(\tau)$ is the vector $\bar{b}b$ (or Y) correlation function, K_{free} is its version corresponding to free propagation of b quarks with a mass $m_b = 4.9$ GeV, and τ is Euclidean time (in GeV^{-1}). The error bars show $F(\tau)$ as derived from experimental data (see text). The more negative values of this quantity at small τ correspond to stronger Coulomb forces at smaller distances between quarks. The solid line corresponds to the Cornell potential, and the dashed line to the Martin one.

Here one averages the exponential “interaction factor” over an ensemble of quantum paths, corresponding to the motion of free quarks.

We have calculated this correlator using the two phenomenological potentials given above. The resulting curves are also shown in Fig. 12. Although the experimental accuracy is not really good enough to make a conclusion, it appears that these data show some preference for the Cornell potential over the Martin one. Improvement in the quality of the data, especially in the measurement of the actual shape of the nonresonance continuum containing a pair of b -flavored hadrons, can clarify this important issue.

Perspectives of $\bar{t}t$ spectroscopy is an interesting subject, which we now address briefly. Because the t quark mass is at least 100–150 GeV or more, its weak decay is too rapid to allow the Coulomb bound states to show up as a set of narrow resonances. However, even if the separate toponium states cannot be seen as well-separated peaks, by integrating the corresponding cross section as above and calculating the correlation function, one may still observe its derivation from that expected for free-moving t quarks and detect a trace of Coulomb-induced effects. This may provide a method to measure Λ_{QCD} .

We conclude this section with a question. It is known

that essentially the same potentials as those used above for heavy quarks produce a reasonable description of the overall spectroscopy of the strange and even of the light mesons and baryons (Capstick, Godfrey, Isgur, and Paton, 1986). It is only necessary to introduce a phenomenological “constituent” quark mass for the light quarks. It would be interesting to know whether such an approach could reproduce the correlation functions associated with the light quarks, especially at smaller distances.

B. Operator product expansion and QCD sum rules

In this section we turn from the simple potential models to a much more complicated approach, that of applying the operator product expansion to correlation functions at small distances. We present only a few important examples of its applications, but actually about a hundred papers have been written on this topic, and it has been reviewed by Novikov *et al.* (1982, 1984), Shuryak (1984, 1988a), Reinders *et al.* (1985), and Shifman (1992).

The general idea (Wilson, 1969) is an expansion of the bilocal operator

$$j(x)j(0) = \sum_n C_n(x) O_n(0) \quad (3.8)$$

in terms of local operators. Here the $C_n(x)$ are coefficients, depending on the distance between the points, and the $O_n(0)$ are operators. If one deals with ordinary functions, one might think of a Taylor-series expansion of $J(x)$ in powers of x , but the dependence on x is quite singular in quantum field theory. However, in massless QCD the powers of x are just determined by dimensional arguments, except for some nontrivial powers of $\ln(x)$.

A formal definition of the OPE is based on a separation between the high-momentum and soft momentum modes of the quantum fields involved. The operators O_n contain a cutoff μ so that they only couple to soft modes, with Euclidean momentum $p^2 < \mu^2$. The coefficients C_n absorb all hard modes of the fields, i.e., those with momenta $p^2 > \mu^2$. If the value of μ is changed, the whole expansion is redefined, however, the sum remains the same, because μ is just an artificial parameter without any physical significance.

There are no averaging symbols in this equation; the expansion is assumed to be valid for any matrix element of this equation. In particular, we may average it over the vacuum state, of course, but the equality should hold for any configuration of the fields separately. We cannot go deeper into the theoretical discussion here, but refer those interested to a recent compilation of main papers (Shifman, 1992), which also has further references.

Two technical points should be noted here. First, since unrenormalized QCD with massless quarks has no di-

mensional parameters,³² the coefficients $C_n(x)$ are just powers of x , depending on the dimension of the corresponding operator O_n . For example, if one deals with the product of two currents, one has an object of total mass dimension 6. Suppose one is interested in the coefficient of gluonic operator $O = (G_{\mu\nu}^a)^2$, which has dimension 4. Without calculations, one sees that the corresponding coefficient must have an x dependence $C_{G^2}(x) \sim 1/x^2$.

Our second remark is that, in practice, people have used a somewhat different form of the OPE, namely, the expansion of the Fourier transform of the correlators $K_{\text{mom}}(Q^2)$ in powers of $1/Q^2$, where Q is the momentum transfer. Roughly speaking, large Q corresponds to small x , but not exactly. Suppose, for example, one has a term proportional to $(1/Q^2)^n$ and takes its Fourier transform. Then, for $n \geq 2$, one gets the power of x^2 dictated by naive dimensional counting times the $\ln(x^2)$. In fact, this logarithm is present because all contributions that are regular at $x=0$, i.e., proportional to $(x^2)^n$ without logarithms, are missing in this approach.³³

The existence of terms regular at $x=0$ is one of the reasons why people in the past avoided the use of coordinate representation. We return to this point at the end of this section.

Let us first show some examples of how the Shifman, Vainshtein, and Zakharov (SVZ) approach works in the space-time representation. Derivation of the formulas can be found in the original papers (Shifman, Vainshtein, and Zakharov, 1979b) or in reviews (e.g., Reinders *et al.*, 1985; Shuryak, 1988a; Shifman, 1992). For clarity, we omit some terms that are, in practice, unimportant, like the $m_q \bar{q}q$ operators. We also did not include the lengthy expressions for higher-dimension operators, because they are not actually used in applications.

In Euclidean time τ , which is the same as the spatial distance x used before, the normalized correlation functions for ρ and A_1 channels are given by (Shifman *et al.*, 1979b):

$$\begin{aligned} \Pi_{\mu\mu}^{\rho, A_1}(\tau) / \Pi_{\mu\mu}^{\text{free}}(\tau) = & 1 + \frac{\alpha_s(\tau)}{\pi} \frac{\langle (gG_{\mu\nu}^a)^2 \rangle \tau^4}{3 \times 2^7} \\ & + \frac{\pi^2 \tau^6}{16} \ln \frac{1}{\tau\mu} \langle O_{\rho, A_1} \rangle + \dots \end{aligned} \quad (3.9)$$

The complicated four-fermionic operators O_{ρ, A_1} are different for the vector and axial channels and are given

by

$$\begin{aligned} O_{\rho} = & \frac{\pi\alpha_s}{2} (\bar{u}\gamma_{\mu}\gamma_5 t^a u - \bar{d}\gamma_{\mu}\gamma_5 t^a d)^2 \\ & + \frac{\pi\alpha_s}{9} (\bar{u}\gamma_{\mu} t^a u + \bar{d}\gamma_{\mu} t^a d) \left[\sum_q \bar{q}\gamma_{\mu} t^a q \right], \end{aligned} \quad (3.10)$$

$$\begin{aligned} O_{A_1} = & O_{\rho} + 2\pi\alpha_s (\bar{u}_L\gamma_{\mu} t^a u_L - \bar{d}_L\gamma_{\mu} t^a d_L) \\ & \times (\bar{u}_R\gamma_{\mu} t^a u_R - \bar{d}_R\gamma_{\mu} t^a d_R), \end{aligned} \quad (3.11)$$

where R, L denote right- and left-hand polarization on the quarks.

Estimates of vacuum expectation values of the above operators were made using the so-called vacuum dominance hypothesis (Shifman *et al.*, 1979b).³⁴ The recipe is as follows: one should try to transform this operator into a product of two scalars, and just include the vacuum state in the sum over intermediate states between the two scalar operators. The vacuum expectation of the scalar will be nonzero if there is a quark condensate, and it is evaluated as such.

For the operators mentioned above the answer is (Shifman *et al.*, 1979b)

$$\langle O_{\rho} \rangle \approx (7 \times 2^4 \pi / 3^4) \alpha_s \langle \bar{\psi}\psi \rangle^2, \quad (3.12)$$

$$\langle O_{A_1} \rangle \approx -(2^5 \pi / 3^4) \alpha_s \langle \bar{\psi}\psi \rangle^2, \quad (3.13)$$

where $\langle \bar{\psi}\psi \rangle$ is the quark condensate. Note that these two expressions have opposite signs.

We can see how well this works in Fig. 13. The phenomenological correlation functions of the previous section are shown by the solid curves, and the OPE predictions by dashed curves. The curves marked ρ, SVZ and A_1, SVZ correspond to the above expression, and, in particular, the short-dashed line shows the OPE prediction, including perturbative and gluon condensate corrections. One can see that the general behavior of these correlation functions is reproduced surprisingly well up to distances of about $\frac{1}{2}$ fm. In particular, (1) the splitting between the vector and axial $I=1$ channels happens exactly in the right place, and (2) the magnitude of the splitting is also correct. Both observations show that the estimates of the vacuum expectation values of these two four-fermion operators are probably reliable.³⁵ As a third point, note that in the vector case the quark and gluon corrections nearly compensate each other, so that

³²Radiative corrections produce terms containing a dimensional parameter Λ_{QCD} , but only in the form of some powers of $\ln(x\Lambda_{\text{QCD}})$, the so-called anomalous dimensions. Since these complications are not very important for our discussion, we shall not introduce them, for the sake of simplicity of presentation.

³³Their Fourier transform is $K_{\text{mom}}(Q^2) \sim \exp(-Q \times \text{const})$, and such terms are more difficult to trace.

³⁴The accuracy of this estimate is an interesting question that can be addressed with lattice data, the IIA, and other vacuum models. The IIA (Shuryak, 1989b) strongly contradicts the vacuum dominance hypothesis for gluonic operators, but more or less agrees with it for the operators in Eqs. (3.10) and (3.11).

³⁵The general discrepancy between OPE curves and experimental ones, about 10% in absolute normalization, may well be due to higher-order radiative corrections. They are also comparable to the experimental uncertainties in the axial channel.

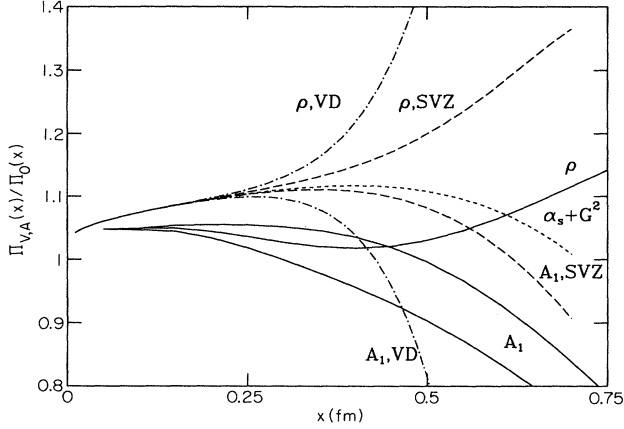


FIG. 13. Ratio of the correlation function to that corresponding to a free-quark propagation vs distance x (fm). One solid line shows the ρ contribution, and two solid lines for the A_1 correspond to experimental data as in Fig. 9. Other curves are different versions of the OPE. The short-dashed line shows the perturbative correction and that due to the gluon condensate: those are the same for both channels. The long-dashed lines marked ρ, SVZ and A_1, SVZ correspond to $1/Q$ expansion, while the dot-dashed ones marked ρ, VD and A_1, VD include regular terms as well.

at least the beginning of superduality is reproduced.

Encouraged by this success, let us look at the pseudoscalar channels. The OPE expression for the pseudoscalar correlators was also given by Shifman *et al.* (1979b). In coordinate representation the correlator can be written as

$$\begin{aligned} \Pi_\pi(\tau)/\Pi_{\text{free}}(\tau) &= 1 + \alpha_s(\tau)/\pi + \langle (gG_{\mu\nu}^a)^2 \rangle \tau^4/384 \\ &+ (\pi^2/48)\tau^6 \ln \frac{1}{\tau\lambda} \langle O_1 + O_2 \rangle, \end{aligned} \quad (3.14)$$

where the four-fermion operators are defined as follows:

$$O_1 = -\pi\alpha_s(\bar{u}\sigma_{\mu\nu}t^a u)(\bar{d}\sigma_{\mu\nu}t^a d) \quad (3.15)$$

$$\begin{aligned} O_2 &= (\pi\alpha_s/2)[(\bar{u}\sigma_{\mu\nu}t^a u)^2 + (\bar{d}\sigma_{\mu\nu}t^a d)^2] \\ &+ (\pi\alpha_s/3)[(\bar{u}\gamma_\mu t^a u)(\Sigma_q \bar{q}\gamma_\mu t^a q)]. \end{aligned} \quad (3.16)$$

The expectation values of these operator products are evaluated according to the vacuum dominance hypothesis, and the main one is³⁶

$$\langle O_2 \rangle \approx (56\pi/27)\alpha_s \langle \bar{\psi}\psi \rangle^2. \quad (3.17)$$

³⁶The operator O_1 , estimated in the same way, has a smaller matrix element. We have separated O_1 because it is the operator that obtains contribution from instanton zero modes. In the instanton liquid model, its vacuum expectation value is actually several times larger than that for O_2 (Shuryak, 1983), but it still does not contribute enough to make a good description of the data.

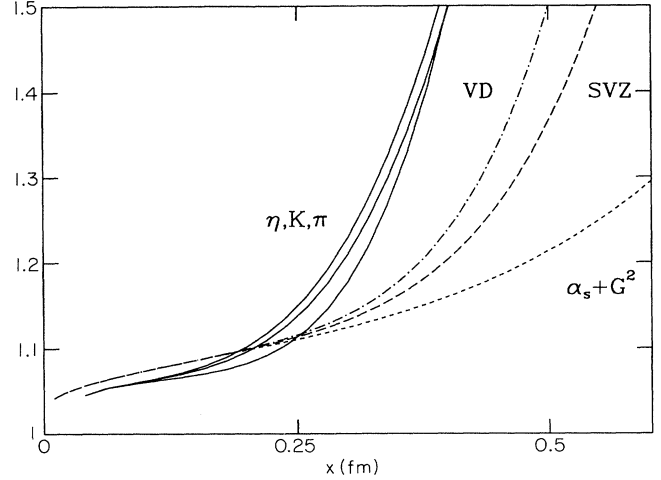


FIG. 14. Same as Fig. 13, but for the pseudoscalar channel. The three solid lines close together correspond to the π , K , and η phenomenological correlators, respectively.

The resulting curves are compared to phenomenological ones for π, K, η mesons in Fig. 14. One sees that the SVZ results have “good intentions” in the sense that the predicted behavior looks similar to the experimental trend, but numerically these effects are too small to reproduce the experimental data. (Remember, coming from $x \sim \frac{1}{4}$ fm to $\frac{1}{2}$ fm means correlators being reduced by $\sim 2^6 = 64$.)

This failure was discussed in the important paper by Novikov *et al.* (1981) entitled “Are all hadrons alike?” The suggested answer was that all spin-zero correlation functions are special: new, important effects show up in these cases, which are not seen in the OPE framework. Attempts to understand how this could come about have led to the instanton theory discussed in the next section.

However, before we go into it, we can take one more step forward. It was noticed at the beginning of this section that the SVZ expressions ignore the part of the correlation functions that is nonsingular at $x=0$. The natural question is what corrections can arise due to them. In fact, the theory of regular terms is even simpler than that of singular ones. In particular, it is not difficult to understand that the constant term at $x \rightarrow 0$ is nothing but the current squared: $K_{\text{regular}}(x \rightarrow 0) = \langle j^2(0) \rangle$. One can also easily evaluate their vacuum expectation values in the same vacuum dominance approximation, gaining some insight into the effect of those regular terms. Moreover, as all currents considered in this section have the simple flavor structure $\bar{u}d$, two quark lines do not mix and one can obtain all $O(\langle \bar{\psi}\psi \rangle^2)$ corrections by using the quark propagator in the form³⁷ $S = S_0 + \frac{1}{12} \langle \bar{\psi}\psi \rangle$. The re-

³⁷This simple way of implementing the vacuum dominance was first used by Ioffe in treating the baryonic sum rules. We come to them in the next section.

sults look as follows:

$$\Pi_{\mu\mu}^{\rho}(\tau)/\Pi_{\mu\mu}^{\text{free}}(\tau) = 1 + \frac{\pi^4 \tau^6}{18} \langle \bar{\psi}\psi \rangle^2, \quad (3.18)$$

$$\Pi_{\mu\mu}^{A_1}(\tau)/\Pi_{\mu\mu}^{\text{free}}(\tau) = 1 - \frac{\pi^4 \tau^6}{18} \langle \bar{\psi}\psi \rangle^2, \quad (3.19)$$

$$\Pi_{\pi}(\tau)/\Pi_{\text{free}}(\tau) = 1 + \frac{\pi^4 \tau^6}{36} \langle \bar{\psi}\psi \rangle^2 \quad (3.20)$$

$$\Pi_{\text{scalar}}(\tau)/\Pi_{\text{free}}(\tau) = 1 - \frac{\pi^4 \tau^6}{36} \langle \bar{\psi}\psi \rangle^2. \quad (3.21)$$

These corrections are added to the SVZ terms discussed above and shown as the dot-dashed curves in Figs. 13 and 14 marked VD (vacuum dominance). We see that in all channels these corrections have signs coinciding with experimental trends. However, the quantitative comparison is not at all satisfactory: although inclusion of the regular corrections makes disagreement in the pseudoscalar case somewhat smaller, it also worsens the agreement in the vector and axial channels.

In summary, the OPE can be used in two forms: as $1/Q$ expansion in momentum space and x expansion in space-time, the latter possessing extra regular terms. Supplemented by the vacuum dominance hypothesis, it predicts correct qualitative behavior of correlators, but it is not able to reproduce them quantitatively.

C. Interacting instanton approximation

A detailed discussion of the theory of instantons and related phenomena cannot be made here. We simply outline the main steps of the development of this theory (presenting the references), then briefly consider some qualitative features of the instanton-induced effects to first order in the instanton-induced 't Hooft effective Lagrangian, defined in Eq. (3.22). After that, jumping over a decade of work, we proceed directly to the particular predictions, including all orders, in this interaction. We end with a brief discussion of the connections between the IIA and lattice data.

Since the discovery of the instanton solution in non-Abelian gauge theories (Belavin, Polyakov, Schwartz, and Tyupkin, 1975), they have been believed to be an important ingredient of strong-interaction physics. Early applications to hadronic physics are discussed in Callan, Dashen, and Gross (1978). The theory is very elegant, using semiclassical theory related to the physics of tunneling.

However, instanton-induced effects appeared to be “too strong” in the following sense: only a few effects, such as the short-distance deviation from asymptotic freedom discussed below, could be understood from a first-order treatment of instantons. Other properties of QCD, such as hadronic masses and coupling constants, could be described only by including many instantons interacting with each other. That is why only recently has

it become possible to create a consistent approximation³⁸ treating the interacting instantons (IIA, for short), which both includes 't Hooft effective interaction to all orders and is simple enough to make calculations practical.

The main steps in the development of this theory were as follows. Phenomenological discussions pioneered by Geshkenbein and Ioffe (1980) and Novikov *et al.* (1981) eventually led to the “instanton liquid model” (Shuryak, 1982a, 1983, through which the qualitative picture of the ensemble of interacting pseudoparticles was significantly clarified. Surprisingly enough, essentially the same picture emerged from the variational approach to the “instanton liquid” (Diakonov and Petrov, 1984). Encouraged by this agreement, much effort was devoted to the study of the approximations involved in this analysis and to the development of a more quantitative theory. A straightforward numerical solution was obtained by the present author (Shuryak, 1988b), who then applied the approximation to the calculation of various mesonic correlation functions (Shuryak, 1989a, 1989c, 1989d. These results are discussed below.

Let us now briefly introduce the reader to some qualitative features of the instanton-induced effects. The main physical phenomenon, a tunneling through a barrier separating gauge fields of different topology, was shown ('t Hooft, 1976) to be related to specific rearrangements of the light quark states: some of them “dive into the Dirac sea” during this process, and some others emerge from it. Without going into details, let us only mention that the tunneling between gauge fields is described by the 't Hooft effective Lagrangian, which has the structure

$$L_{\text{eff}} \sim \sum_f (\bar{q}_f \psi_0) (\bar{\psi}_0 q_f). \quad (3.22)$$

Here q_f is a quark field of flavor f ($f = u, d, s$), while ψ_0 is the so-called fermionic zero mode, a solution of the Dirac equation $\hat{D}\psi_0(x) = 0$ in the field of the instanton. These zero modes play the role of wave functions of quark states, in which they are produced or absorbed during the tunneling; they depend in a known way on collective variables of the instanton.³⁹ Important for us is the following fact: these zero modes have chirality, directly related to the topological charge of the gauge field: there is only a left-handed solution for the instantons and a right-handed one for the anti-instanton. Thus the quark

³⁸The status of this activity is somewhat intermediate between what is usually called a “model” and a “theory.” Unlike the “instanton liquid model” of the early '80s, now it does not contain any model-dependent elements; its statistical sum is, in principle, directly derived from QCD. But it is also not a complete theory: it is restricted to the sum over gauge-field configurations of a certain type, a superposition of some number of instantons and anti-instantons.

³⁹There are 12 collective degrees of freedom in QCD: the size ρ , the four-dimensional position of the instanton center, and seven (out of eight) color rotation angles.

Lagrangian generated by a single instanton or anti-instanton has an effective interaction like $\bar{q} \frac{L}{f} q_f^R$ (or $R \leftrightarrow L$), but never $\bar{\psi} \frac{L}{f} \psi_f^L$ (or $\bar{\psi} \frac{R}{f} \psi_f^R$). The Dirac structure of the helicity-flip interaction contributes only to scalar and pseudoscalar correlators. Noting also the specific flavor-changing structure of this Lagrangian, we find that the interaction has the following important properties:

(1) The first-order corrections in the 't Hooft effective interaction are present in the scalar and pseudoscalar correlators, but absent in the vector and axial ones.

(2) These corrections have the opposite sign for the scalar and pseudoscalar channels.

(3) These corrections have the opposite sign for the isospin 1 and 0 channels.

All three points are welcomed to reconcile the disagreements in the previous section. The first point accounts for the nature of the disagreement in the pseudoscalar case, while preserving the good agreement for the axial and vector cases. The last two points show how this interaction has exactly the structure of the amplitude K_{--} , which was demanded at the end of Sec. II to provide a qualitative explanation of the behavior of all four spin-zero correlators. Unfortunately, one can use the first-order results only at small distances, where the instanton-induced effects are small corrections to the perturbative correlation functions.

To go beyond the first-order effects, one can numerically model an ensemble of interacting instantons, using a partition function of the form

$$Z = \int \Pi_i [d\Omega_i \exp(-S_i)] \exp(S_{\text{int}}) \Pi_{f=1, N_f} [\det(i\hat{D} + im_f)]. \quad (3.23)$$

Here we have denoted by $d\Omega_i$ the measure in space of collective coordinates of the i th instanton. $S_i = 8\pi^2/g^2(\rho_i)$ is the action corresponding to individual instantons. S_{int} describes the classical (gluonic) interaction between instantons and anti-instantons. At large distances it is known to be a dipole interaction (Callan *et al.*, 1978), but at finite distances this quantity requires a specific definition. Starting with Diakonov and Petrov (1984), a set of trial functions of growing complexity was used (Shuryak, 1988c). However, the most natural collective coordinates for the instanton-anti-instanton problem can be obtained by "descending down the valley" (Shuryak, 1988d), solving the so-called streamline equation (Yung, 1988). This was done for gauge fields in Verbaarschot (1991), where one can find a detailed discussion of this interaction.⁴⁰

The last (and the most complicated) factor in (3.23) is the so-called fermionic determinant, which describes

quark-induced interactions. It is evaluated by division into two terms, that due to zero and nonzero modes. The former can be written as the $N \times N$ matrix in the so-called zero-mode subspace, where N is the number of instantons (and anti-instantons) considered. Its determinant is evaluated directly for each configuration, which is equivalent to inclusion of all diagrams in the 't Hooft interaction to N th order.

This system is somehow more complicated than the traditional systems considered in statistical mechanics: the fermion determinant induces a very nonlocal interaction. Therefore in simulations one has to deal with about 20–60 instantons. The question of whether or not chiral symmetry is broken becomes a matter of calculation, similar to the question of whether a collection of atoms behaves as a conductor or an insulator. The situation is also complicated by the fact that the ensemble of instantons is not "frozen" into a periodic structure, but remains liquid-like. However, this problem still is enormously simpler than lattice gauge theory. In fact, one needs only about 10 parameters to describe field in the volume 1 fm^4 , instead of 10^5 or more used for the same purpose in current lattice calculations. We also have some evidence that these variables are in fact the main ones (see below).

After this brief introduction, a sample of results is in order. In Fig. 15 the $I=1$ mesonic correlation functions presented in Shuryak (1989a, 1989b, 1989c, 1989d) are shown, in the form of $\Pi_i(x)/\Pi_{\text{free}}(x)$. Qualitative behavior of all correlators agrees well with our discussion. In particular, there is strong attraction in the octet pseudoscalar case, causing the curve to go up starting from rath-

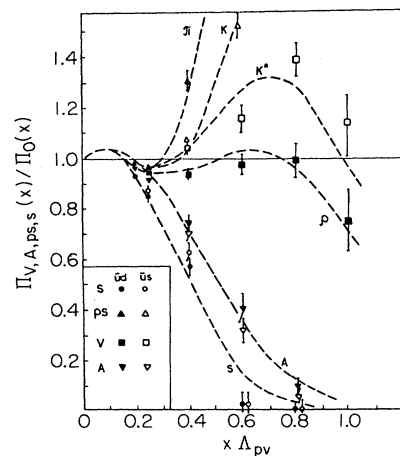


FIG. 15. Ratio of the various correlation functions to that corresponding to the free-quark propagation vs distance $x\Lambda_{PV}$ (normalized to the Pauli-Villars Λ_{PV} parameter, roughly in fm). The points correspond to the calculation in the IIA framework (Shuryak, 1989a) for scalar (S), pseudoscalar (PS), vector (V), and axial (A) channels with the flavor structure $\bar{u}d, \bar{u}s$ (closed and open points, respectively). The dashed curves are the three-parameter fit described in the text.

⁴⁰Recently this interaction has attracted much attention in connection with possible baryon number violation by weak interaction (see Khoze and Ringwald, 1991; Shuryak and Verbaarschot, 1992).

er small distances. There is very good superduality in the vector channels. No resonance, it is amusing to note, is needed to fit the scalar channel: the correlator found is consistent with just a continuum threshold at sufficiently high masses. This prediction is intriguing in its correlation with phenomenology.

Moreover, the results are in quantitative agreement with the data. The dashed curves are the three parameter fits for the data points, with resonance mass m , its coupling, f , and continuum threshold E_0 obtained for each channel.⁴¹ Further studies of a wide set of correlation functions in the IIA are now in progress.

Let us now briefly discuss connections between IIA and LGT. In order to see the instantons in LGT, one must “cool” the lattice configurations of gauge fields by damping out the quantum fluctuations. This leaves a configuration of only classical gauge fields, which can be examined. Kremer *et al.* (1988) have shown that the classical fields remaining after cooling are essentially the instantons, and their density is roughly comparable to what is used in the IIA. Second, these instantons are related to fermionic zero modes, which strongly contribute to the quark condensate (Hands and Teper, 1990). Third, it was recently found (Chu and Huang, 1991) that cooling affects the correlation functions surprisingly weakly; so hadronic masses and coupling constants determined from the full QCD and from the cooled, instanton-dominated configurations are practically the same. However, these studies are in their initial stages and the accuracy of the numerical results should be improved. Further references on studying the IIA with lattice methods may be found in the recent lattice conference proceedings [Lattice 90 (1991); Teraflop 1992].

We conclude this section by listing the main phenomena that can be explained using the IIA:

(1) We found that the IIA accounts for the chiral symmetry breaking of the QCD vacuum, including the value of the quark condensate (Shuryak, 1989b) at $T=0$, as well as for the chiral symmetry restoration at higher temperatures (Ilgenfritz and Shuryak, 1989).

(2) As will be discussed in Secs. IV.A and IV.B, the IIA produces an effective mass for the quark of about 300–400 MeV. This is the constituent quark, the main building block of all hadronic masses.

(3) The IIA gives the absolute magnitude and quantum numbers of $\bar{q}q$ effective interaction at small distances, especially in the scalar and pseudoscalar channels.

(4) The IIA reproduces some delicate effects, such as the superduality in the vector channels or the absence of isovector scalar resonances.

It perhaps can account for some other phenomena discussed in literature, such as (5) spin splittings of baryons, especially explaining why the nucleon is so light (see Sec. IV.D); (6) part of the NN potential and the experimental

absence of a well-bound dihyperon H (Takeuchi and Oka, 1991); and (7) the suppression of the singlet axial charge of the proton (known as the “spin crisis”) or, in other words, the strong polarization of the gluonic field in the polarized protons (Forte and Shuryak, 1992).

However, the IIA certainly does not explain the important QCD phenomenon of quark confinement. This may be seen from the fact that in the “instanton liquid” the static potential between a pair of heavy quarks tends at large distances toward a constant (Shuryak, 1989d).⁴²

IV. OTHER CORRELATION FUNCTIONS

A. Light-and-heavy mesons

The central idea of our discussion has been that the correlation functions have quite different properties depending on the quantum numbers of the channel considered, which means that a realistic $\bar{q}q$ interaction is rather complicated and that by no means does it reduce to a simple universal confining potential. In this section we shall continue these studies, considering now the qq interactions.

However, before addressing the issue of interquark interaction in two- (or three-) body systems, it would be logical to study first the propagation in the QCD vacuum of a single quark. However, as the quark propagator is not a gauge-invariant quantity, it cannot by itself have any physical meaning; one has either to fix the gauge, or, following Schwinger, to switch from the ordinary propagator S to its gauge-invariant version \tilde{S} :

$$\tilde{S}(x) = \langle \bar{\psi}(x) P \exp \left[(ig/2) \int_0^x A_\mu^a t^a d\tau \right] \psi(0) \rangle, \quad (4.1)$$

where t^a are Gell-Mann matrices of the color group, and the path-ordered exponent contains an integral to be taken over the straight line, going from 0 to x . In other words, one can simply supplement our light dynamical quark with a static, very heavy antiquark, considering a heavy-light meson instead of a single quark. Of course, this now changes the long-distance physics: the light quark becomes bound by the confining potential to the heavy one. However, at the small distances we are going to be studying, these confining forces are not crucial, and the static charge of the heavy quark produces only small

⁴²The reader may be puzzled about how an approximation can produce correct hadronic masses without this important piece of physics. Instanton-induced forces are strong enough to make effective masses of quarks and to bind them together into mesons and, perhaps, even baryons. However, even if those have reasonable parameters, there also should be some false states related to free propagation of “dressed” quarks. So far the behavior of the correlation functions in IIA has not revealed this unphysical component, which probably means that the false states do not contribute very much.

⁴¹A table of the numbers is given in Shuryak (1989a).

(and calculable) corrections. This is the line of reasoning that has led us to study such mesons. In a sense, it is the simplest system with light quarks, so to say, a hydrogen atom of hadronic physics.

Certainly, there is some empirical information about charmed and bottom mesons. For simplicity we concentrate on the simplest case, in which the light quark mass is put to zero and that of the heavy one is considered large on the hadronic scale: $m_q \ll \Lambda, m_Q \gg \Lambda$. Discussion of the corresponding correlation functions in the OPE framework was started in Shuryak (1982b). In a more general context, discussion of some effective theory excluding the heavy quarks was initiated by Isgur and Weise (1991) and applied to various decay form factors, etc., which can be related to multipoint correlation functions.

Returning to our main object, the two-point correlators, we shall discuss the correlation functions of the following type,

$$K_i(\tau) = \langle \bar{Q}(\tau) \Gamma_i q(\tau) \bar{q}(0) \Gamma_i^+ Q(0) \rangle, \quad (4.2)$$

where Γ_i is some gamma matrix, τ is the Euclidean time difference between the two points, and Q, q stand for the field of heavy (light) quarks. We assume that the heavy antiquark just stays at $\mathbf{x}=0$ all the time. All energies are naturally measured relative to the heavy quark mass M_Q . Additional simplification due to the large M_Q limit is the absence of a spin splitting: the spin direction of the superheavy quark cannot be of any importance. Thus the pseudoscalar and the vector mesons are degenerate, as well as the scalar and the axial ones. Therefore, we consider only the splitting in parity P , negative ($-$) for the first two cases and positive ($+$) for the two latter ones, denoting these correlators by $K_-(\tau)$ and $K_+(\tau)$. These functions were evaluated numerically both on the lattice (Boucaud *et al.*, 1988; Bernard, Heard, Labrenz, and Soni, 1992) and in IIA (Shuryak, 1989d; see below).

Experimental data on heavy-flavored mesons are still very incomplete. Some masses of flavored mesons have been compiled in Table II. We included strange mesons as well as charmed and bottom mesons, although the s quarks and probably even the c quarks are not sufficiently heavy to have the above approximation applied to them. However, the data are useful for showing the trends. We express these masses in terms of the excess energy above the heavy quark mass,

$$E(J^\pi) = m(J^\pi) - m_q.$$

Using the values of s , c , and b quark masses from the

TABLE II. Masses of some heavy-light mesons (in MeV), according to *Particle Data Table*.

J^P	0^-	1^-	1^+	0^+
$\bar{s}u$	497	892	1270,1400	1430
$\bar{c}u$	1865	2007	2422	
$\bar{b}u$	5278	5327		

QCD sum-rule analysis $m_s \approx 150$ MeV, $m_c \approx 1250$ MeV, and $m_b \approx 4800$ MeV (Shifman, 1986) and assuming that the spin splitting is caused by the $S_1 S_2$ -type interaction, we have the following equation for the spin-averaged excess energies of the negative- and the positive-parity states

$$E^\pm = \frac{3}{4}E(1^\pm) + \frac{1}{4}E(0^\pm), \quad (4.3)$$

where 1,0 label spin. Using the experimental numbers, one concludes that the spin-averaged $P=-1$ state is separated from the quark mass by $E^- \approx 640, 520$, and 475 MeV for s, c , and b quarks, respectively. Splitting of the two parity states $\delta E = E^+ - E^-$ is roughly 600 and 450 MeV for s and c cases. From this we conclude that for the superheavy mesons the excess energies are probably

$$E^- \sim 450 \text{ MeV}, \quad E^+ \sim 900 \text{ MeV}. \quad (4.4)$$

For the small-distance behavior of the corresponding correlation functions, we see that the trivial limit is given by the product of free propagators

$$K^{\text{free}}(\tau) = \text{Tr}[S_q^{\text{free}}(\tau) \Gamma S_Q^{\text{free}}(\tau) \Gamma], \quad (4.5)$$

where

$$S_q^{\text{free}}(\tau) = -\gamma_0 / (2\pi^2 \tau^3), \quad S_Q^{\text{free}}(\tau) \sim (1 + \gamma_0). \quad (4.6)$$

Here we have dropped all unimportant factors in the heavy quark propagator.

As before, we consider the ratio of the true correlation function to the free one, $R(\tau) = K(\tau) / K^{\text{free}}(\tau)$. First, for the OPE coefficient of the leading operator, the light quark propagator is modified due to the presence of the nonzero quark condensate as follows (Shuryak, 1982b),

$$S_q(\tau) = -\gamma_0 / (2\pi^2 \tau^3) + \langle \bar{q}q \rangle / 12 + \dots \quad (4.7)$$

This yields

$$R_\pm(\tau) = 1 - (\pm) \frac{\pi^2 \tau^3}{6} |\langle \bar{q}q \rangle| + \mathcal{O}(\tau^5). \quad (4.8)$$

In this equation, the \pm stands for the parity of the state considered, and we use the modulus of the quark condensate to avoid any sign confusion. Thus one can see that the nonzero quark condensate naturally produces the splitting of the correlation functions with the opposite parity. The OPE suggests a simple symmetry splitting of the two correlation functions considered: the odd-parity correlator curves up, which means these mesons are lighter, and the even-parity one curves down, which means these mesons are heavier. These predictions certainly agree with phenomenology.

Following the usual OPE descriptions, some further terms were evaluated and the resulting correlator was fit (Shuryak, 1982b) with the usual parametrization of the

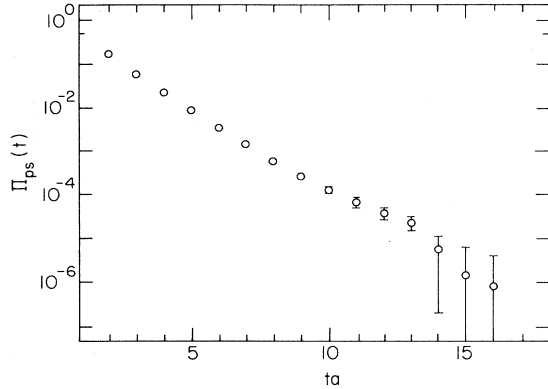


FIG. 16. Correlation functions for the B -type meson (arbitrary units) vs Euclidean time t (in lattice units a), evaluated in (Maiani, Martinelli, and Sachrajda, 1992).

physical spectral density⁴³

$$\text{Im}K(E) = f_{\text{res}}^2 M_Q \delta(E - E_{\text{res}}) + (3E^2/\pi)\theta(E - E_0). \quad (4.9)$$

The fit E_{res} corresponds to the meson mass; the corresponding excess masses found were

$$E^- = 400 \pm 100 \text{ MeV}, \quad (4.10)$$

$$E^+ - E^- = 800 \pm 250 \text{ MeV}. \quad (4.11)$$

Comparing this with the data discussed earlier, one can see that the E^- was evaluated correctly, while the splitting $E^+ - E^-$ was overestimated, roughly by about a factor of 2.

Let us now present an example of point-to-point correlation functions measured on the lattice. In Fig. 16 one can see a set of early data by Boucaud *et al.* (1988) corresponding to the B -type (which means pseudoscalar light-and-heavy quark) meson.⁴⁴

At small distances ($\tau = 1a - 3a$) they are in a reasonable agreement with a free propagator; but at large distances they fall with distance very rapidly, and one finds the excess energy of the lowest state $E^- \sim 1 \text{ GeV}$, about twice larger than expected phenomenologically. The reason is not difficult to trace: the pointlike superheavy quark has a divergent self-energy, $\delta M_Q \sim 1/a$, and one should subtract this unphysical quantity. Another way out is to

⁴³One may be surprised by the appearance of a large quantity, the heavy quark mass, in this equation. In the limit $M_Q \rightarrow \infty$, the combination $f_{\text{res}}^2 M_Q$ tends to constant, equal to $12\pi n$, where n is the density of a light quark at the origin.

⁴⁴Later data, corresponding to much larger statistics and larger lattices, can be found, for example, in Allton *et al.* (1991), Lubicz *et al.* (1992), and Bernard *et al.* (1992), together with further discussion of how the large-mass limit on the lattice can be reached, Maiani *et al.* (1992).

evaluate both $P = \pm 1$ correlators and consider their ratio: then the mass difference between the two lowest mesons can be calculated without this problem.

Finally, let us turn to the calculations of these correlation functions in the IIA (Shuryak, 1989d). Omitting all details, we come directly to the results shown in Fig. 17. Although the splitting between two parity channels still is significant, the whole picture looks quite different from the symmetric $1 \pm \text{const} \times \tau^3$ behavior suggested by the OPE. The solid lines are again the three-parameter fit by the standard equation (4.12), but now with the following values of the parameters:

$$E^- = (2 \pm 0.4)\Lambda, \quad E_0^- = 3.2\Lambda, \quad (4.12)$$

$$E^+ = (4.5 \pm 1)\Lambda, \quad E_0^+ = 5.5\Lambda, \quad (4.13)$$

where Λ is the QCD scale parameter. With the experimental values $\Lambda = 150 - 200 \text{ MeV}$ it gives $E^- = 330 - 440 \text{ MeV}$ and $E^+ - E^- = 350 - 460 \text{ MeV}$, in reasonable agreement with the empirical energy excesses.

B. Does the constituent quark model make sense?

The nonrelativistic quark model of the '60s suggest a simple picture of hadrons as relatively loose bound states of constituent quarks with masses of about 350 MeV. During its long history, this idea obtained impressive phenomenological support (DeRujula, Georgi, and Glashow, 1975; Isgur and Karl, 1978), reproducing many properties of the baryons, such as masses and magnetic moments.

Another simple argument in favor of the nonrelativistic quark model presents itself when one considers the correlation functions: although the masses and the cou-

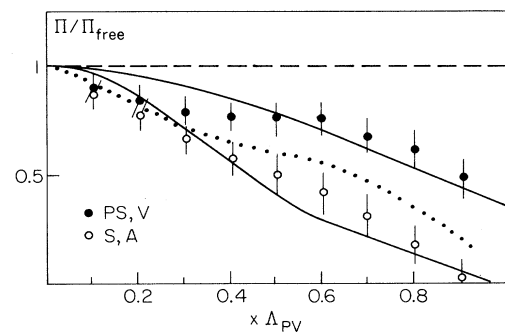


FIG. 17. Correlation functions for B -type mesons, normalized to the free propagator, vs distance $x \Lambda_{PV}$ (normalized to the Pauli-Villars Λ_{PV} parameter, roughly in fm). The points correspond to the calculation in the IIA framework (Shuryak, 1989d). The closed and open points correspond to negative-parity channels [pseudoscalar (PS) and vector (V) ones] and positive-parity ones [the scalar (S) and axial (A) channels], respectively. The solid curves are the three-parameter fit described in the text. The dotted line shows the common contribution of the nonzero fermionic modes.

plings of the lowest states strongly depend on the quantum numbers of the channel, the continuum thresholds are always about $E_0 = 1.3-1.5$ GeV. Now, if confinement demands production of an extra pair of constituent quarks, these thresholds should be roughly $4M_{\text{eff}}$ in order to produce an extra pair, which indeed corresponds well with observation. Unfortunately, it is very difficult to understand how the constituent quark model may be derived from QCD.

Considering correlators for light-and-heavy mesons, one may wonder how a “bare” quark becomes a “dressed” one. For example, what are the distance scales involved, and what is the spin structure of the light quark propagator? To be specific, let us consider the following linear combinations of the two correlation functions discussed above:

$$S_{\text{flip}} = \frac{1}{4} \text{Tr}[\tilde{S}(\tau)] \sim [K^+ - K^-], \quad (4.14)$$

$$S_{\text{nonflip}} = \frac{1}{4} \text{Tr}[\gamma_0 \tilde{S}(\tau)] \sim [K^+ + K^-], \quad (4.15)$$

where “flip” and “nonflip” refer to the light quark chirality, \tilde{S} is the gauge-invariant quark propagator (4.1), and K^+, K^- are the correlators for light-heavy mesons with different parity (discussed above). These quantities are shown in Figs. 18 and 19, as calculated using the IIA (Shuryak, 1989d). In the constituent quark model, one expects that these two amplitudes will be given by the following simple formulas

$$S_{\text{flip}}(\tau) \sim Z^2 m D(m, \tau), \quad (4.16)$$

$$S_{\text{nonflip}}(\tau) \sim Z^2 \partial_\tau D(m, \tau), \quad (4.17)$$

where m is the constituent quark mass, $D(m, \tau)$ is the

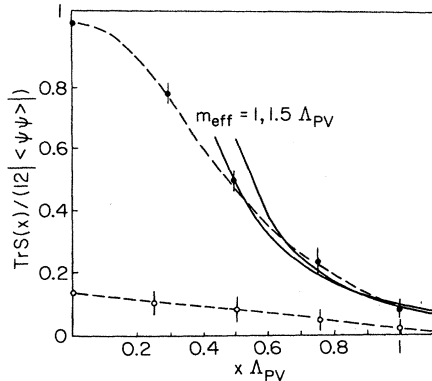


FIG. 18. Spin-flip propagator of the light quark normalized to the value of the quark condensate, $\frac{1}{12} \text{Tr} S(x) / \langle \bar{q}q \rangle$ vs distance $x \Lambda_{PV}$, normalized to the Pauli-Villars Λ_{PV} parameter. Closed points are the result of the calculation in the IIA framework (Shuryak, 1989d; open ones show the contribution of the nonzero modes). The dashed lines are simply a fit to the points, while the two solid lines correspond to the constituent quark model with a fixed value of the quark effective mass $m_{\text{eff}} = 1, 1.5 \Lambda_{PV}$.

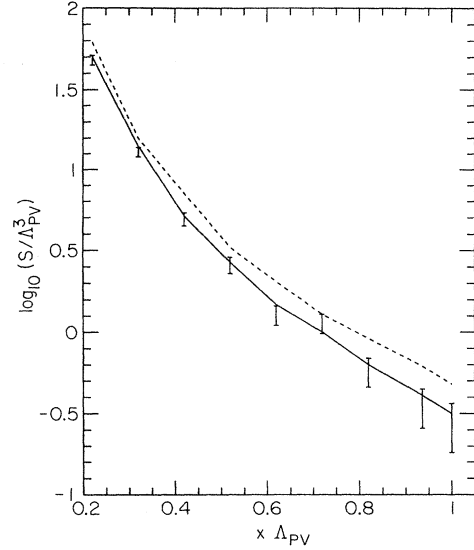


FIG. 19. Same as in Fig. 18, but for the spin-nonflip component of the propagator S (in units Λ_{PV}^3) vs distance x (in units $1/\Lambda_{PV}$). Dots correspond to IIA calculations (Shuryak, 1989d), and the dashed and solid lines correspond to the constituent quark model with $m_{\text{eff}} = 0.15 \Lambda_{PV}$, respectively.

propagator of a scalar particle at distance τ , and Z is the coupling constant of the constituent quark to the bare or “current” quark. Note that m in the propagator and in the numerator of S_{flip} should be the same, if this model is to make sense.

The results of the calculations are indeed reproduced by these simple formulas well enough, with $Z=1$ and a quark effective mass of about $(1.5-2)\Lambda$. This fact is quite surprising. Particularly unexpected is the result that $Z=1$ within the error limits; it means that for unknown reasons the current quarks become constituent quarks without any admixture of more complicated states!

The fit is not perfect, of course: in fact, looking at S_{flip} , we observe that this model works only for $\tau > 0.5$ fm; so one gets an idea of the distances at which the constituent quark mass is formed. This agrees with the OPE-based estimates (Shuryak, 1982b) of the effective mass at small distances:

$$m_{\text{eff}}(x) = (\pi^2/3) |\langle \bar{\psi}\psi \rangle| x^2, \quad (4.18)$$

if one assumes that this equation is valid up to $m_{\text{eff}} \sim 300$ MeV is formed.

Recently, lattice measurements of the light quark propagator, taken in a variety of gauges, were reported by Bernard, Murphy, Soni, and Yee (1990). Remarkably, the gauge dependence turns out to be relatively weak, and the data can be more or less described by a simple constituent quark model with a similar mass value. We think this interesting point deserves further study.

C. Diquarks and baryons containing a heavy quark

In contrast to the $\bar{q}q$ channels, we know very little about the qq interaction. Empirical information must come from baryons, but it is nontrivial to deal with a system containing three light quarks. The logical extension of what we did in the preceding section is to work with a qq pair, adding a heavy static quark Q to produce a physical gauge-invariant object.

Masses of the corresponding charmed baryons are known:

$$\begin{aligned} M(\Lambda_c) &= 2284.9 \pm 1.5 \text{ MeV} , \\ M(\Sigma_c^{++}) &= 2452.2 \pm 1.7 \text{ MeV} , \\ M(\Xi_c) &= 2460 \pm 19 \text{ MeV} . \end{aligned} \quad (4.19)$$

If one ignores the kinetic energy and any interactions with the charmed quark, the following conclusions emerge.

(1) Subtracting m_c , one finds that the excess energy as-

$$K_\Lambda(\tau) = \langle [u_i^T(\tau)C\gamma_5 d_m(\tau)]^\dagger \epsilon_{lmn} P \exp \left[(ig/2) \int_0^\tau A_\mu^a t^a d\tau \right]_{nk} [u_i^T(0)C\gamma_5 d_j(0)] \epsilon_{ijk} \rangle , \quad (4.20)$$

$$K_\Sigma(\tau) = \langle [u_i^T(\tau)C\gamma_\mu d_m(\tau)]^\dagger \epsilon_{lmn} P \exp \left[(ig/2) \int_0^\tau A_\mu^a t^a d\tau \right]_{nk} [u_i^T(0)C\gamma_\mu d_j(0)] \epsilon_{ijk} \rangle , \quad (4.21)$$

where T means transposition and C charge conjugation.

D. Ordinary baryons. Why is the nucleon so light?

As mentioned earlier, we want to learn about the interaction between quarks by studying the baryonic correlation functions. Unfortunately, we do not have as much experimental information about baryons as we have about mesons. What we actually know is essentially only the baryonic masses⁴⁵; but as we have those for all members of octet and decuplet, it is still possible to get some information from them.

We start this section with a presentation of lattice data on hadronic masses, using the so-called Edinburgh plot, the ratio m_N/m_ρ versus m_π/m_ρ . In Fig. 20 are data taken from Teraflop (1992).⁴⁶ None of these points so far correspond to quarks being as light as they are in Nature. Nevertheless, one can see that these data are all consistent with the naive quark model,

$$m_N/m_\rho = \frac{3}{2} . \quad (4.22)$$

⁴⁵In principle, exclusive reactions with baryons at high-momentum transfer (e.g., elastic form factors) provide some information about the probability of finding three quarks at the same point, in definite spin and color state.

⁴⁶We discuss recent large-lattice data with dynamical fermions (Brown *et al.*, 1991) below. A review of the current situation can be found in the talk given by Toussaint (1992).

sociated with two light quarks is rather large: it is about 1 GeV. It is also about twice the minimal energy of the light quark E_- , estimated above, for the light-heavy mesons; so these numbers are consistent.

(2) The Σ - Λ splitting yields the difference between energies of the spin-0 and spin-1 diquarks to be about 170 MeV.

(3) The Ξ - Σ difference is 175 ± 20 MeV, more or less consistent with the standard value of the strange quark mass.

Unfortunately, we are not aware of any studies of the corresponding correlation functions (besides some preliminary discussion in Shuryak, 1982b). Therefore we simply indicate which correlation functions we suggest in this respect.

For simplicity, let us take two quarks of different flavors, say, u, d ones. We consider a heavy quark mass to be infinitely large; so it only propagates in the (Euclidean) time direction. Thus one may consider the following correlation functions:

Unfortunately, this is 25% higher than the empirical ratio.

Recently, large-scale lattice simulations with dynamical fermions were reported by the Columbia group (Brown *et al.*, 1991). They were able to come down in quark masses to the values $ma = 0.01$ and even to 0.004 (for the valence quarks only)⁴⁷; and even in this case the N/ρ mass ratio is found to be 1.527(11), or still much too large.

Although the history of lattice simulations has shown that such problems should disappear if larger and finer lattices are used, it is always instructive to ask what particular effect requires such a fine-grained lattice. For the N/ρ mass ratio, we do not know; but we can speculate. Note that the mass of the $\Delta(\frac{3}{2}, \frac{3}{2})$ is phenomenologically in better shape. Thus it is more probable that something is wrong with the nucleon itself: for some reason it is not as light as it should be on the lattice. The nucleon differs by having $s=0$ qq pairs; so our speculation is that there is a short-ranged attraction between quarks in this channel.

Let us examine the general origin of the spin splitting

⁴⁷Those numbers roughly correspond to bare masses at lattice scales of about 15 and 7 MeV in absolute units. In other words, in the $ma = 0.004$ case, the pion mass is already nearly as small as it is in the real world.

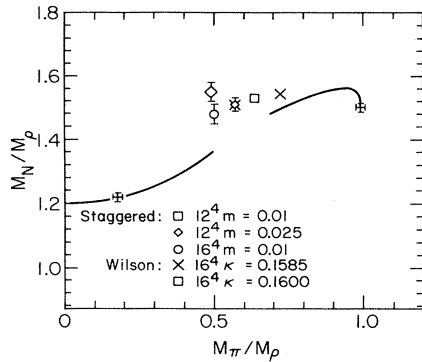


FIG. 20. Compilation of lattice data obtained by the HEMCGC Collaboration [this figure is taken from the review Teraflop (1992)] on the plot m_N/m_ρ vs m_π/m_ρ . The dagger in the left corner is the experimental point, that at the right is the one at $(1, \frac{3}{2})$ expected for very heavy quarks. The line at large masses corresponds to the nonrelativistic potential model, while the line at small ones corresponds to chiral perturbation theory. Data points correspond to different lattices and fermion masses, explained in the figure.

in an effort to understand why lattice simulations may have problems reproducing them. It is instructive to start with a somewhat simplistic discussion of light-heavy hadrons. In Sec. IV.A we concluded that the minimal energy of a light quark is about $E^- \sim 450$ MeV, ignoring here the energy of the interaction with the static quark. In Sec. IV.C we found that an average diquark has an energy about twice that. Does that imply that the typical three-quark baryon should have a mass about $3E^- \approx 1.3-1.4$ GeV, even larger than $\frac{3}{2}M_\rho$?

No, if the mutual qq interaction is significant: in the three-quark system it may be much more important than in the two-quark one. Checking whether the simple idea of binary interactions can explain this difference, we follow a simple analysis by Shuryak and Rosner (1989). They used a nonrelativistic quark model, in which light and strange quarks had some energies E_q, E_s together with additional negative interaction for spin-zero diquarks $\delta E, \delta E_s$. All masses of the baryon octet and decuplet can be very well described by this primitive model, with the following values of the parameters:

$$\begin{aligned} E_q &= 412.9 \text{ MeV}, & E_s &= 557.5 \text{ MeV}, \\ \delta E &= -200.5 \text{ MeV}, & \delta E_s &= -132.7 \text{ MeV}. \end{aligned} \quad (4.23)$$

We make the following observations on these quantities: (1) E_q is indeed consistent with the magnitude of the light quark energy in light-heavy hadrons; and (2) δE is also close to the binary interaction found from the splitting in the light-heavy baryons. The strange sector also leads to no surprises: (3) the difference is given by $E_s - E_q \approx 145$ MeV, close to the standard estimates of m_s ; and (4) the ratio $\delta E_s / \delta E \approx 0.66$ is close to the ratio of the magnetic moments and to the ratio of the energies themselves.

To summarize, the baryon mass systematics suggests

that the nucleon is light because it contains spin-zero qq pairs, which have attractive interactions.

Two mechanisms have been suggested as the cause of this attraction: (a) a perturbative spin-spin interaction due to gluon-magnetic moments (DeRujula *et al.*, 1975); and (b) the instanton-induced interaction (Betman and Laperashvili, 1985; Kochelev, 1985; Shuryak and Rosner, 1989; Takeuchi and Oka, 1991).

How can one distinguish these two mechanisms? One possible way is a comparison of the ud and us pairs, related to point (4) in the discussion above. The conclusion drawn above is often taken as a proof that the spin splitting mechanism is due to a gluon-magnetic spin-spin interaction; but, as shown in Shuryak and Rosner (1989), the instanton-induced forces lead to precisely the same prediction.

Another possible way is to look at the corresponding correlation functions. Even if both mechanisms are tuned to fit the observed mass splittings, they have, in general, a different spatial dependence. In fact, both are rather short-range forces; but still they should have different systematic errors on the lattice. If, as it follows from IIA, the typical instanton radius is as small as $\frac{1}{3}$ fm (Shuryak, 1982a; Diakonov and Petrov, 1984; Shuryak, 1988b), one still may have problems, even with the lattice spacing being about $a \sim 0.1$ fm. And, certainly, correlation with instantons can be studied on the lattice on a configuration-by-configuration basis.

The last topic in this section is the OPE analysis of the baryonic correlators, as initiated by B. L. Ioffe and collaborators (Ioffe, 1981; Belyaev and Ioffe, 1982; see also Farrar, Zhaoang, Ogloblin, and Zhitnitsky, 1981 and Reinders, Rubinstein, and Yazaki, 1983). The results obtained in these papers show some remarkable features (which were partly unnoticed in the original papers), well correlated with our discussion above.

We shall use Ioffe's nucleon and Δ currents, which are defined as (Ioffe, 1981)

$$\eta_N = (u^T C d)u - (u^T C \gamma_5 d)\gamma_5 u, \quad (4.24)$$

$$\eta_{\Delta, \mu} = (u^T C \gamma_\mu u)u, \quad (4.25)$$

where C is the charge-conjugation matrix, and T stands for transposition. We gave suppressed color indices, which are, as usual, convoluted with $\epsilon^{i,j,k}$. Convolution of the spinor indices is prescribed by brackets; the current is a spinor itself, and its index is the same as that of the quark field in the last position in this formula.

One can consider the nucleon (or the Δ) correlation functions with or without a spin flip; so, in fact, one still has a variety of correlation functions to be discussed. Deviating slightly from Ioffe in this respect, I consider the simplest traces⁴⁸

⁴⁸One can consider other traces, say, without γ_0 , which actually was used by Ioffe as well. Certainly, our discussion of baryonic correlators is not complete; we have picked up the sum rule which is assumed to be the best.

$$K_N(\tau) = \text{Tr}[\gamma_0 \langle \bar{\eta}_N(\tau) \eta_N(0) \rangle], \quad (4.26)$$

$$K_\Delta(\tau) = \text{Tr}[\gamma_0 \langle \bar{\eta}_{\Delta,\mu}(\tau) \eta_{\Delta,\mu}(0) \rangle]. \quad (4.27)$$

The two points are separated by the Euclidean time τ .

Both correlation functions are nonzero in the free-quark approximation; so, as above, we normalize the correlators to these values:

$$K_N^{\text{free}}(\tau) = \frac{6}{\pi^6 \tau^9}, \quad (4.28)$$

$$K_\Delta^{\text{free}}(\tau) = \frac{18}{\pi^6 \tau^9}. \quad (4.29)$$

Let us now present the OPE predictions by Ioffe (1981) and Belyaev and Ioffe (1982)⁴⁹:

$$R_N(\tau) = 1 + \frac{\tau^4}{3 \times 2^7} \langle (gG_{\mu\nu}^a)^2 \rangle + \frac{\pi^4 \tau^6}{72} \langle \bar{\psi}\psi \rangle^2 (1 - \tau^2 m_0^2 / 32) + \dots, \quad (4.30)$$

$$R_\Delta(\tau) = 1 - \frac{\tau^4 5^2}{3 \times 2^{11}} \langle (gG_{\mu\nu}^a)^2 \rangle + \frac{\pi^4 \tau^6}{12} \langle \bar{\psi}\psi \rangle^2 (1 - 7\tau^2 m_0^2 / 96) + \dots. \quad (4.31)$$

Here $m_0^2 = -ig \langle \bar{\psi} \sigma_{\mu\nu} t^a G_{\mu\nu}^a \psi \rangle / \langle \bar{\psi}\psi \rangle$, according to Ioffe, it is rather large, of the order of $0.5-1 \text{ GeV}^2$. Note that these $\langle \bar{\psi}\psi \rangle^2$ corrections correspond to straightforward application of the vacuum dominance hypothesis (see Sec. III.B). Radiative corrections to them, $O(\alpha_s) \ln(1/\tau\mu)$, which played an important role for vector mesons, are not included.

The corresponding curves are displayed in Figs. 21 and 22. The short-dashed, long-dashed, and dot-dashed lines are OPE corrections including all terms up to gluonic condensate, quark condensate, and quark-gluon condensates. One can probably trust the last line up to, say, $x=0.7 \text{ fm}$ before it starts to bend too much.⁵⁰

As we do not have experimental data for this correlator, we can only compare it to predictions for these correlators, which are actually based on similar equations. If we parametrize the imaginary part in the usual way, we get

$$K_N(x) = \beta_1^2 D'(m_N, \tau) + \frac{1}{2^8 \pi^4} \int_{W_N}^{\infty} ds s^2 D'(s^{1/2}, \tau), \quad (4.32)$$

⁴⁹These formulas have been recalculated in the space-time representation from the original expressions given in Borel-transformed form. The vacuum expectation values of operators were evaluated using the vacuum dominance hypothesis.

⁵⁰In general, behavior like this is typical for any power expansion of a rapidly falling function. The subsequent terms are sign changing and tend to compensate each other.

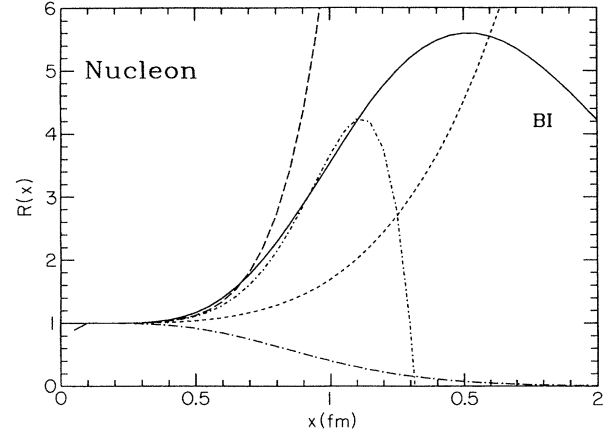


FIG. 21. Ratio of the nucleon correlation function (see text) to that corresponding to the free propagation of three quarks vs distance x (in fm). The short-dashed, long-dashed, and short-dot-dashed lines are the OPE predictions including the gluon condensate, the gluon and quark condensates, and the gluon, quark, and mixed condensates, respectively. The solid line is the resulting prediction of Belyaev and Ioffe, (1982), to be compared with the resulting OPE line at $x < 1 \text{ fm}$. (The long-dot-dashed line shows the contribution of the continuum states, apart from that of the nucleon itself.)

$$K_\Delta(x) = 2\lambda^2 D'(m_\Delta, \tau) + \frac{3}{2^8 \pi^4} \int_{W_\Delta}^{\infty} ds s^2 D'(s^{1/2}, \tau), \quad (4.33)$$

where $D'(m, \tau) = -d/d\tau D(m, \tau)$. The parameter values suggested by Belyaev and Ioffe (1982) are

$$W_N \approx 1.5 \text{ GeV}, \quad \beta_1^2 \approx 0.45 \text{ GeV}^6 (2\pi)^4, \quad (4.34)$$

$$W_\Delta \approx 2.1 \text{ GeV}, \quad \lambda^2 \approx 2.3 \text{ GeV}^6 (2\pi)^4. \quad (4.35)$$

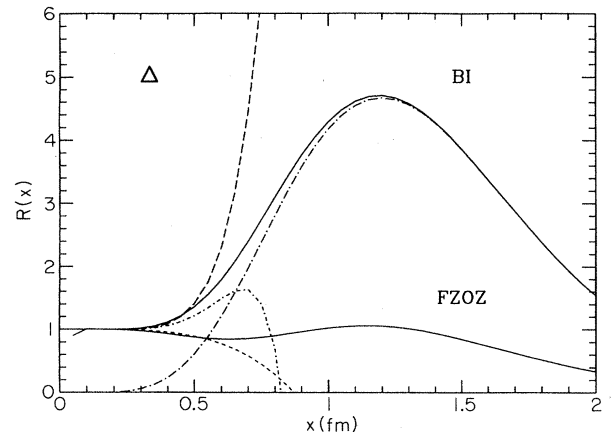


FIG. 22. Same as in Fig. 21, but only for the Δ correlation function. In this case we have shown by two solid lines predictions of two groups: BI (Belyaev and Ioffe, 1982) and FZOZ (Farrar *et al.*, 1981).

The corresponding prediction correlators are also shown in Figs. 21 and 22 as the solid lines. Here BI stands for the predictions of Belyaev and Ioffe (1982), while FZOZ corresponds to Farrar *et al.* (1981), where the baryonic parameters were obtained from a somewhat different set of sum rules (Chernyak and Zhitnitsky, unpublished). The latter work obtained similar parameters for the nucleon, but significantly smaller coupling for the Δ , $\lambda^2 \approx 0.5 \text{ GeV}^6 (2\pi)^4$. The agreement between the OPE and the predicted curves in some regions of τ is not surprising: the parameters of these curves were obtained from essentially the same sum rules.

What is surprising is the large predicted magnitude of the nucleon correlator at distances of from 1–2 fm, where they are essentially larger than the perturbative ones. Comparing this curve with the mesonic ones discussed in Sec. II, one sees that they are reminiscent of the pseudoscalars, for which strong attractive forces certainly exist.

It seems the curves for the Δ have less pronounced peak than those for the nucleon, if the FZOZ numbers are used. Is it because the Δ contains only diquarks of spin one, similar to the ρ , while the nucleon also has scalar diquarks, similar to scalar and pseudoscalar mesons with strong instanton-induced interactions?

Although these curves seem to support our discussion, it remains to be proven whether these OPE predictions are really true, and it is not actually applicable at such large distances.

Recently the first attempt to calculate the instanton-induced corrections to baryonic correlation functions in first order in 't Hooft interaction was made. Kochelev (1990) reported a significant improvement of the sum rules compared to the Ioffe OPE-based results. Similar work in the IIA framework is now in progress, including the evaluation of all orders of the 't Hooft interaction.

We have seen that a number of approaches, including the naive quark model and the OPE, suggest the existence of an attractive qq interaction inside the nucleon. The attraction is less pronounced inside the Δ and therefore is attributed to the spin-0 isospin-0 diquarks. If the attraction is there, it can explain why the nucleon is so light and its coupling to the Ioffe current is so large. The nature of these forces remains an open question. We also do not understand why lattice simulations have problems in reproducing them.

V. CORRELATION FUNCTIONS AT NONZERO TEMPERATURES AND/OR DENSITIES

A. Melting the QCD vacuum

Because the QCD vacuum is a complicated medium made out of nonperturbative fluctuations of quark and gluon fields, one naturally arrives at the idea of trying to “melt” it. The present understanding is that at some critical temperature or density it undergoes a transition to another phase called the quark-gluon plasma

(Shuryak, 1980). This transition can be studied experimentally in heavy-ion collisions at high energies. Such experiments are under way at CERN and Brookhaven [see Quark Matter-89 (1990) and Quark Matter '90 (1991)]. Construction of a large, dedicated facility in Brookhaven, the Relativistic Heavy Ion Collider (RHIC), was begun in 1991, and there are plans to use, in the study of this transition, the future Large Hadronic Collider at CERN as well.

This problem can be studied theoretically in the framework of various models and, from the first principles of QCD, by numerical simulations on the lattice. This work is very active at the moment [see Lattice 88 (1989); Lattice 89 (1990); Lattice 90 (1991)]. The proposed TERAFLAP project⁵¹ (Teraflop, 1992) in the United States promises to increase the computer power involved by 2–3 orders of magnitude.

Readers interested in finite temperature QCD in general are directed to Shuryak (1980), Gross, Pisarski, and Yaffe (1981), Shuryak (1988a), and Hwa (1990). In this section we shall concentrate on the correlation functions at finite temperature.

Two main qualitative features of the QCD vacuum will disappear at a high enough temperature: one expects deconfinement and chiral symmetry restoration. Figure 23, taken from a recent paper by the Columbia group (Brown *et al.*, 1990), makes a brief summary of our present understanding of the corresponding phase diagram. Two observations are important: (1) The two phase transitions mentioned seem to be well separated, which supports the idea that they are based on completely different physics. (2) The real world seems to be outside of the first-order transition regions, but still very close to the line of the chiral one.⁵²

Speaking about the QCD vacuum more quantitatively, one may ask why typical energy density⁵³ is needed to melt it? For deconfinement one may take as a guess something similar to the MIT bag constant,

$$B_{\text{MIT}} \sim 50 \text{ MeV}/\text{fm}^3. \quad (5.1)$$

For the energy density related to chiral symmetry restoration, one may take the simple estimates (Asakawa and Yazaki, 1989; Li, Bhalrao, and Bhadury, 1991) in the Nambu–Jona-Lasinio model. This is essentially an estimate of how much energy will be gained if the quarks in the negative-energy Dirac sea are correlated, making the quark condensate and the massive constituent quarks.

⁵¹Similar projects are developing in Europe and Japan as well, but none have been approved yet.

⁵²We shall use the notion of critical temperature T_c , meaning the one at which specific heat is maximal and chiral symmetry is “practically restored.” Numerically it is expected to be about 150–180 MeV.

⁵³We do not speak here about the temperature T , because the energy density is much more relevant for experiments.

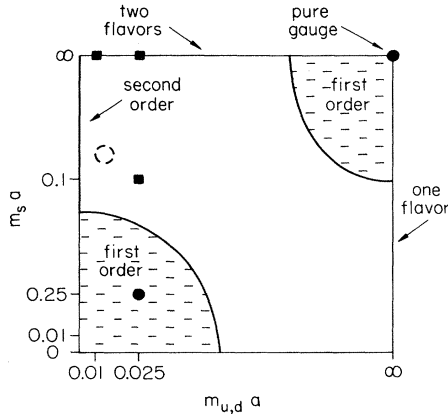


FIG. 23. Diagram of the QCD phase transitions, given in the m_u, m_s plane (the light and strange quark masses, respectively) according to Brown *et al.* (1990). In the lower left corner, one observes a first-order chiral restoration transition, and in the upper right a first-order deconfinement. The experimental point is shown by the dashed circle.

Without going into details, we conclude only that this leads to a magnitude of chiral energy density comparable to the B_{MIT} value.

However, it is important to realize that the total non-perturbative energy density of the QCD vacuum is much larger: using the trace anomaly relation and the value of the gluon condensate (Shifman *et al.*, 1979b), one obtains (Shuryak, 1978a)

$$B_{\text{NP}} = \frac{11N_c/3 - 2N_f/3}{128\pi^2} \langle (gG_{\mu\nu}^a)^2 \rangle \sim 500 \text{ MeV/fm}^3, \quad (5.2)$$

where N_c, N_f are the number of quark colors and flavors. Therefore one may conclude that some important non-perturbative effects should be present even at T larger than that needed for deconfinement and chiral restoration; and in order to obtain the quasi-ideal quark-gluon plasma, one actually needs to surpass this energy density. That is why the planned energy of the heavy-ion collider is chosen to be so high.

The hadrons are expected to melt along with the vacuum as one approaches the phase transition. Presumably, hadrons gradually become unstable in hot matter and finally fail to represent the main degrees of freedom of the system. To discuss hadrons at finite temperature is rather tricky, because we have to define precisely the objects of discussion at nonzero T .

The correlation functions, on the contrary, have the same definition below or above T_c and retain essentially the same physical meaning. The only obvious modification in their definition is that the averaging changes its meaning, the angular brackets here representing the statistical average over the Gibbs ensemble, characterized by the temperature T and possibly by chemical potentials, for finite charge or flavor densities.

We have discussed in the preceding sections what kind of information is currently available about the correlation functions at $T=0$. Roughly speaking, phenomenology tells us that the physical spectral density can usually be represented by two distinct components,

$$\text{Im}K(s) = f^2\delta(s-m^2) + \theta(s-E_0^2)\text{Im}K_{\text{pert}}(s), \quad (5.3)$$

describing propagation of bound quarks at large distances and of free quarks at small distances.

Is this general structure preserved at $T \neq 0$? Let us take it as a rough working hypothesis. If so, the general question formulated above is reduced to a question about the temperature and density dependence of these three parameters, $f, m,$ and E_0 .

We have already mentioned two phenomena that are expected to occur at high temperature—deconfinement and restoration of chiral symmetry. As one signal for deconfinement, one can consider “hadron swelling,” presumably detectable in the correlation functions as a strong decrease of the coupling constants f to local currents.⁵⁴ Another possible signal might be a drop of the observed threshold E_0 : the threshold under confinement may be interpreted as $4m_{\text{eff}}$ (see discussion in Sec. IV), and we expect it to drop to something like $2m_{\text{eff}}$ at the point where deconfinement takes place.

So far there has not been much discussion in the literature of the effect of phase transitions on the correlators. Rather, the main focus has been on “dropping masses” $m(T)$. There were suggestions that parity doublet hadronic modes could be formed ($\pi-\sigma, \rho-A_1, N-N^*$, etc.) above T_c (DeTar and Kogut, 1987). Another interesting suggestion is that masses of many hadronic modes should vanish at the critical point, because they are related to the vanishing quark condensate (Brown, 1991), and this phenomenon may cause much more smooth behavior at the phase transitions (Brown, Bethe, and Pizzochero, 1991) compared to naive estimates with free pions and quark-gluon plasma.

Let us add to this list of general questions a few more that are related to specific channels. As we have mentioned, the isovector scalar channel most probably has no “normal” $\bar{q}q$ mesons; so these correlators are mainly related to the quark continuum. As T approaches T_c , does the $I=1$ scalar resonance go down in mass to meet its parity partner, the pion, and become a visible resonance, or does one have simply a cut with a decreasing threshold, going down as the temperature approaches T_c ? Can the scalar-pseudoscalar mode, representing large fluctuations in $\bar{q}q$, persist even above T_c ?

The next very interesting channel is the η' , the isoscalar pseudoscalar channel. It is well known that $U_A(1)$

⁵⁴The usual order parameters used for the deconfinement on the lattice, such as the expectations of Wilson or Polyakov loops, are not really useful in theories with light quarks, because forces between static quarks are screened.

chiral symmetry is explicitly broken by the instanton-induced interaction, and therefore it is never restored in a strict sense. However, at some temperature it is restored for practical purposes, in the sense that differences between singlet (η') and octet (K, π, η) correlation functions become small.

Thinking about the mixing of hadrons made of quarks with glueballs, one may naturally ask whether the quark-related and the gluon-related correlators approach their high- T limit at the same or at different temperatures. In particular, it is known that quark-made mesons are much lighter than glueballs: does this imply that one will need higher temperatures to “melt” the glueballs?

In the remainder of this section we shall review what is known on this topic. Investigations are only recently started, so only a few of these questions have answers.

B. The low-temperature and low-density limits

The Gibbs averaging of the correlation functions can be written, in general, as the sum over stationary states

$$K_T(x) = \langle \langle j(x)j(0) \rangle \rangle = \sum_n \langle n | j(x)j(0) e^{(\Omega - E_n)/T} | n \rangle . \quad (5.4)$$

If the temperature and baryon density are small enough, the matter will be normal hadronic, made of well-separated particles: pions at low T or nucleons at low densities n_b . Therefore, to first order in matter density, one need consider only the one-body states in the statistical sum. This makes finite density corrections calculable, provided the corresponding matrix element over the hadronic state can be estimated.

Let us restrict our discussion to the case of zero density of all charges and divide the low T range into two separate regions: (a) parametrically small temperatures, meaning that power series in T may be terminated at the lowest nonvanishing terms, and (b) any T below T_c , excluding the vicinity of the transition region.

In the former case, one can use such general methods as the partially conserved axial current hypothesis (PCAC) and the Weinberg effective Lagrangian. In the latter case, one should use some more involved parametrization of the empirical interaction between particles involved. Note that in the latter case the conclusions are essentially model independent, but their accuracy is limited by the accuracy of the corresponding data.

As an example of the general statements valid at parametrically small temperatures, we consider vector and axial correlators with ρ, A_1 quantum numbers, following Dey, Eletsky, and Ioffe (1990). At low temperature, the vacuum has added a dilute gas of pions; so finite temperature expectation values can be expressed in terms of the thermal density of pions $n_\pi(T)$ as

$$\langle M \rangle_T = \langle M \rangle + n_\pi(T) \langle \pi | M | \pi \rangle .$$

To evaluate $\langle \pi | V^a(x) V^b(0) | \pi \rangle$, one can use PCAC and replace it by vacuum averages of the type $\langle AVVA \rangle$.

Here A, V are axial and vector currents, and their upper indices are, for example, those of the SU(2) isospin group. Then, using commutator relations

$$[A_0^a, V_\mu^b] = f^{abc} A_\mu^c, \quad [A_0^a, A_\mu^b] = f^{abc} V_\mu^c, \quad (5.5)$$

it can be further reduced to a combination of $T=0$ vector and axial correlators. The results can be written in the following elegant form, expressing the small- T correlators in terms of vacuum correlators:

$$K_{\mu\nu}^V(T) = (1 - \epsilon) K_{\mu\nu}^V(T=0) + \epsilon K_{\mu\nu}^A(T), \quad (5.6)$$

$$K_{\mu\nu}^A(T) = (1 - \epsilon) K_{\mu\nu}^A(T=0) + \epsilon K_{\mu\nu}^V(T). \quad (5.7)$$

The admixture coefficient is simply

$$\epsilon = \int \frac{4d^3k}{(2\pi)^3 2k} \frac{1}{\exp(k/T) - 1} = \frac{T^2}{6F_\pi^2}. \quad (5.8)$$

As both vector and axial correlators at $T=0$ are known (see Sec. II), we therefore know both correlators at finite but parametrically small T , $\epsilon \ll 1$. In a later paper (Eletsky, 1990) a similar statement was also proven for positive- and negative-parity baryonic currents. From this general approach, one has learned that vector and axial correlators start to merge at small T . By the time $T > T_c$, they should become identical.

Unfortunately, this general approach is very restricted in its applicability, as the following argument shows. What has been taken into account is essentially the forward-scattering amplitude of a pion on virtually a ρ meson or nucleon. This is indeed known at low pion momenta from quite general considerations. However, this region ends as soon as the thermal pion energy becomes large enough to hit the first resonance, say, A_1 in the $\pi\rho$ channel or Δ in the πN case. This condition actually restricts T to a level below 100 MeV or so.

However, using the experimentally measured forward-scattering amplitudes, one can get realistic estimates of the modification of hadrons at low T . Such calculations for π, K, ρ, ω , and other mesons, modified in the pion gas, were made in Shuryak (1991) and Shuryak and Thorsson (1992). Without going into details here, let us only mention some main conclusions. In all the cases hadronic dispersion curves $\omega(k)$ were found to shift down with increasing T . However, the magnitude of the effect was found to be rather modest, even at $T=150-200$ MeV, where the phase transition is expected. Roughly speaking, the corresponding collective potentials are of the order of the nuclear potential well, say, -50 MeV, an order of magnitude smaller than mesonic masses themselves.

These calculations show that the hadronic masses can significantly drop only very close to T_c , where the calculations are inapplicable due to possible multiple particle interactions. Whether the masses really drop or not remains an open question.

C. Quark propagation in the quark-gluon plasma at high temperatures

At very high temperatures (and/or densities) matter is believed to be a nearly ideal gas of fundamental constituents, the so-called quark-gluon plasma. Discussion of this statement in the framework of the perturbation theory and beyond it can be found in Shuryak (1980, 1988a) and Gross *et al.* (1981). Without going into detail here, many phenomena were found to be analogous to those in ordinary electromagnetic plasmas. For example, electric fields are known to be screened, there are plasma oscillations, etc. Only the long-range gluo-magnetic field may have a specific nonperturbative structure at the scale g^2T .

If hot plasma is made of nearly noninteracting quarks, one may expect that the correlators correspond to independent propagation of quarks, described by the ordinary loop diagram with thermal quark propagators, below denoted by $S_T(x)$. Such zero-order diagrams were first evaluated for the vector correlator at $T \neq 0$ by Bockarev and Shaposhnikov (1986), and for the nucleon current by Adami and Zahed (1990). These authors used a Borel-transformed representation of the correlator, which made the derivation rather complicated.

Calculations are significantly simplified in the coordinate representation. In the zeroth order, one has a completely independent propagation of quarks; so mesonic or baryonic correlators are reduced essentially to the square or cube of the thermal quark propagator. For simplicity, we ignore the quark masses and consider correlators in the spatial direction only.⁵⁵

There are three ways of getting the thermal quark propagator: (1) use the standard Feynman rules in the Matsubara formalism and then make a Fourier transform; (2) use a real-time formalism and look at all scattering processes; or (3) solve the Dirac equation in space-time with Matsubara antiperiodic boundary conditions. The first way leads to the sum

$$S_T(x) = (\gamma_x \partial_x) T \sum_n \int \frac{d^3k}{(2\pi)^3} \frac{\exp(ikx)}{k^2 + [\pi T(2n-1)]^2}, \quad (5.9)$$

where n ranges over all integers, positive and negative. The second method leads to

$$S_T(x) = (\gamma_x \partial_x) \int \frac{d^3k}{(2\pi)^3} \exp(ikx) \left[\frac{1}{2} - \frac{1}{1 + \exp(k/T)} \right], \quad (5.10)$$

where the last term is the Fermi occupation factor, and the third to

$$S_T(x) = (\gamma_x \partial_x) T \sum_n (-1)^n \frac{1}{x^2 + (\tau - n/T)^2}, \quad (5.11)$$

where an antiperiodic scalar propagator is written as a sum over paths with different "winding number." These different methods give the same results, which can be expressed in terms of a universal temperature modification factor f ,

$$S_T(x) = S_0(x) f(\pi T x), \quad (5.12)$$

where, at $T=0$, one has $f(0)=1$, $S_0(x)=1/(2\pi^2x^3)$ and at $T \neq 0$

$$f(z) = z \exp(-z) \frac{z+1+(z-1)\exp(-2z)}{[1-\exp(-2z)]^2}. \quad (5.13)$$

At small z , f may be expanded as

$$f = 1 - (7/360)z^4 + O(z^6). \quad (5.14)$$

The meaning of the fourth-order coefficient and the reason why lower powers vanish will be discussed in Sec. V.E. Consider now another limit: why does this function decrease exponentially, $f(z)=z^2 \exp(-z)$, at large z ? This behavior implies that the thermal propagator decoupled from low-energy quark states, although they certainly exist in the noninteracting gas of massless quarks.

Some readers are probably satisfied by the formal answer to this question based on Matsubara formalism (Eletsky and Ioffe, 1988): the lowest Matsubara frequency for fermions is (πT) . It may also be seen in perhaps more physical terms by looking at the second equation (5.11) containing the combination $[\frac{1}{2} - n_f(k)]$ with the Fermi occupation factor. In the case of Bose statistics, one has instead a much more familiar combination $[\frac{1}{2} + n_B(k)]$, due to zero-point motion and thermal excitations, respectively. In our case these two terms have the same interpretation as well. At $k=0$ one has exactly $n_f = \frac{1}{2}$; there is cancellation due to the destructive interference of zero-point fluctuations and excitations.

One may also rewrite $[\frac{1}{2} - n_f(k)]$ as $\frac{1}{2}[(1 - n_F) - n_F]$, so that the particle-hole symmetry $n_F \leftrightarrow (1 - n_F)$ becomes obvious. If the situation near $n_f=0$ and $n_f=1$ is physically similar, up to a sign of the propagator, it is natural that the point where occupation is exactly $n_F = \frac{1}{2}$ is special; here the particle and hole terms compensate each other.

We now use these formulas to compare the expected high- T behavior of the correlation functions with what is known in the vacuum ($T=0$). In Figs. 24 and 25 comparison is made for the vector-axial and nucleon- Δ correlators. This comparison indicates that the axial correlator should show the weakest T dependence in the interval of distances considered, the ρ and Δ ones should show somewhat stronger T dependence, and the nucleon correlator should depend most strongly on T . We have not discussed scalar and pseudoscalar cases, but from our discussion in Sec. III.A and Fig. 24 it may be inferred that in these cases the T dependence should be even more dramatic.

⁵⁵In general, there will be different functions for spatial and time separations, because the thermal system is not Lorentz invariant.

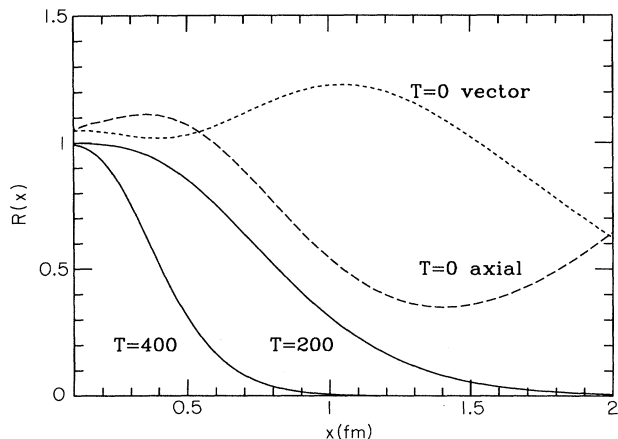


FIG. 24. Ratio of correlation function to that corresponding to free-quark propagation, vs distance x (in fm). The dashed curves correspond to ρ and A_1 channels at zero temperature, as derived from experimental data in Sec. II. Two solid lines correspond to the factor $f^2(\pi T x)$, describing modification of quark propagators in the quark-gluon plasma; they are shown for $T=200$ and 400 MeV.

D. Lattice data

1. Screening masses

Lattice studies of correlation functions at nonzero T were pioneered by DeGrand and DeTar (1986), who observed the exponential decay with distance and interpreted it as the existence of hadronic modes, even at high $T > T_c$. As it was in apparent contradiction with popular ideas about deconfinement and even with perturbative Debye screening of color charges in the plasma phase, it

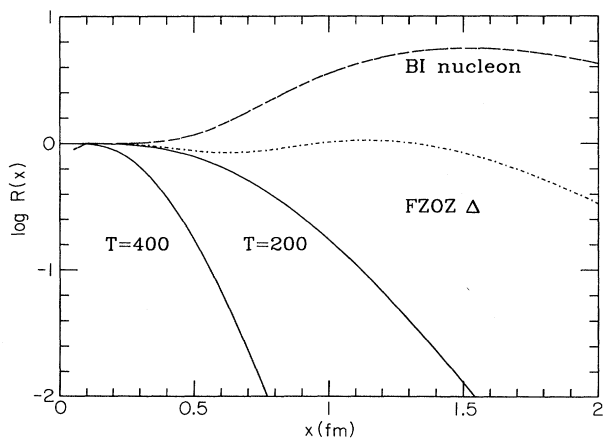


FIG. 25. Same as Fig. 24, but for baryonic currents. Two solid curves for $T=200$ and 400 MeV correspond to the factor $f^3(\pi T x)$; the dashed ones are Belyaev-Ioffe (BI) predictions (Belyaev and Ioffe, 1982) for the nucleon and Farrar *et al.* (FZOZ) ones for the Δ (Farrar *et al.*, 1981) discussed in Sec. V.

looked very mysterious. However, as it was shown in the previous section, even for independent quark propagation, a destructive interference of two terms in the quark propagator $[n_F(E) - \frac{1}{2}]$ leads to such exponential decay.

A set of lattice data compiled by Gocksch (1991) is plotted in Fig. 26 in the form of the so-called screening masses as a function of temperature. The screening mass is defined as

$$M = - \lim_{x \rightarrow \infty} \frac{d \ln K(x)}{dx} . \quad (5.15)$$

Its value at low T should coincide with the masses of the lowest hadrons in the corresponding channels. At $T > T_c$, data for vector mesons and baryons show that M/T is essentially constant. Moreover, although it is not exactly 2π and 3π , they agree reasonably well with the corresponding values after finite-size corrections (Born *et al.*, 1991).

The following observations can also be made on the basis of these results.

(a) The lattice results clearly show one of the anticipated phenomena, parity doubling. At $T > T_c$ vector-axial and scalar-pseudoscalar correlators, etc., become identical, which is a direct consequence of the restored chiral symmetry.

(b) For the vector and baryonic correlation functions, the asymptotically high- T form is smoothly reached already near T_c , without any noticeable discontinuities.

(c) For the scalar-pseudoscalar case, one observes much smaller screening lengths than those corresponding to Matsubara frequencies.

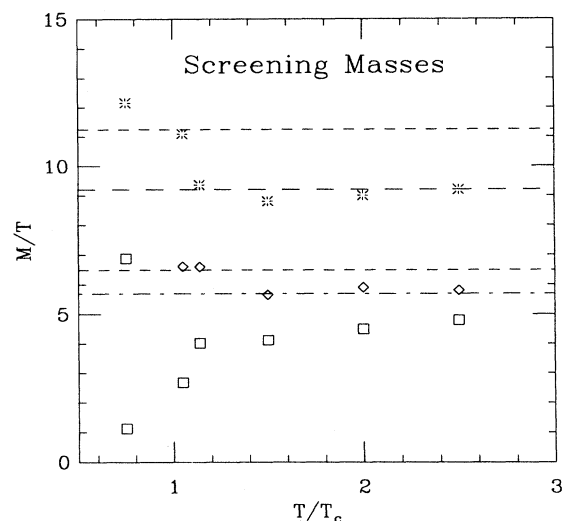


FIG. 26. Compilation of screening masses (Gocksch, 1991) obtained on the lattice for different correlators vs temperature T (scaled in units of the critical one, T_c). The short-dashed curves show values $2\pi T, 3\pi T$ corresponding to the lowest Matsubara frequencies in the continuum, while the long-dashed ones show their values for the finite lattices used.

2. Binding of $\bar{q}q$ pairs propagating in spatial direction

The question of whether $\bar{q}q$ pairs are correlated or move independently was addressed in the recent lattice study by Bernard, DeGrand, DeTar, Gottlieb, Krasnitz, Ogilvie, Sugar, and Toussaint (1991). It was demonstrated that if the $\bar{q}q$ pair is forced to propagate large distance in, say, the z direction, it moves in the transverse x, y plane in a correlated way. The corresponding wave function at finite T happens to be similar to that at $T=0$, and it even has a smaller radius. This result has created some excitement and we believe, some misinterpretation.

The key technical point, important for the understanding of the terminology used, is an interchange of the time t and z axis. After transformation to this new space, one deals with a system at zero temperature in a periodic box in the z direction, with periodicity $\beta=1/T$. Using this language it is obvious that in the high- T limit the so-called dimensional reduction takes place, and a 1+3 dimensional gauge theory becomes a 1+2 dimensional one (Appelquist and Carrazzone, 1975).

The main physical point is that in the high- T limit the motion of a quark in the new space is dominated by its momentum in the z direction, which, as a result of the antiperiodic boundary conditions, is given by πT . For the motion in the transverse directions x, y , this momentum acts just like a mass:

$$M_{\text{eff}} = \sqrt{m^2 + \pi^2 T^2}. \quad (5.16)$$

As at a high temperature, M_{eff} becomes very large, any attractive potential can bind the quarks in the transverse direction.

Qualitative features of the related quantum electrodynamic problem of $d=2$ positronium were recently discussed in Hanson and Zahed (1991): apart from the effective mass just mentioned, another important ingredient is the logarithmic Coulomb potential in two dimensions. More quantitative analysis of this problem was made by Koch *et al.* (1991).

Turning to the QCD case and using the old dimensional reduction argument (Appelquist and Carrazzone, 1975), one realizes that one has to deal in this case with $d=2+1$ Yang-Mills theory, which is far from simple. In particular, as argued in D'Hoker (1982), it has a linear confining potential, as do $d=1+1$ and $d=1+3$ (the real QCD!) theories.

In the high- T limit quarks have large effective mass, similar to superheavy quarkonia (Appelquist and Politzer, 1975); so the size of the bound state is small $R \sim 1/gT$ and the Coulomb potential is justified. However, one cannot compare this picture with the available lattice data because the temperature is too low. The lesson learned from quarkonium physics is that the nonrelativistic approach based on an effective potential works very well. Such effective potential, in fact, was numerically studied some time ago by Manoussakis and Polonyi

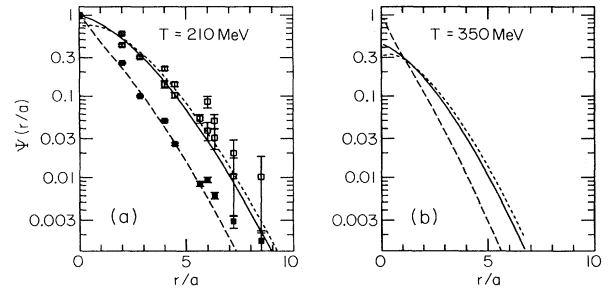


FIG. 27. Wave functions for ρ, π channels at $T=250$ MeV (a) and $T=350$ MeV (b), as a function of r/a ($a \approx 0.22$ fm). The lines are solutions of the $d=2$ Schrödinger equation with the potential discussed in the text from Koch *et al.* (1991), while the points are from lattice measurements by Bernard *et al.* (1991). The solid line and the short-dashed line correspond to ρ with spin projections $S_z = \pm 1$ and 0, respectively, while the long-dashed line corresponds to the pion wave function. In (a) normalization is arbitrary, while in (b) all cases are normalized in the same way.

(1987), who found for the potential⁵⁶

$$V = -a/r + \sigma r \quad (5.17)$$

with $a = 0.184 \pm 0.02$, $\sqrt{\sigma} = 0.22 \pm 0.03$. This should be compared to the $T=0$ parameters, $a = 0.25$, $\sqrt{\sigma} = 0.22 \pm 0.02$. Thus the potential measured in the space direction appears to be essentially T independent.

In Koch *et al.* (1992) spin-dependent forces due to a Fermi-Breit interaction are discussed in detail. In particular, this paper points out that the vector states ρ, ω are split into separate states at high temperature, depending on the spin projection S_z on the propagation axis. All these splittings are proportional to one common parameter, the effective color charge, and more detailed lattice study can check the Fermi-Breit splitting mechanism well enough. Presumably, it is the only mechanism to survive at high T , while at low T nonperturbative phenomena discussed in previous sections should also be involved.

With a potential fixed, one can proceed further and solve numerically the $d=2$ Schrödinger equation and compare it with lattice data, as shown in Fig. 27. Comparing data for the ρ, π channels, one can observe a significant difference between the two cases. The average size of the pion is significantly smaller and, in particular, at small distances $r \leq 2a$, the pion wave function is much

⁵⁶One may compare these data with the potential corresponding to quarks propagating in time direction. Not only are the confinement forces absent above the deconfinement temperature, but even the Coulomb part is much smaller, due to screening effects.

more prominent,⁵⁷ with $|\psi(0)|^2$ about 4 times greater than in the ρ -meson case. Let us also note that spin-dependent forces explain not only the difference in wave functions, but also large splitting of the screening masses discussed in the previous section.

We have discussed in this section correlation functions in the spatial direction at high temperature. Unlike for $T=0$, these spectra are by no means related to the energy spectra of hadronic modes. However, the corresponding momentum or “screening masses” spectra, as well as the corresponding wave functions, happen to be very similar to those at $T=0$. This may be explained by the $d=2$ Schrödinger equation with an effective mass (5.16) and potential (5.17).

3. Baryonic number susceptibility

As a final topic, we mention an interesting set of lattice data (Gottlieb *et al.*, 1987) related to the so-called baryon number susceptibility (McLerran 1987):

$$\chi_b = (1/T) \int d^3x \langle \langle n_b(x) n_b(0) \rangle \rangle, \quad (5.18)$$

where n_b is the baryon density. Such an integral measure of the SU(3) singlet vector correlator (a combination of ω, ϕ ones) was found to jump significantly at T_c , as shown in Fig. 28, soon reaching about $\frac{2}{3}$ of its asymptotic value corresponding to the free thermal motion of light quarks. Shown also in the same figure, the nonsinglet susceptibility with the quantum numbers of ρ has the same behavior, and within the error limits (Gottlieb *et al.*, 1987). The definitions for singlet and nonsinglet cases can also be written as derivatives with respect to the chemical potentials,

$$\chi_{S,NS} = (\partial/\partial\mu_u \pm \partial/\partial\mu_d)(n_u \pm n_d). \quad (5.19)$$

One may be puzzled by this jump after our previous experience of smooth behavior in the screening lengths. As the magnitude of χ_b is comparable to that expected for free quarks at high temperature, the real question is, why is χ_b so small below T_c ?

One can answer this question in two ways. First, the nucleons are the lowest baryons and they are rather heavy. Therefore below T_c we expect their density to be low, and the effects of changes in chemical potential will be small. Thus the data shown in Fig. 28 suggest the baryonic masses do not drop significantly, until maybe very close to T_c .

Second, one can relate this susceptibility to the vector

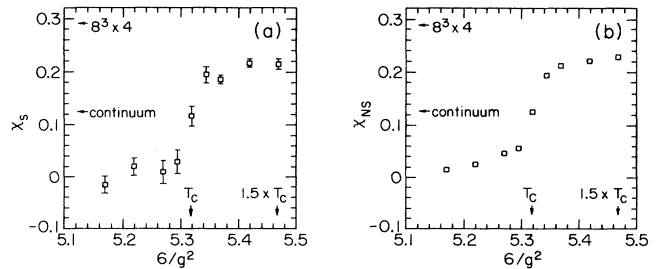


FIG. 28. Baryonic charge susceptibility for singlet (a) and nonsinglet (b) definitions (5.17) vs the bare coupling constant g (arrows show positions of the corresponding chiral restoration temperature T_c and $1.5T_c$, from Gottlieb *et al.*, 1987).

correlation functions integrated over space-time.⁵⁸ The integrated correlators vanish at $T=0$, which can be explained as follows (McLerran, 1987). The general structure of the vector correlator at $T=0$ is $\Pi_{\mu\nu} = (\partial_\mu \partial_\nu - \partial^2 g_{\mu\nu}) \Pi(x)$, and the density-density correlator is the Π_{00} component. The two terms generally compensate time derivatives, and the spatial integral over spatial derivatives vanishes.

At nonzero temperature this simple form for the vector correlator is no longer valid. There exist other transverse tensors, because the thermal rest frame is special. Thus χ_b can be nonzero. However, Fig. 28 suggests that no significant modification in vector correlators takes place until T is very close to T_c .

Certainly, much more work is needed to reach a real understanding of these data. It would be helpful to measure the entire point-to-point correlation functions $F_T(R)$ on the lattice, not just its derivative, (the screening length) or an integral (the susceptibility).

E. Sum rules based on the operator product expansion at finite temperatures and densities

Generalization of the QCD sum rules for nonzero temperatures was pioneered by Bochkarev and Shaposhnikov (1986), and for nonzero baryonic density by Drukarev and Levin (1990). These two important papers have created quite a substantial literature, which can only be discussed in full in a specialized review. Our discussion below concentrates on a few key points, some of them being firmly established and others remaining open questions. We conclude with a sample of the results. Even more than for the vacuum case, the status of these predictions is not completely clear, but they are certainly very interesting. In any case, they have raised many new physical questions and have given a new perspective in the area of finite temperature and density QCD.

⁵⁷On the topic of pion wave functions, the $T=0$ pion wave function by Bernard *et al.* (1991) is sensibly the same as the zero-temperature Bethe-Salpeter amplitude calculated by Chu, Lissia, and Negele (1991).

⁵⁸A warning: we have up to now ignored contact terms, but they do contribute to the integrals.

1. Modifications of the operator product expansion

In Sec. III.B we saw that many questions related to the domain of applicability of the OPE remain open even for the vacuum. In the case of nonzero temperature or density we certainly have to face extra complications. All finite temperature complications can be put into two categories: (a) modification of the OPE itself, because in matter one has to include a wider set of operators on the left-hand side; and (b) the physical spectral density on the right-hand side is more complicated, containing not only production processes but also scattering on matter constituents. In this section we mainly concentrate on the first set of questions, holding to our general idea that predictions for the correlation functions are interesting even without empirical information, for comparison with other (e.g., lattice) studies.

Let us first recall that the OPE has a generic scale μ used for the separation of the low and high frequencies, with which the matrix elements and coefficients of the operators are constructed. At finite temperature or nonzero chemical potential, one should first decide on the relationship between T and μ . If $T \ll \mu$, coefficients C_i are not modified and only the operator matrix elements $\langle\langle O_i \rangle\rangle$ are changed, including new contributions from the heat bath.

The major difficulty with the finite temperature OPE is that the set of contributing operators is no longer limited to Lorentz scalars but includes all symmetric tensors. This is, of course, due to the existence of a preferred frame, the thermal rest frame. Let us define the unit four-vector of the thermal frame, n_μ . If, for example, one considers a correlation function of scalar or pseudoscalar operators, the OPE equation would have the form

$$K(x) = \Sigma C^{(i)} x_{\alpha_1}, \dots, x_{\alpha_n} \langle\langle O_{\alpha_1 \alpha_n}^{(i)} \rangle\rangle \quad (5.20)$$

and the thermal average of the operator would give factors $n_{\alpha_1}, \dots, n_{\alpha_n}$. In simpler terms, one simply has to expand separately in powers of time and the space interval.

The kinematics are slightly more involved for vector and axial currents, but it is essentially the same as the

one for deep-inelastic scattering. As at $T=0$, the Fourier transform of the correlator

$$T_{\mu\nu}(q) = i \int d^4x e^{iqx} \langle\langle j_\mu(x) j_\nu(0) \rangle\rangle \quad (5.21)$$

can be considered as a physical scattering amplitude, say, of forward photon scattering on the heat bath, and its imaginary part has all the usual analytic properties, although it depends on the energy transfer $\omega=(qn)$ and momentum transfer separately. Standard notations for vector current describe the corresponding physical spectral density in terms of the two functions W_1 and W_2 :

$$\frac{1}{2\pi} \text{Im} T_{\mu\nu}(q) = -W_1(q)(g_{\mu\nu} - q_\mu q_\nu / q^2) + n_\mu^T n_\nu^T W_2(q). \quad (5.22)$$

Here the transverse part of the vector \mathbf{n} is $n_\mu^T = n_\mu - (nq)q_\mu / q^2$. This parametrization satisfies gauge invariance of electrodynamics,⁵⁹ which demands that $(Tq)=0$.

The main new operators are the so-called leading twist quark operators (Politzer, 1974) of the kind

$$O_{\mu_1, \mu_2, \dots, \mu_n} = \bar{\psi} \gamma_{\mu_1} \partial_{\mu_2} \dots \partial_{\mu_n} \psi. \quad (5.23)$$

The origin of these operators is easily explained. These operators are associated with a process in which a quark is created at point 0, travels from 0 to x , and then is returned to the heat bath. Its amplitude can be written as $\bar{\psi}(0)\Gamma(\gamma_\mu x_\mu)/(2\pi^2 x^4)\Gamma\psi(x)$, where $\Gamma = \gamma_\mu$ or γ_5 for vector and pseudoscalar currents, respectively. All that remains to be done is to simplify γ matrices and expand $\psi(x)$ in a Taylor series in x .

The lowest of these operators, with only two indices, has dimension 4 and is nothing other than the quark stress tensor. That is why our small-distance expansion of the quark propagator (5.14) started with the x^4 term. Furthermore, the $O(T^4)$ coefficient is nothing more than a pressure of the plasma made of free quarks.

Now let us display few OPE terms of the lowest dimension, measuring the correlation function in a spatial direction x ,

$$\begin{aligned} K(x)/K_{\text{free}}(x) = & 1 + x^4 [C_1 \langle E^2 - B^2 \rangle + C_2 \langle E^2 + B^2 \rangle + C_3 \langle \bar{\psi} \gamma_1 \partial_1 \psi \rangle] \\ & + x^6 [C_4 \langle \bar{\psi} \psi \rangle^2 + C_5 \langle (\bar{\psi} \gamma_1 \psi)(\bar{\psi} \gamma_1 \psi) \rangle + C_6 \langle \bar{\psi} \gamma_1 \partial_1^3 \psi \rangle \dots]. \end{aligned} \quad (5.24)$$

This equation includes some operators that have not yet been studied in the literature, in particular, the gluonic stress tensor (C_2) and the square of the vector current (C_5).

2. Operator expectation values

The next set of questions concerns the temperature dependence of the operator averages. Generally speak-

ing, one cannot answer these questions without an understanding of the underlying nonperturbative dynamics. However, some statements can be made about the matrix

⁵⁹For the nonconserved axial current there are four functions: two additional ones can be chosen to be proportional to $q_\mu q_\nu$ and $q_\mu n_\nu + n_\mu q_\nu$.

elements, and we briefly review some ideas suggested in the literature.

Let us start with the leading twist operators just discussed. In Bochkarev and Shaposhnikov (1986) and in many later papers on the subject, the diagrams were evaluated using the thermal quark propagator $S_T(x)$ instead of $S_0(x)$. It seems like a logical thing to do, but actually this prescription has a limited region of validity. It involves the operators mentioned above, but perturbatively, which means that their average values are automatically taken for an ideal quark gas.

Such estimates of these matrix elements may be used at high $T > T_c$, where matter is indeed the quark plasma, but they are not valid otherwise. Therefore the simplified procedure based on thermal propagators overestimates the temperature dependence of the correlation functions at $T < T_c$. In the opposite limit of low T , one can evaluate the quark part of the thermal energy density as $\epsilon_q(T) = \chi_q \epsilon_\pi(T)$, where $\epsilon_\pi(T)$ is the energy density of a dilute pion gas and χ_q is the quark share of the pion momenta. This share is about $\chi_q \sim \frac{1}{2}$, inferred from empirical pion structure functions.

In OPE-based sum rules, one of the essential ingredients is the *gluon condensate*, $\langle G_{\mu\nu}^2 \rangle$. In matter one has to include two separate operators: essentially the electric- and magnetic-field strength squared. An argument was proposed (Bochkarev and Shaposhnikov, 1986) that the correction is connected with the average at small T over the pion state $\langle \pi | G_{\mu\nu}^2 | \pi \rangle$ are small because they are proportional to the pion mass.⁶⁰ In Adami, Hatsuda, and Zahed (1991) lattice data were used to conclude that although these quantities decrease with T , the decrease occurs near T_c and is roughly a factor of 2. The IIA also predicts a qualitatively similar behavior of the instanton-induced gluonic fields. It can be parametrized, for example, as follows:

$$\langle \langle E^2 \rangle \rangle = \langle \langle H^2 \rangle \rangle \sim \exp(-T^2/T_0^2), \quad (5.25)$$

where T_0 is of the order of T_c , but actually has nothing to do with it. For example, there is a systematic suppression of the instantons of size $\rho T > 1$, but they certainly *do not disappear at the chiral symmetry restoration point T_c* : the so-called instanton-anti-instanton molecules do exist even in the chirally symmetric phase.

The next important ingredient of the OPE-based sum rules is specific *four-fermionic operators*. Their analogs at finite T are, generally speaking, a set of all symmetric tensors, and the corresponding OPE formulas are very complicated.⁶¹ In Bochkarev and Shaposhnikov (1986), estimates of their expectation values were obtained as fol-

lows: they were rewritten as a sum of squares of some currents, with quantum numbers of different mesons. At small T , one therefore may start with a simple pion loop diagram, making a unique estimate of the T dependence of the corresponding matrix element. For example, for the operator O_ρ entering the ρ -meson sum rules, this pion loop leads to a negative correction; so its expectation value diminishes with temperature.

Another simple way of reasoning (Furnstahl, Hatsuda, and Lee, 1990; Adami *et al.*, 1991) leading essentially to the same conclusion is as follows. According to the vacuum dominance hypothesis (Shifman *et al.*, 1979b), VEV of four-fermionic operators can be expressed via *quark condensate squared*. If so, it is natural to expect *all of them to vanish at the chiral symmetry restoration point $T = T_c$* . The specific parametrization usually used is then

$$\frac{\langle \langle O_{4 \text{ fermion}}(T) \rangle \rangle}{\langle \langle O_{4 \text{ fermion}}(T=0) \rangle \rangle} \approx \frac{\langle \langle \bar{\psi}\psi(T) \rangle \rangle^2}{\langle \langle \bar{\psi}\psi(0) \rangle \rangle^2} \approx 1 - T^2/T_c^2. \quad (5.26)$$

The last parametrization is used because it is simple and reproduces lattice data.

3. Some results

We now apply the above approximations to the vector and axial correlators. Specifically, we start with the OPE expression at $T=0$, modify the quark loop with the factor $f^2(\pi TR)$, and take the condensates to have a temperature dependence given by Eq. (5.26). The results are shown in Fig. 29. We see that both vector and axial correlators converge rapidly and join smoothly to the expected high-temperature curves. Next, one can make fits to such curves⁶² to a parametrized spectral density, deriving the temperature dependence of the parameters involved.

As discussed earlier, the spectral density is usually expressed with three parameters, the resonance mass m , its coupling to the current f , and the threshold energy E_0 .

Bochkarev and Shaposhnikov (1986) first analyzed the temperature dependence of the ρ channel in this way, and they concluded that all three parameters decrease with T , with E_0 dropping much faster than the others. However, several later papers addressing the same issue (Dosch and Narison, 1988; Furnstahl *et al.*, 1990; Adami *et al.*, 1991) found somewhat weaker temperature dependence of all three parameters in the vector channel, still with the main T dependence seen in E_0 . Figure 30 shows the typical results taken from Adami *et al.* (1991).

⁶⁰We recall that due to an anomaly relation this operator can be considered as a trace of the energy-momentum tensor.

⁶¹The relevant formulas were derived for *higher twist* corrections to deep-inelastic scattering (Jaffe and Soldate, 1982; Shuryak and Vainshtein, 1982a, 1982b).

⁶²Actually, it is traditionally done in Borel representation, with the so-called Borel parameter playing the role of distance in our approach. Let us repeat that there are no real advantages behind this trick, which makes the whole presentation much less transparent.

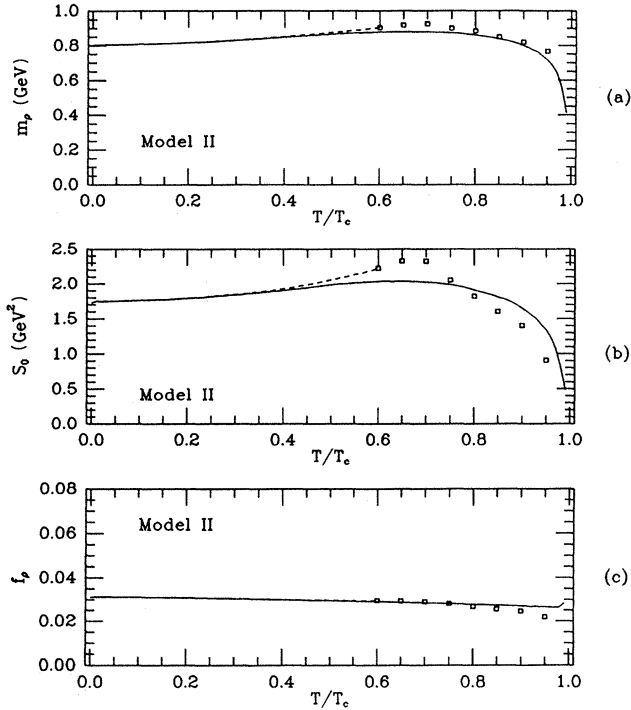


FIG. 29. Schematic OPE predictions for vector (solid lines) and axial (dashed ones), given by the ratio of the correlation function to that for free quarks vs distance x (in fm). Four solid lines correspond to $T=0, 140, 200, 400$ MeV (from upper curve down), and the dashed lines correspond to $T=0$ and 140 MeV (in the last two cases, above T_c , they coincide with solid ones).

Effects in the ρ channel may be weaker than the other channels, because the ρ correlator is close to free-quark propagation, as we saw in Sec. II. It would be interesting and relatively simple to generalize the analysis done for vector current to the axial case, where we have π, A_1 contributions and nonperturbative corrections acting in the same direction.

Another suggestion is to focus on ω, ϕ mesons, for reasons related to experiment (Shuryak, 1991). Their widths are small enough so that even a relatively small shift of the mass could be observable. On the other hand, their widths are large enough to give them a chance to decay inside the “fireball” created in heavy-ion collisions. Even in the environment of heavy-ion collisions, one can observe two decay modes, e^+e^- and K^+K^- , and thus measure the coupling to the current. Therefore in these cases the resonance modification with temperature can be subjected to direct experimental testing.

Finally, consideration has also begun of correlation functions in dense nuclear matter: Drukarev and Levin (1990), Cohen, Furnstahl, and Griegel (1991), and Hatsuda and Lee (1991). There are corrections of first order in density that also contain certain nucleon matrix elements. Fortunately, these can be determined empirically from deep-inelastic scattering. The results suggest that nuclear matter produces significantly larger corrections,

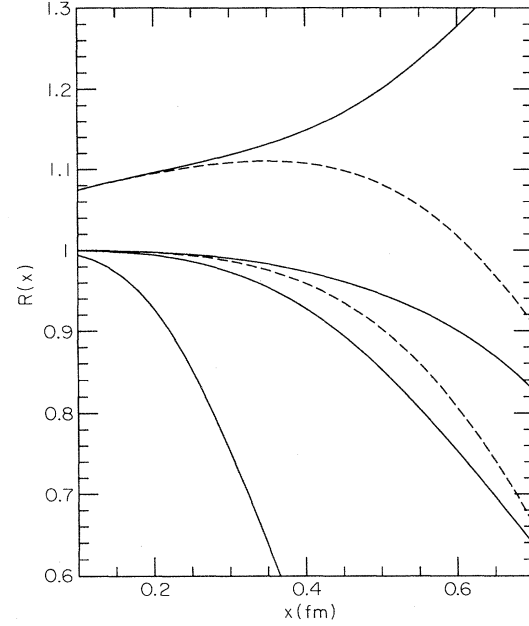


FIG. 30. Solid lines show predictions of the temperature dependence of the ρ meson mass and of the threshold parameter of the continuum S_0 and the coupling constant F_ρ , derived in Adami *et al.* (1991) from the OPE-based sum rules. (The points are a slightly different calculation and can be disregarded.) The “Model II” used corresponds roughly to a condensate modification discussed in the text and to the correlation function shown in Fig. 29.

compared to the pion gas of comparable density, and makes the nucleon lighter. Whether the next-order corrections produce positive shifts in the nucleon mass, as would be required to saturate nuclear matter (see Drukarev and Levin, 1990), is still unclear.

The current state of the art of QCD sum rules at finite T does not allow firm conclusions. However, there is some understanding of how the correlation functions are modified with temperature, and also what physical meaning these modifications may have. A lot of work, both analytic and numerical, is needed and is currently under way.

VI. SUMMARY AND DISCUSSION

A. Summary of phenomenological observations

In Sec. II we discussed the phenomenology of mesonic correlation functions and showed that existing experimental data not only fixed the logarithmic derivative of the correlation functions at large distances, the hadronic masses, but, in several important cases, they also provided a good description of the whole function.

Using these data one can conclude that a realistic $\bar{q}q$ interaction is much more complicated than just a universal confining potential. Various channels show very

different trends, and their deviations from a perturbative picture of free-quark propagation in some cases occurs at such small distances, where confinement effects are yet unimportant. Several phenomena have been observed, in particular:

(1) We have seen the superduality in the ρ and other vector channels, giving unexpectedly small deviations from the free-quark behavior. These deviations are within 10–20% up to very large distances 1–1.5 fm, while the correlation function changes in this interval by several orders of magnitude. In other words, in all vector cases all nonperturbative corrections in this range of distance are remarkably canceled. No explanation for this phenomenon is known.

(2) It was shown that ρ and ω correlators are identical within errors in a wide range of distances. Not only the masses of these particles, but also the coupling constants and even the production amplitudes of the nonresonance states are very similar. This means that the famous Zweig rule forbidding flavor mixing is unexpectedly strict in the vector channels: it holds up to distances $x \sim 2$ fm, where the correlations are extremely small.

(3) The last interesting observation related to vector channels is that even for the K^*, ϕ channels involving strange quarks a similarity to all other vector correlators persists up to distances of about 1 fm. The effect of larger masses is partially compensated by larger coupling constants, and all curves go together as shown in Fig. 31. In other words, all corrections proportional to the strange quark mass are canceled separately.

Taken together, observations (1)–(3) show that all point-to-point vector correlators in coordinate representations are more similar than the cross sections from

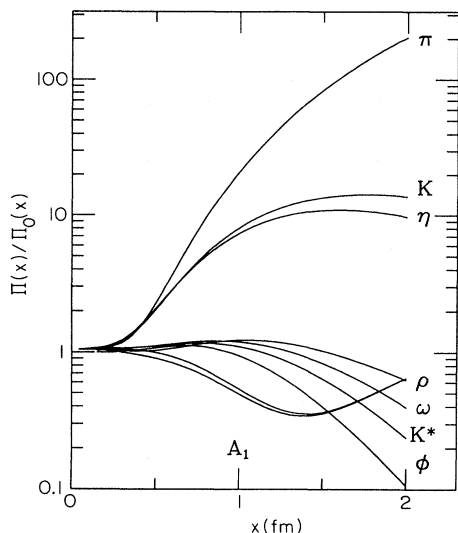


FIG. 31. Phenomenological information on the various mesonic correlation functions discussed (same as in Fig. 2, etc.). Different vector correlators were derived from completely different sets of data, but they are very consistent with one another and demonstrate a systematic trend.

which they were calculated. This clearly demonstrates our main point: these correlators are more fundamental objects than particular hadronic states and their excitation amplitudes involved.

(4) Comparing the axial and vector correlators, one observes quite different behavior. This axial-vector difference is due to chiral asymmetry of the QCD vacuum and should therefore gradually decrease with temperature, disappearing at the chiral restoration point $T = T_c$.

(5) The octet pseudoscalar correlators, including the π , K , and η channels, are very similar at distances up to $x = 0.5$ fm. In all cases the effect of a very strong $\bar{q}q$ attraction is seen already at $x \sim \frac{1}{3}$ fm.

(6) The SU(3) singlet (η') pseudoscalar correlator shows completely different behavior. No trace of attractive quark interaction is observed, at least at distances $x > 0.5$ fm, where it is presumably dominated by the evaluated η' contribution.

Let us also point out that in none of the pseudoscalar channels is any trace of the Zweig rule seen: on the contrary, the flavor-changing amplitudes seem to be the dominant effect.

(7) Radiative J/ψ decays provide valuable information on the $\eta, \eta', \eta(1440)$ couplings to gluonic pseudoscalar operator $G\bar{G}$. Deviations from asymptotic freedom in this case take place at very small distances $x \sim \frac{1}{4}$ fm, as in quark-related pseudoscalar channels. Similarly, also the sign of these deviations indicates the presence of a strong attraction.

(8) Qualitative comparison of all four spin-zero channels (scalars and pseudoscalars, octets and singlets) made in Sec. II.H leads to the following conclusion: all deviations from the asymptotic freedom can presumably be explained by the dominance of one particular amplitude (denoted K^{--}) changing both quark flavor and chirality.

B. What new experiments are needed?

Electromagnetic and weak currents are the only local probes available in nature, and their relations to fundamental quark fields are by now well established. The cross sections of $e^+e^- \rightarrow \text{hadrons}$ and $\tau \rightarrow \nu_\tau + \text{hadrons}$ are giving us fundamentally important information, in particular, information about the correlation functions in the QCD vacuum discussed in this review.

In view of significant efforts devoted to understanding QCD (heavy-ion collider projects like RHIC, or new large-scale lattice simulations like the TERAFLOP project), one may also think about new generations of e^+e^- and τ -lepton-related experiments providing more accurate data than those available today. Discussion of various c and b “factories” is under way in many places around the world, which may be the basis for some optimism in this respect. Here are some possibilities related to our discussion.

(1) In principle it seems feasible to achieve an experimental accuracy of a few percent in the e^+e^- cross section resolved into $I=0, 1$ channels. If so, one will have

vector (ρ, ω) correlation functions with similar accuracy. At the moment, the uncertainty in the correlators is dominated by the poor accuracy ($\sim 30\%$) of the data in the energy region $E = 1.5 - 3$ GeV. This corresponds to the very interesting intermediate-distance region, $x = 0.2 - 0.6$ fm. If the gap is filled, we shall be able to tell whether these correlators follow the OPE formulas and, if so, to measure directly the vacuum expectation values of the operators involved.

(2) A new generation of τ lepton hadronic decay experiments is very interesting as the best source of information on axial and strange vector correlators. The particular region of hadronic states with invariant mass above the A_1 mass is of main interest, since the available data are very poor in this region.

(3) Our discussion in the η' correlator, the axial anomaly, and the gluonic matrix elements was based on a rather old set of data on J/ψ radiative decays. These studies, done mainly at SPEAR a decade ago, have found many interesting phenomena, but many related questions remain unanswered. As it is the best way we know to approach the mysterious world of gluonic states and corresponding matrix elements, further experiments are justified.

(4) Much better data on $\bar{b}b$ production above the $\bar{B}B$ threshold can help to measure the magnitude of the strong Coulomb potential. This is a new and potentially fruitful method of measuring Λ_{QCD} . Observable effects are large, but they are of a perturbative nature and allow for reliable evaluation by standard methods.

(5) Although the t quark seems to be too heavy to form narrow states, the shape of the $\bar{t}t$ production threshold can still be used to measure Coulomb-type strong forces.

(6) Last, but not least, hadron modification at finite temperatures and densities can be studied in high-energy collisions of heavy ions. Instead of lepton annihilation into hadrons, one observes the inverse process, a hadronic production of lepton pairs, to detect the melting of the ρ , ω , ϕ , and ψ mesons.

C. Further lattice studies

The main suggestion for immediate study is as follows: It would be very interesting to supplement current efforts oriented to measurements of hadronic masses by a set of data on point-to-point correlation functions. The most interesting region is at intermediate distances $x = 0.2 - 1$ fm, which corresponds to a few lattice spacings. For obvious reasons, such data can be statistically more accurate and also less affected by the finite-size effects, presumably making their comparison with phenomenology more conclusive. Some details of this suggestion are discussed below.

(1) Generally speaking, any integration of the correlation functions leads to some loss of information, and measurements with nonlocal sources certainly cannot tell us much about the short-range interaction of quarks and gluons. Separation of the contributions of short- and

long-range correlations in the vacuum is the natural thing to do. In particular, it is important to understand at which distances one should trust OPE-based expressions in various channels.

(2) It has been shown that several correlation functions are experimentally known at all distances; so their comparison with lattice data can provide a much better test. In particular, one may wonder if lattice simulation can reproduce such delicate phenomena as superduality in the vector channels, their splittings from the axial one, or short-range attraction in pseudoscalar channels.

(3) In this paper the ratio of the correlation functions to those corresponding to free-quark motion is systematically used. If one normalizes the lattice data in a similar way, some systematic errors, such as finite-size corrections, can be canceled or reduced. Moreover, using such normalized correlators, one can avoid the problem of the absolute scale of lattice units.

(4) It would be very interesting to study flavor-changing correlation functions. The so-called two-loop diagrams have not yet been studied because of the problems with statistics, but presumably correlation functions at intermediate distances are still measurable. Hadronic phenomenology tells us that these correlators are strongly suppressed in all vector channels, but enhanced in the pseudoscalar ones. It would be interesting to see whether LGT reproduces these observations, even qualitatively.

(5) Studies of light-heavy systems can easily be extended to various angular momenta and parities, but so far most of the work has been concentrated on the pseudoscalar channel. It was argued above that the pattern of splittings of such mesonic correlators in parity could shed some light on the old question of the applicability of the constituent quark model. The point is whether the model can describe both the spin-flip and the spin-nonflip part of the propagator. Data on the light-heavy baryons can similarly clarify the properties of the qq interaction. In particular, studies defining at which distances and how the Σ and Λ -type correlators become different can tell a lot about the mechanism of spin splitting in baryons. There are two candidates: gluon exchanges and instanton-induced forces, and on the lattice one can invent a number of ways to tell the difference between them. For example, one may study spin splittings by applying the so-called lattice cooling, thereby killing the perturbative component but preserving instantons.

(6) A technical point: the three-parameter fit for the spectral density, with a δ plus a θ function, has proved to be very accurate in most cases studied. It is even more accurate than a four-parameter fit with two exponents used in some lattice works, because it has both long- and short-distance limits right. We recommend using it as the standard parametrization of the correlators.

D. Theoretical problems

The list of questions formulated below is certainly related to phenomena discussed above, but they are listed

in order of their theoretical importance, from the more general to the more specific.

(1) *Why are the quark-made hadronic states much lighter than the glueballs? Or, speaking in terms of the correlation functions, why are gluonic fields uncorrelated at much smaller distances than the quark ones?* Certainly, there should be a big difference between the space-time distribution of gluon and quark fields in the QCD vacuum. One example is provided by IIA, which suggests a picture of the vacuum as a very inhomogeneous instanton liquid. According to it, gluonic fields are concentrated in small fluctuations, the instantons, while quarks have another role: they jump from one instanton to another, filling the whole space-time more or less homogeneously. LGT also reproduces these qualitative features of correlators, but it is at the moment very difficult to say whether it is consistent with this explanation.

(2) It was argued earlier that correlation functions tell us that, in fact, $\bar{q}q$ and qq interaction is much more complicated than just simple universal confining forces. After many years of studies of individual hadrons, only now is an attempt being made to understand first the much simpler objects, the small-size wave packets that are the intermediate states of the correlators. The long-range effects (confinement) are in this case much less important, but some others (like spin-spin interactions) are enhanced. We have found the strongest deviation from perturbative behavior at small distances in the case of octet pseudoscalars, where attraction dominates at distances as small as $\frac{1}{4}$ fm. The OPE formulas do not reproduce the effect.⁶³ *What is the physical nature of the short-range $\bar{q}q$ attractive interaction?*

(3) Considering these data (which are also combined with some limiting information about other spin-zero channels, the η' one and the scalars), we have concluded that the quantum numbers of them in corrections point toward the amplitude K^{--} , which changes both *chirality and flavor* of participating quarks. The quantum numbers of this interaction fit into the *instanton-induced 't Hooft interaction*; so it is the best candidate we know. However, to make our arguments convincing, it would be interesting to measure all these correlators on the lattice. *Is there a window in which one may use the 't Hooft interaction in first order, avoiding complicated IIA calculations?*

(4) Now we come to a set of questions related to the qq interaction and baryons. *Why is the nucleon so light, compared to current lattice calculations? Is the OPE-based conclusion really true, and is there a maximum in $K_N(x)/K_N^{free}(x)$ in which the nucleon contribution is several times larger than the perturbative one? Is it also*

true for the $I=\frac{3}{2}(\Delta)$ correlator? More generally, how do the spin-splitting interactions depend on interquark distances?

(5) Let us ask some questions about the propagation of a single quark in the QCD vacuum, assuming such questions can be given physical meaning. *Does the constituent quark model make sense? Is it indeed true that quarks are "dressed smoothly," with Z factors close to 1, and more or less independently from one another? Is it true, as is sometimes conjectured, that the size of the constituent quark is significantly smaller than 1 fm, a hadronic radius?*

(6) Modification of all correlators with temperature and density is a vast region for investigation. In particular, the correlators were decomposed above out of several components: resonance and nonresonance hadronic states. *Do these components depend on temperature similarly, or quite differently? What is "melted" first, the resonance contribution or the continuum threshold? Which correlation functions are discontinuous following the chiral or confinement phase transitions? What is the nature of strong deviation of the scalar-pseudoscalar screening length from $2\pi T$, which is not observed in other channels?*

In conclusion of this review, let us return to a general point considered in the Preface. The QCD-related studies is a vast field. Many particular problems were analyzed in detail, and we have a vast phenomenology and great potential for better experiments and lattice simulations. Even so, these new efforts will be more successful if they are also supplemented by some work aimed on their synthesis, consolidating all studies to the common set of observables and problems. Whatever goals this paper has reached, it is an attempt in this direction.

Notes added in proof

Since this paper was submitted, some extremely important new developments have taken place in the field, and in this note we cite the main ones.

One of the main suggestions of this paper is to perform detailed lattice studies of point-to-point correlation functions. Now the first such measurements have been made by (Chu, Grandy, Huang, and Negele, 1992). Another idea emphasized above was to get much more accurate results from the instanton-based models, and those are also now available, both for the simplest case or "random instanton liquid" (Shuryak and Verbaarschot, 1992a, 1992b, 1992c), and interacting instantons (Shuryak and Verbaarschot, 1992d).

A selection of the most important data for lattice and random instantons is shown in Fig. 32: they are surprisingly consistent with each other in all cases. For mesons, they are also very close to phenomenological expectations. For baryons, both show a remarkably different behavior for nucleons and Δ 's, strongly supporting Chernyak-Zhitnitsky predictions (Farrar, Zhoang, Ogloblin, and Zhitnitsky, 1981) over Belyaev-Ioffe ones

⁶³Unless one increases VEV of some four-fermion operators by more than one order of magnitude compared to the "standard" estimates.

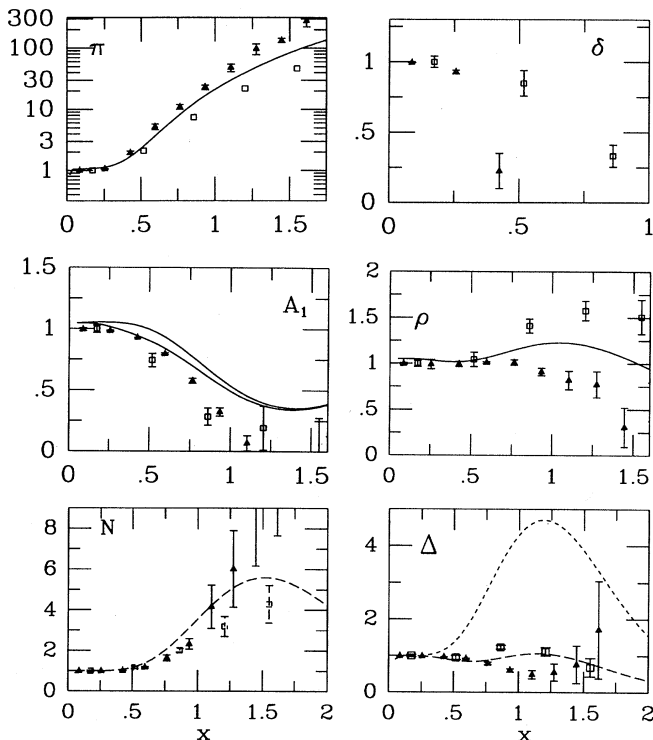


FIG. 32. Correlation functions for the isovector pseudoscalar (π), vector (ρ), scalar (δ), axial-vector (A_1), nucleon (N), and delta (Δ) channels, as a function of distance x in fm, and normalized by corresponding correlators for free massless quarks. Squares and triangles show lattice results by Chu *et al.* (1992) and random instanton vacuum (Shuryak and Verbaarschot, 1992b, 1992c), respectively. Solid lines correspond to experimental data; long-dashed (Farrar *et al.*, 1981) and short-dashed (Belyaev and Ioffe, 1982) ones show different predictions of the QCD sum rules.

(Belyaev and Ioffe, 1982). As argued above, this provides a completely new perspective in our understanding of baryon structure.

At the same time more detailed studies of interacting instantons (Shuryak and Verbaarschot, 1992d) have revealed a problem: the “streamline”-generated interaction leads to too strongly bound instanton–anti-instanton pairs, which spoils a good description of correlators reached in a random (=noninteracting) instanton vacuum. However, an additional repulsive core-type interaction does solve a problem, and leads to even better agreement with data, especially for scalar and η' channels.

New important results concerning the quark-gluon plasma phase have been reported by Boyd, Gupta, and Karsch (1992). In agreement with our arguments, they have clearly observed the appearance of effective quark mass πT if the quark propagates in spatial directions, but only small perturbative mass for quarks propagating in the time direction.

Our last comment deals with QCD sum rules at low temperatures: our discussion of all these works above is

very critical. A recent paper (Hatsuda, Koike, and Lee, 1992) has addressed this criticism and deals with the problem in a much more consistent way. However, it still is incomplete (tensor operators are not really included) and, by construction, restricted to the very-low- T region. Therefore, we still think some main conclusions of this paper (e.g., qualitatively different modification of ρ and ω mesons, predicted there) still may be revised by further works.

ACKNOWLEDGMENTS

Most of what I have learned about correlation functions has been gained through discussions with my old friends A. I. Vainshtein, M. A. Shifman, V. I. Zakharov, and V. L. Chernyak. The idea for writing this paper presented itself naturally, because its substance was part of a course on nonperturbative QCD in Stony Brook in 1990, a project which would never have materialized without the practical help and everlasting curiosity of G. E. Brown. I am also much indebted to S. I. Eidelman, who supplied relevant experimental data, and to G. Bertsch and J. Verbaarschot, who took on the painful task of reading this voluminous manuscript and making numerous suggestions. I should also mention that this paper was finished at the Aspen Summer Institute, which I thank for its hospitality. This work is partly supported by the U.S. Department of Energy under Grant No. DE-FG02-88ER40388.

REFERENCES

- Adami, C., T. Hatsuda, and I. Zahed, 1991, Phys. Rev. D **43**, 921.
 Adami, C., I. Zahed, 1990, “Finite temperature QCD sum rules for the nucleon,” SUNY preprint NTG-90-37.
 Adler, S. L., 1969, Phys. Rev. **177**, 2426.
 Albrecht, H., *et al.*, 1986, Z. Phys. C **33**, 7.
 Allton, C. R., C. T. Sachrajda, V. Lubicz, L. Maiani, and G. Martinelli, 1991, Nucl. Phys. B **349**, 598.
 Appelquist, T., and J. Carazzone, 1975, Phys. Rev. D **11**, 2856.
 Appelquist, T., and H. D. Politzer, 1975, Phys. Rev. Lett. **34**, 43.
 Asakawa, M., and K. Yazaki, 1989, Nucl. Phys. A **509**, 608.
 Barkov, L. M., *et al.*, 1985, Nucl. Phys. B **256**, 365.
 Barkov, L. M., *et al.*, 1988, Sov. J. Nucl. Phys. **47**, 248.
 Belavin, A. A., A. M. Polyakov, A. A. Schwartz, and Y. S. Tyupkin, 1975, Phys. Lett. B **59**, 85.
 Bell, J. S., and R. Jackiw, 1969, Nuovo Cimento A **60**, 47.
 Belyaev, V. M., and B. L. Ioffe, 1982, Sov. Phys. JETP **83**, 976.
 Bernard, C., D. Murphy, A. Soni, and K. Yee, 1990, Nucl. Phys. B Proc. Suppl. **17**, 593.
 Bernard, C., T. DeGrand, C. DeTar, S. Gottlieb, A. Krasnitz, M. Ogilvie, R. Sugar, and D. Toussaint, 1991, “The spatial structure of screening propagators in hot QCD,” preprint AZPH-TH/91-60.
 Bernard, C., C. Heard, J. Labrenz, and A. Soni, 1992, “Decay constants and wave functions of heavy-light pseudoscalars,” Brookhaven National Laboratory preprint BNL-45097. Also in Proceedings of Lattice 91, Tsukuba, Japan.

- Betman, R. G., and L. V. Laperashvili, 1985, *Sov. J. Nucl. Phys.* **41**, 295.
- Bochkarev, A. I., and M. E. Shaposhnikov, 1986, *Nucl. Phys. B* **268**, 220.
- Born, K. D., S. Gupta, A. Irbäck, F. Karsch, E. Laermann, B. Petersson, and H. Satz, 1991, *Phys. Rev. Lett.* **67**, 302.
- Boucaud, P., *et al.*, 1988, “*B*-meson mass and decay constant from lattice QCD,” CERN-TH.5269/88.
- Boyd, G., S. Gupta, and F. Karsch, 1992, “The quark propagator at finite temperature,” preprint CERN-TH.6482/92.
- Brown, G. E., 1991, *Nucl. Phys. A* **522**, 397.
- Brown, G. E., H. A. Bethe, and P. M. Pizzochero, 1991, *Phys. Lett.* **B263**, 337.
- Brown, F. R., F. P. Butler, H. Chen, N. H. Christ, Z. Dong, W. Schaffer, L. I. Unger, and A. Vaccarino, 1990, *Phys. Rev. Lett.* **65**, 2491.
- Brown, F. R., F. P. Butler, H. Chen, N. H. Christ, Z. Dong, W. Schaffer, L. I. Unger, and A. Vaccarino, 1991, *Phys. Rev. Lett.* **67**, 1062.
- Callan, C. G., R. Dashen, and D. J. Gross, 1978, *Phys. Rev. D* **17**, 2717.
- Capstick, S., S. Godfrey, N. Isgur, and J. Paton, 1986, *Phys. Lett.* **175B**, 457.
- Capstick, S., and N. Isgur, 1986, *Phys. Rev. D* **34**, 2809.
- Chu, M.-C., J. Grandy, S. Huang, and J. Negele, 1992, “Lattice calculation of QCD vacuum correlation functions,” CTP 2113, *Phys. Rev. Lett.*, in press.
- Chu, M.-C., and S. Huang, 1991, “The relevance of dilute instanton ensemble to light hadrons,” preprint MAP-138.
- Chu, M., M. Lissia, and J. Negele, 1991, *Nucl. Phys. B* **360**, 31.
- Cohen, T., R. Furnstahl, and D. K. Griegel, 1991, *Phys. Rev. Lett.* **67**, 961.
- Cordier, A., D. Bisello, J.-C. Bizot, J. Buon, B. Delcourt, L. Fayard, and F. Mané, 1982a, *Phys. Lett.* **B109**, 129.
- Cordier, A., D. Bisello, J.-C. Bizot, J. Buon, B. Delcourt, L. Fayard, and F. Mané, 1982b, *Phys. Lett.* **B110**, 335.
- Cosme, G., *et al.*, 1979, *Nucl. Phys. B* **152**, 215.
- DeGrand, T. A., and C. E. DeTar, 1986, *Phys. Rev. D* **34**, 2469.
- DeRujula, A., H. Georgi, and S. L. Glashow, 1975, *Phys. Rev. D* **12**, 147.
- DeTar, C., and J. B. Kogut, *Phys. Rev. D* **36**, 2828.
- Dey, M., V. L. Eletsky, and B. L. Ioffe, 1990, *Phys. Lett. B* **252**, 620.
- D’Hoker, E., 1982, *Nucl. Phys. [FS4] B* **200**, 517.
- Diakonov, D. I., and V. Y. Petrov, 1984, *Nucl. Phys. B* **245**, 259.
- Dolinsky, S. I., *et al.*, 1989, “Review of e^+e^- experiments with neutral detector. . . .” INP preprints 89-68 and 89-104 (in Russian), Novosibirsk.
- Dosch, H. G., and S. Narison, 1988, *Phys. Lett. B* **203**, 155.
- Drukarev, E. G., and E. M. Levin, 1990, *Nucl. Phys. A* **511**, 679.
- Eichten, E., K. Gottfried, T. Kinoshita, K. D. Lane, and T. M. Yan, 1980, *Phys. Rev. D* **21**, 203.
- Eletsky, V. L., 1990, *Phys. Lett. B* **245**, 229.
- Eletsky, V. L., and B. L. Ioffe, 1988, *Sov. J. Nucl. Phys.* **48**, 384.
- Farrar, G., H. Zhaoang, A. A. Ogloblin, and I. R. Zhitnitsky, 1981, *Nucl. Phys. B* **311**, 585.
- Forte, S., and E. Shuryak, 1991, *Nucl. Phys. B* **357**, 153.
- Furnstahl, R. J., T. Hatsuda, and S. H. Lee, 1990, *Phys. Rev. D* **42**, 1744.
- Gasser, J., and H. Leutwyler, 1987, *Phys. Lett. B* **184**, 83.
- Gell-Mann, M., and M. Levi, 1960, *Nuovo Cimento* **16**, 705.
- Gell-Mann, M., R. Oakes, and B. Renner, 1968, *Phys. Rev.* **175**, 2195.
- Geshkenbein, B. V., and B. L. Ioffe, 1980, *Nucl. Phys. B* **166**, 340.
- Gocksch, A., 1991, “Chiral symmetry in hot QCD,” Brookhaven National Laboratory preprint BNL-46286.
- Godfrey, S., and N. Isgur, 1985, *Phys. Rev. D* **32**, 189.
- Gottlieb, S., W. Liu, D. Toussaint, R. L. Renken, and R. L. Sugar, 1987, *Phys. Rev. Lett.* **59**, 2247.
- Gross, D. J., R. D. Pisarski, and L. G. Yaffe, 1981, *Rev. Mod. Phys.* **53**, 43.
- Hands, S., and M. Teper, 1990, *Nucl. Phys. B* **347**, 819.
- Hanson, T., and I. Zahed, 1991, Stony Brook preprint SUNY-NTG-91-44.
- Hatsuda, T., and S. H. Lee, 1991, preprint YSTP-91-10.
- Hatsuda, T., Y. Koike, and S. H. Lee, 1992, “Finite temperature QCD sum rules reexamined,” University of Maryland preprint 92-203.
- Hernández, J. J., *et al.*, 1990, *Phys. Lett. B* **239**, 1.
- Hwa, R., 1990, Ed., *Quark-gluon plasma*, Advanced Series on Directions in High Energy Physics, Vol. 6 (WSPC, Singapore).
- Ilgenfritz, E. M., and E. Shuryak, 1989, *Nucl. Phys. B* **319**, 511.
- Ioffe, B. L., 1981, *Nucl. Phys. B* **188**, 317.
- Isgur, N., 1989, *Phys. Rev. D* **39**, 1357.
- Isgur, N., and G. Karl, 1978, *Phys. Rev. D* **18**, 4187.
- Isgur, N., and M. B. Weise, 1991, *Phys. Rev. Lett.* **66**, 1130.
- Ivanov, P., L. M. Kurdadze, M. Yu. Lechuk, V. A. Sidorov, A. N. Skrinsky, A. G. Chilingarov, Yu. M. Shatunov, B. A. Shwartz, and S. I. Eidelman, *Phys. Lett. B* **107**, 297.
- Jaffe, R. L., and M. Soldate, 1982, *Phys. Rev. D* **26**, 106.
- Khoze, V., and A. Ringwald, 1991, *Phys. Lett. B* **259**, 106.
- Koch, V., E. V. Shuryak, G. E. Brown, A. D. Jackson, 1992, *Phys. Rev. D* **46**, 3169.
- Kochelev, N. I., 1985, *Sov. J. Nucl. Phys.* **41**, 291.
- Kochelev, N. I., 1990, *Z. Phys. C* **46**, 281.
- Kremer, M., A. Kronfeld, M. Laursen, G. Schierhilt, C. Schleiermacher and U. J. Wiese, 1988, *Nucl. Phys. B* **305**, 109.
- Kurdadze, L. M., M. Yu. Le’chuk, E. V. Pakhtusova, V. A. Sidorov, A. N. Skrinskiĭ, A. G. Chilingarov, Yu. M. Shatunov, B. A. Shvarts, and S. L. Éidel’man, 1988, *JETP Lett.* **47**, 512.
- Lattice 88, 1989, *Nucl. Phys. B Proc. Suppl.* **9**, 1. Fermilab, Chicago, 1988.
- Lattice 89, 1990, *Nucl. Phys. B Proc. Suppl.* **17**, 1. Capri, Italy, 1989.
- Lattice 90, 1991, *Nucl. Phys. B Proc. Suppl.* **20**, 1. Tallahassee, Florida, 1990.
- Lattice 91, 1992, *Nucl. Phys. B Proc. Suppl.* **26**, 1. Tsukuba, Japan, 1991.
- Li, S., R. S. Bhalrao, R. S. and R. K. Bhadury, 1991, *Int. J. Mod. Phys. A* **6**, 501.
- Lubicz, V., G. Martinelli, M. McCarthy, and C. T. Sachrajda, 1992, *Phys. Lett. B* **274**, 415.
- Mackenzie, P., 1992, in “Lattice 91,” Tsukuba, Japan.
- Maiani, L., G. Martinelli, and C. T. Sachrajda, 1992, *Nucl. Phys. B* **368**, 281.
- Mané, F., D. Bisello, J.-C. Bizot, J. Buon, A. Cordier, and B. Delcourt, 1982, *Phys. Lett. B* **112**, 178.
- Manousakis, E., and J. Polonyi, 1987, *Phys. Rev. Lett.* **58**, 847.
- Martin, A., 1981, *Phys. Lett. B* **100**, 511.
- McLerran, L., 1987, *Phys. Rev. D* **36**, 3291.
- Novikov, V. A., M. A. Shifman, A. I. Vainshtein, and V. I. Zakharov, 1980, *Nucl. Phys. B* **165**, 55.
- Novikov, V. A., M. A. Shifman, A. I. Vainshtein, and V. I. Zakharov, 1981, *Nucl. Phys. B* **191**, 301.
- Novikov, V. A., M. A. Shifman, A. I. Vainshtein, and V. I. Za-

- kharov, 1982, *Sov. Phys. Usp.* **136**, 553.
- Novikov, V. A., M. A. Shifman, A. I. Vainshtein, and V. I. Zakharov, 1984, *Fortschr. Phys.* **32**, 585.
- Peccei, R., and J. Sola, 1987, *Nucl. Phys. B* **281**, 1.
- Politzer, H. D., 1974, *Phys. Rep.* **14**, 130.
- Quark Matter '88, 1989, *Nucl. Phys. A* **498**, 1.
- Quark Matter '90, 1991, *Nucl. Phys. A* **525**, 1.
- Reinders, L. J., H. Rubinstein, and S. Yazaki, 1983, *Phys. Lett. B* **120**, 209.
- Reinders, L. J., H. Rubinstein, and S. Yazaki, 1985, *Phys. Rep.* **127**, 1.
- Shifman, M., 1992, Ed., *Vacuum Structure and QCD Sum Rules* (North-Holland, Amsterdam), in press.
- Shifman, M. A., 1986, *Charmed and Beautiful Hadrons*, International Symposium on Production and Decay of Heavy Hadrons, Heidelberg, 1986, *Sov. Phys. Usp.* **30**, 91 (1987).
- Shifman, M. A., A. I. Vainshtein, and V. I. Zakharov, 1979a, *Nucl. Phys. B* **147**, 385, 448, 519.
- Shifman, M. A., A. I. Vainshtein, and V. I. Zakharov, 1979b, *Nucl. Phys. B* **147**, 385, 448, 519.
- Shuryak, E., 1978a, *Phys. Lett. B* **79**, 135.
- Shuryak, E., 1978b, *Zh. Eksp. Teor. Fiz.* **74**, 408.
- Shuryak, E., 1980, *Phys. Rep.* **61**, 72.
- Shuryak, E., 1982a, *Nucl. Phys. B* **203**, 116, 140, 237.
- Shuryak, E., 1982b, *Nucl. Phys. B* **198**, 83.
- Shuryak, E., 1983, *Nucl. Phys. B* **214**, 237.
- Shuryak, E., 1984, *Phys. Rep.* **115**, 151.
- Shuryak, E., 1988a, *The QCD Vacuum, Hadrons and the Superdense Matter* (World Scientific, Singapore).
- Shuryak, E., 1988b, *Nucl. Phys. B* **302**, 559, 574, 599, 621.
- Shuryak, E., 1988c, *Nucl. Phys. B* **302**, 574.
- Shuryak, E., 1988d, *Nucl. Phys. B* **302**, 621.
- Shuryak, E., 1989a, *Nucl. Phys. B* **328**, 102.
- Shuryak, E., 1989b, *Nucl. Phys. B* **319**, 541.
- Shuryak, E., 1989c, *Nucl. Phys. B* **319**, 102.
- Shuryak, E., 1989d, *Nucl. Phys. B* **328**, 85.
- Shuryak, E., 1991, *Nucl. Phys. A* **533**, 761.
- Shuryak, E., and J. L. Rosner, 1989, *Phys. Lett. B* **218**, 72.
- Shuryak, E., and V. Thorsson, 1992, *Nucl. Phys. A* **536**, 739.
- Shuryak, E., and A. I. Vainshtein, 1982a, *Nucl. Phys. B* **199**, 451.
- Shuryak, E., and A. I. Vainshtein, 1982b, *Nucl. Phys. B* **201**, 141.
- Shuryak, E., and J. J. M. Verbaarschot, 1992, *Phys. Rev. Lett.* **68**, 2576.
- Shuryak, E., and J. J. M. Verbaarschot, 1992a, "Quark propagation in random instanton vacuum," Stony Brook preprint SUNY-NTG-92-39.
- Shuryak, E., and J. J. M. Verbaarschot, 1992b, "Mesonic correlation functions in random instanton vacuum," Stony Brook preprint SUNY-NTG-92-40.
- Shuryak, E., and J. J. M. Verbaarschot, 1992c, "Baryonic correlation functions in random instanton vacuum," Stony Brook preprint SUNY-NTG-92-41.
- Shuryak, E., and J. J. M. Verbaarschot, 1992d, "Interacting instantons in the QCD vacuum," Stony Brook preprint SUNY-NTG-92-42.
- Shuryak, E., and O. V. Zhirov, 1987, *Nucl. Phys. B* **292**, 714.
- Takeuchi, S., and M. Oka, 1991, *Phys. Rev. Lett.* **66**, 1271.
- Teraflop, 1992, "Physics Goals of the QCD Teraflop Project," *Int. J. Mod. Phys.*, in press.
- 't Hooft, G., 1976, *Phys. Rev. D* **14**, 3432.
- Toussaint, D., 1992, Talk given at Lattice 91, Tsukuba, Japan.
- Verbaarschot, J., 1991, *Nucl. Phys. B* **362**, 33.
- Weinberg, S., 1967, *Phys. Rev. Lett.* **18**, 507.
- Weinberg, S., 1975, *Phys. Rev. D* **11**, 3583.
- Weingarten, D., 1983, *Phys. Rev. Lett.* **51**, 1830.
- Wilson, K. G., 1969, *Phys. Rev.* **179**, 1499.
- Witten, E., 1983, *Phys. Rev. Lett.* **51**, 2351.
- Yung, A., 1988, *Nucl. Phys. B* **297**, 47.